AD-A152 027 VERY LARGE ARRAY OBSERVATIONS OF CORONAL LOOPS AND RELATED OBSERVATIONS O.. (U) TUFTS UNIV MEDFORD MA DEPT OF PHYSICS K R LANG 29 JAN 84 AFOSR-TR-85-0256 1/2

UNCLASSIFIED AFOSR-83-0019 F/G 3/2 NL

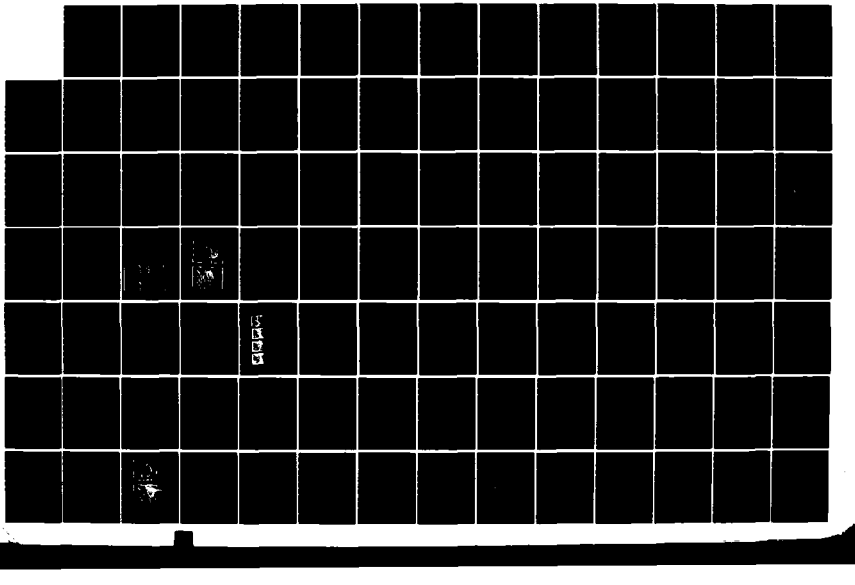

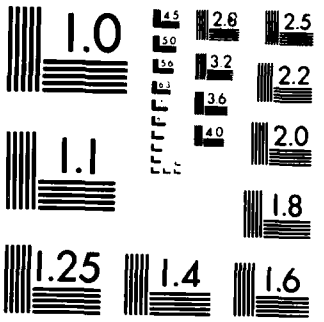

SECURITY CLASSIFICATION OF THIS PAGE (When Data Entered)

REPORT DOCUMENTATION PAGE		READ INSTRUCTIONS BEFORE COMPLETING FORM
1. REPORT NUMBER AFOSR-TR- 85-0256	2. GOVT ACCESSION NO.	3. RECIPIENT'S CATALOG NUMBER
4. TITLE (and Subtitle) VERY LARGE ARRAY OBSERVATIONS OF CORONAL LOOPS AND RELATED OBSERVATIONS OF SOLAR TYPE STARS		5. TYPE OF REPORT & PERIOD COVERED Annual Scientific Report 1 Jan. 1984 to 31 Dec. 1984
		6. PERFORMING ORG. REPORT NUMBER
7. AUTHOR(s) Kenneth R. Lang		8. CONTRACT OR GRANT NUMBER(s) AFOSR-83-0019
9. PERFORMING ORGANIZATION NAME AND ADDRESS Tufts University Department of Physics and Astronomy Medford, MA 02155		10. PROGRAM ELEMENT, PROJECT, TASK AREA & WORK UNIT NUMBERS 61102 F 2311/A1
11. CONTROLLING OFFICE NAME AND ADDRESS AFOSR/NP Bolling Air Force Base, Bldg. No. 410 Washington, D.C. 20332		12. REPORT DATE 29 January 1984
		13. NUMBER OF PAGES 118
14. MONITORING AGENCY NAME & ADDRESS(if different from Controlling Office)		15. SECURITY CLASS. (of this report) Unclassified
		15a. DECLASSIFICATION DOWNGRADING SCHEDULE

16. DISTRIBUTION STATEMENT (of this Report)

Approved for public release - distribution unlimited

17. DISTRIBUTION STATEMENT (of the abstract entered in Block 20, if different from Report)

18. SUPPLEMENTARY NOTES

19. KEY WORDS (Continue on reverse side if necessary and identify by block number)

Coronal Loops - Radio Radiation, Polarization, Evolution, Temperature, Density, Magnetic Field, Thermal Cyclotron Lines, Very Large Array, Solar Bursts - Origin, Prediction, Preburst Heating, Changing Magnetic Fields, Coherent Maser-Like Emission, Flare Build-Up, Nearby Stars - Coronae, Bursts, Slowly Varying Emission International Ultraviolet Explorer Satellite

20. ABSTRACT (Continue on reverse side if necessary and identify by block number)

Observations of solar active regions with the Very Large Array (V.L.A.) have led to a new understanding of the origin and prediction of the solar bursts which disrupt communication systems and interfere with high-flying aircraft. The V.L.A has been used to delineate the temperature and magnetic structure at different heights in coronal loops, and the magnetic field strength has also been determined. Much of the visible solar disk has been resolved at 20 cm wavelength with 2.6" angular resolution. Snapshot maps at intervals of 3 seconds have been

DD FORM 1 JAN 73 1473

SECURITY CLASSIFICATION OF THIS PAGE (When Data Entered)

used to specify changes in the temperature and the magnetic field before and during solar bursts. These snapshot maps ~~have~~ also ~~been~~ were used to investigate the flow of plasma within coronal loops during solar bursts. Postflare loop systems ~~have been~~ were similarly investigated. Our V.L.A. observations ~~have also~~ provided new information on coronal heating and emerging magnetic loops that may trigger the emission of solar bursts. Some of the V.L.A. data were taken within several bands near 20 cm, leading to the probable detection of thermal cyclotron lines. This antenna is the only one capable of resolving the individual emitters of these lines. Detection of the thermal cyclotron lines provides a new sensitive tool for measuring the magnetic field strength in the solar corona. We have also completed related investigations of the quiescent and burst emission from the coronae of nearby stars of late spectral type. The V.L.A. has been used to detect coronal loops and measure burst spectra on these stars. The Arecibo Observatory has been used to obtain accurate polarization and rapid (less than one millisecond) time sampling of the stellar bursts. These studies of radio bursts from the Sun and nearby stars provide a deeper knowledge of the triggering mechanisms of solar bursts, and may lead to new methods of predicting when they will occur.

A summary of the research performed under this grant is given in Section II. The abstracts for four observational programs carried out at the Very Large Array in 1984 are given in Section III. One of these programs included several simultaneous observations with the International Ultraviolet Explorer (I.U.E.) satellite. Section IV contains the titles of six papers presented at professional meetings or workshops in 1984. The titles and references for six papers published in 1984 are given in Section V, and reprints of these six papers can be found in Section VI. They are followed by the abstracts of four observational programs with the Very Large Array that have been accepted for 1985 (Section VII). The titles for five papers accepted for presentation at professional meetings and workshops in 1985 are found in Section VIII, whereas the references and abstracts for five papers accepted for publication in 1985 are given in Sections IX and X. The final Section XI provides a brief summary of the work proposed during the continuation of this grant in 1985.

TABLE OF CONTENTS

VERY LARGE ARRAY OBSERVATIONS OF CORONAL LOOPS AND

RELATED OBSERVATIONS OF SOLAR TYPE STARS

Grant AFOSR-83-0019 B
Interim Scientific Report
for 1 Jan. 1984 to 31 Dec. 1984

TABLE OF CONTENTS (Continued)

I. INTRODUCTION

This is the 1984 interim scientific report for grant AFOSR-83-0019 B entitled Very Large Array Observations of Coronal Loops and Related Observations of Solar Type Stars. The primary purpose of the research proposed in this grant is to use the Very Large Array (V.L.A.) to gain new insights into solar active regions and the powerful bursts that erupt from them. Studies of bursts from nearby flare stars provide new perspectives for our understanding of solar bursts. Our investigations of solar active regions and nearby flare stars have important practical implications in predicting and understanding the Sun's emission of energetic particles that disrupt and interfere with satellites and high flying aircraft.

The status of the research proposed for 1984 is discussed in Section II. We have completed all of the proposed research obtaining important new information about radio bursts from coronal loops and the magnetic changes and preburst heating that trigger solar eruptions. Observations of thermal cyclotron lines are also summarized in Section II. This section concludes with a brief summary of observations of nearby flare stars with the Very Large Array (V.L.A.) and the International Ultraviolet Explorer (I.U.E.) satellite.

In Section III we present the abstracts for our V.L.A. observing applications that were accepted and carried out in 1984. These observing programs involved roughly three weeks of observing scattered throughout the year, and six days of simultaneous observations with the I.U.E. satellite. Analysis of this data involves months of subsequent computer computations. Our requests to use the billion-dollar V.L.A. have never been rejected. This is essentially because we have a strong reputation for carrying out unique, publishable observations in an efficient manner.

In Section IV we provide the titles for six (6) papers presented at professional meetings and workshops in 1984. The titles and references for six (6) papers published in 1984 are given in Section V and reprints of these papers are given in Section VI.

The abstracts of our V.L.A. observing applications for 1985 are given in Section VII. They will provide an introduction to our future research plans that are given in greater detail in Section XI. Of course, additional observations with the V.L.A., the I.U.E. and the Solar Maximum Mission (S.M.M.) satellite will also be completed in 1985.

In Section VIII we provide the titles for five (5) papers accepted for presentation at professional meetings and workshops in 1985. The titles and references for five (5) papers accepted for publication in 1985 are given in Section IX, and the abstracts for these papers are given in Section X.

Our plans for future research are discussed in Section XI. They are the subject of the 1985 continuation of grant AFOSR-83-0019.

II. STATUS OF RESEARCH PROPOSED FOR 1984

A. PROPOSED OBSERVATIONS OF RADIO BURSTS FROM CORONAL LOOPS

We have completed the proposed observation of radio bursts from coronal loops using the V.L.A. at 20 cm wavelength. The B configuration was employed to provide 2.6" angular resolution for all active regions on the visible solar surface. The structure and evolution of six solar bursts have been described in the paper by R.F. Willson and Kenneth R. Lang (Astrophysical Journal 279, 427-437 (1984) and paper VI D). The sizes (total length $L \sim 3 \times 10^9$ cm), temperatures ($T_B \sim 10^7$ to 10^8 K) and degrees of circular polarization ($\rho_c \lesssim 90\%$) have been established for the bursting loops. Snapshot maps made at intervals as short as 10 seconds have been used to study changes in temperature (total intensity) and magnetic field (circular polarization) structure during the bursts. These changes occur on time intervals of 10 seconds or less. The individual peaks of one multiple-component burst originated in different locations within a magnetically complicated region. Preburst heating occurred minutes before the onset of the impulsive phase of another burst. In one case, a loop system emerged in the vicinity of the impulsive source, and two adjacent loop systems may have emerged and triggered the burst.

Additional 20 cm observations of bursts from coronal loops are described in the papers given in Sections VI A, VI B and X A. These ubiquitous loops, which are the dominant structural element in the solar corona, have previously been detected with satellite observations at soft X-ray wavelengths; but we have now shown that their structure can be delineated using ground-based V.L.A. observations at 20 cm wavelength. The unique aspect of the V.L.A. observations is that they can be used to specify the structure and strength of the coronal magnetic field. This is not possible with any other technique either at optical or X-ray wavelengths.

The region of particle energy acceleration and microwave energy release

is at the apex of the coronal loops, and between the flaring Hα kernels that mark the footpoints of the magnetic loops. The release of energy in the coronal part of the magnetic loop impulsively heats the plasma in this region--perhaps through magnetic reconnection or by a tearing mode instability. A nonthermal tail of high energy electrons (energies up to a few hundred keV) may also be produced at this time. The hot plasma is probably confined between a pair of conduction fronts that propagate down the legs of the magnetic loops. The scattering of electrons by electrostatic plasma waves may partially account for the concentration of microwave burst emission near the apex of coronal loops.

B. PROPOSED OBSERVATIONS OF MAGNETIC CHANGES AND PREBURST HEATING IN CORONAL LOOPS

We have completed the proposed observations of magnetic changes and preburst heating in coronal loops. Perhaps the most dramatic evidence for these effects is found in the paper by Robert F. Willson (Solar Physics 92, 189-198 (1984) and paper VI C). The 20 cm V.L.A. observations show that one coronal loop began to heat up and change its structure about 15 minutes before the eruption of two impulsive bursts. The first of these bursts occurred near the top of the loop that underwent preburst heating, while the second occurred in an adjacent loop. The observations suggest that coronal loops twist, develop magnetic instabilities and then erupt. The V.L.A. observations have been combined with GOES satellite X-ray data to infer a peak electron temperature $T_e = 2.5 \times 10^7$ K and an electron density of $N_e = 10^{10}$ cm^{-3} in the coronal loop during the preburst heating phase.

Additional observations of magnetic changes and preburst heating that trigger solar eruptions are given in the COSPAR paper by Kenneth R. Lang and Robert F. Willson (paper VI F and in the review article to be published in Science (by Kundu and Lang- paper X A). The high angular resolution provided

by the V.L.A. has shown that changes in active region microwave emission precede solar eruptions on time scales of a few minutes to an hour, and that these changes are related to preburst heating in coronal loops and to changes in the coronal magnetic field topology. The results indicate that magnetic energy is dissipated in one of three different ways - magnetic changes in a single coronal loop, emerging coronal loops, and interaction between coronal loops.

Single coronal loops or arcades of loops often begin to heat up and change structure about 15 minutes before the eruption of impulsive bursts. The preburst heating and magnetic changes can occur in either a bursting loop or in loops that are adjacent to, but spatially separated from, the sites of impulsive bursts. There is also some evidence for the sequential triggering of impulsive bursts in adjacent coronal loops.

New bipolar loops can emerge and interact with preexisting ones. When the polarity of the new emerging flux differs from that of the preexisting flux, current sheets are produced that trigger the emission of bursts. A similar process can occur when preexisting adjacent loops undergo magnetic changes and trigger eruptions in nearby coronal loops.

The V.L.A. observations have also supplied direct evidence of magnetic reconnection in microwave bursts. In one case, the burst source structure changed and developed into two oppositely polarized bipolar regions or a quadruple structure. A current sheet developed at the interface of the two closed loops, thereby triggering the burst onset. The impulsive energy release occurred during magnetic reconnections of the field lines connecting the two oppositely polarized bipolar regions.

C. PROPOSED OBSERVATIONS OF THERMAL CYCLOTRON LINES FROM CORONAL LOOPS

We have completed the proposed observations of thermal cyclotron lines from coronal loops. The individual cyclotron lines occur at low harmonics of

the electron gyrofrequency; but they can only be detected at high levels in the solar atmosphere where the magnetic fields are relatively constant and by observing at wavelengths near 20 cm where the linewidths are narrow enough to be detected.

Evidence for the detection of thermal cyclotron lines from small sources in active regions is found in the paper by Robert F. Willson (Solar Physics 89, 103-113 (1984) - paper VI C), and in a more comprehensive paper to be published in the Astrophysical Journal (paper X C). The V.L.A. maps of active regions at up to ten closely spaced frequencies between 1420 MHz (or 21 cm) and 1720 MHz show significant changes in the brightness temperature within this narrow range in frequency or wavelength. These changes cannot be attributed to either thermal bremsstrahlung or gyroresonance emission from a coronal loop in which the temperature, density or magnetic field vary uniformly with height. The brightness changes are attributed to the brightness spectrum of cyclotron line emission from a narrow layer where the temperature is elevated above the surrounding part of the loop.

The detection of thermal cyclotron lines has important implications for the measurement of coronal magnetic fields. For example, a change in the magnetic field strength of only 20 Gauss produces a 170 MHz shift in the central frequency of the cyclotron line. Measurements of the wavelength or frequency of the cyclotron lines therefore provide sensitive and accurate measurements of the coronal magnetic field strength. Small regions with angular sizes θ = 10" to 30" have been observed with magnetic field strengths H = 125 to 180 Gauss.

D. PROPOSED OBSERVATIONS OF SOLAR TYPE STARS

We have completed the observations of solar type stars that were proposed in 1984; but this remains a vital aspect of our future research discussed in

Section XI. The results of a V.L.A. search for microwave emission from 32 nearby stars of late spectral type are given in paper X E. Radio emission was detected for four RS CVn stars and four dwarf M flare stars - UV Cet, AD Leo, EQ Peg and YZ Cmi.

Some general characteristics of microwave emission from dwarf M flare stars are discussed in papers VI A, VI E, and X A. These nearby stars exhibit slowly varying, circularly polarized microwave emission that is analogous to the quiescent, or non-flaring, microwave emission from solar active regions. However, brightness temperatures comparable to that of the Sun's quiescent microwave emission ($T_B \approx 10^6$ K are only obtained if the stellar emitting region is three times as large as the visible star. If the detected emission from dwarf M flare stars is due to gyroresonant emission from thermal electrons, then they must have gigantic coronal loops that vastly exceed the star in size. Alternatively, the nonthermal gyrosynchrotron emission of a small number of energetic electrons in star spots may account for the stellar microwave emission.

The dwarf M flare stars also exhibit microwave bursts that are similar to those emitted by the Sun. These bursts are part of an ongoing study using both the Very Large Array and the International Ultraviolet Explorer Satellite. Although ultraviolet bursts have been detected from YZ Cmi, most of the microwave bursts have not been detected at ultraviolet wavelengths. This suggests that the stellar bursts originate in, and are confined to, the stellar coronae. Detailed examination of the microwave bursts suggests nonthermal, coherent radiation mechanisms with brightness temperatures $T_B > 10^{15}$ K and brightness structures that change over narrow frequency intervals $\Delta\nu \approx 200$ MHz or at about 0.1 times the observing frequency.

III. VERY LARGE ARRAY OBSERVING APPLICATIONS ACCEPTED FOR 1984

1. VLA OBSERVATIONS OF HIGH ENERGY SOLAR JETS

Abstract

High resolution rocket observations of the quiet Sun at ultraviolet wavelengths have revealed the presence of energetic, small-scale transient events in the chromosphere and the transition region. We propose 2 cm VLA observations of the quiet Sun that should lead to the detection of these events. Their two-dimensional structure and magnetic field strengths may be determined. New information on the solar granulation, bright points and small ephemeral active regions will also be obtained from the proposed 2 cm observations of the transition region.

2. JOINT VLA - I.U.E. OBSERVATIONS OF FLARE STARS

Abstract

We propose simultaneous ultraviolet and radio wavelength observations of the nearby dwarf M stars YY Gem, YZ Cmi and AD Leo which are known to emit frequent and powerful flares. The combined observations will determine physical conditions such as electron temperature, electron density and magnetic field strength at a variety of levels in the stellar atmosphere. They will provide valuable new insights to such things as the difference between coronal and chromospheric flares, the flare energy budget, the flare conditions in the transition region and corona, the magnetic field strength and size of the emitter, the response of the stellar atmosphere to nonthermal events, the location of flare energy

release, and preburst heating or magnetic changes that may trigger flare emission.

3. COLLABORATIVE MULTIPLE WAVELENGTH OBSERVATIONS OF SOLAR ACTIVE REGIONS

Abstract

Collaborative multiple wavelength observations of solar active regions are proposed for the RATAN 600, WSRT and VLA telescopes. The combined data will describe the three dimensional structure of solar active regions and resolve a controversy over the radiation mechanism of coronal loops. Radio emission from the legs of magnetic loops will also be observed, and we will attempt to detect thermal cyclotron lines. Observations of solar bursts will include studies of preburst heating, magnetic field changes before and during bursts, and the evolution of solar bursts.

4. VLA OBSERVATIONS OF SLOWLY VARYING EMISSION FROM SOLAR TYPE STARS

Abstract

Main sequence stars of late spectral type exhibit variable continuum emission that has its origin in active regions in the vicinity of both star spots and chromospheric plage. We propose to observe this emission from both RS CVn and UV Ceti stars at 2 cm, 6 cm and 20 cm wavelength in order to determine the radiation mechanism and establish the physical properties of the emitter. Electron temperatures, emission measures and magnetic field strengths will be inferred. This will provide valuable information about the star spots and surface plage of solar-type stars. We will also attempt to observe thermal cyclotron lines from the RS CVn stars.

IV. PAPERS ACCEPTED FOR PRESENTATION AT PROFESSIONAL MEETINGS AND WORKSHOPS IN 1984

"Very Large Array Observations of Coronal Loops and Related Observations of Solar Type Stars", Kenneth R. Lang and Robert F. Willson, 163 Meeting of the American Astronomical Society, Las Vegas, January 9-11, 1984.

"Very Large Array Observations of Coronal Loops and Related Observations of Solar Type Stars", Kenneth R. Lang, Union Radio Scientifique International (URSI), Commission J, Special Session on Solar Radio Astronomy, Boulder, January 10-13, 1984.

"The Solar-Stellar Connection", Kenneth R. Lang, INDO-US Workshop on Solar-Terrestrial Physics, January 30-February 3, National Physical Laboratory, New Delhi, India.

"Preflare Activity in Solar Active Regions", Kenneth R. Lang and Robert F. Willson, Third Solar Maximum Mission Workshop, Goddard Space Flight Center, February 13-17, 1984.

"Short Term Prediction of Solar Bursts - Radio Wavelength Precursors", Kenneth R. Lang, Solar Terrestrial Prediction Workshop, Observatoire de Paris, Meudon, June 18-22, 1984.

"VLA Observations of Flare Build Up in Coronal Loops on the Sun and Solar Type Stars", Kenneth R. Lang and Robert F. Willson, Committee on Space Research (COSPAR) - 25th Plenary Meeting, Solar Maximum Analysis, June 25 to July 7, 1984.

V. PAPERS ACCEPTED FOR PUBLICATION IN 1984

"The Solar-Stellar Connection", Kenneth R. Lang, Proceedings of the INDO-US Workshop on Solar-Terrestrial Physics, New Delhi, India, 1984.

"Observations of Preburst Heating and Magnetic Field Changes in a 20cm Loop", Robert F. Willson, Solar Physics, (1984).

"Probable Detection of Thermal Cyclotron Lines from Small Sources within Solar Active Regions", Robert F. Willson, Solar Physics, (1984).

"Very Large Array Observations of Solar Active Regions IV. Structure and Evolution of Radio Bursts from 20 cm Loops", Robert F. Willson and Kenneth R. Lang, Astrophysical Journal, April (1984).

"Short Term Prediction of Solar Bursts - Radio Wavelength Percursors", Kenneth R. Lang, Proceedings of the Solar Terrestrial Prediction Workshop, Observatoire de Paris, Meudon, 1984.

"VLA Observations of Flare Build Up in Coronal Loops on the Sun and Solar Type Stars", Kenneth R. Lang and Robert F. Willson, Advances in Space Research, Proceedings of the 25th Plenary Meeting of COSPAR (Committee on Space Research), Pergamon Press, London, 1984.

VI. REPRINTS OF PAPERS PUBLISHED IN 1984.

A. THE SOLAR-STELLAR CONNECTION

Kenneth R. Lang

Department of Physics and Astronomy

Tufts University

Medford, MA 02155

Presented at the Second INDO-US Workshop on Solar Terrestrial Physics, January 30 to February 3, 1984, National Physical Laboratory, New Delhi, India.

ABSTRACT

Nearby main-sequence stars of late spectral type exhibit quiescent X-ray emission whose absolute luminosity may be as much as 100 times that of the Sun. This suggests that these stars have large-scale coronal loops and intense magnetic fields that are similar to those found in solar active regions. In this paper we review high resolution V.L.A. observations of the microwave emission from solar active regions, and then use the solar analogy to interpret the microwave emission of nearby dwarf M flare stars.

The three dimensional structure of solar active regions is specified using multiple wavelength V.L.A. observations. The strength, evolution and structure of the coronal magnetic field are uniquely specified. The slowly varying component of solar microwave emission is due to thermal electrons trapped within the ubiquitous coronal loops. Either bremsstrahlung or gyroresonant radiation can dominate the microwave emission, depending upon the wavelength and physical conditions in the active region.

Microwave solar bursts are attributed to the synchrotron radiation of mildly relativistic electrons. The region of particle acceleration and microwave energy release is at or near the apex of coronal loops. Twisting coronal loops, emerging coronal loops, and the interaction of coronal loops precede the emission of solar bursts. These magnetic changes may trigger the release of energetic particles from the Sun while providing the necessary magnetic energy.

Nearby dwarf M flare stars exhibit slowly varying (tens of minutes to hours), circularly polarized ($\rho_c \lesssim 30\%$) microwave emission that is analogous to the slowly varying component of microwave radiation from solar active regions. Thermal bremsstrahlung cannot explain this quiescent stellar emission; but it

can be explained by gyroresonant radiation from gigantic coronal loops that are about three times the size of the stellar photosphere. Alternatively, the slowly-varying stellar emission could be due to synchrotron radiation from smaller emitting regions.

Dwarf M flare stars emit highly polarized ($\rho_c \lesssim 100\%$), relatively brief (a few minutes) microwave bursts that are similar to those emitted by the Sun. Bright, rapid spikes from the M dwarf AD Leo have rise times of $\tau \lesssim 200$ milliseconds with 100 % left-hand circular polarization. The rise times provide an upper limit to the linear size $L < 6 \times 10^9$ cm for the emitter under the assumption that it cannot move faster than the velocity of light. Sizes that are a hundred times smaller are inferred if the Alfvén velocity is used. Provided that the source is symmetric, it has an area that is between 3×10^{-6} and 3×10^{-2} of the star's surface area, and a brightness temperature of $T_B > 10^{13}$ to 10^{17}° K. These spikes may be explained by electron-cyclotron maser emission. Microwave bursts from the Sun also occasionally exhibit highly-polarized, millisecond time structure that requires a similar coherent radiation mechanism.

I. INTRODUCTION

Nearby main sequence stars of late spectral type exhibit a variety of phenomena that are closely related to our understanding of solar active regions including dark spots, strong magnetic fields, activity cycles, and flare emission at optical, ultraviolet, radio and X-ray wavelengths. A consideration of solar active regions may therefore provide a useful background for future studies of solar-type stars. The solar analogy is, in fact, particularly relevant for the dwarf M flare stars that exhibit slowly varying quiescent, or non-flaring, microwave emission and microwave bursts that are very similar to those of solar active regions.

In this paper, we first describe high-resolution microwave observations of solar active regions, and then use the solar analogy to interpret the microwave emission of nearby dwarf M flare stars. In Section II we use multiple wavelength Very Large Array (V.L.A.) observations of the quiescent emission to specify the three dimensional structure of solar active regions. The strength, evolution, and structure of the coronal magnetic field are uniquely specified. The quiescent emission is thermal in nature. Either the bremsstrahlung or the gyroresonant radiation of the thermal electrons can dominate the microwave emission, depending upon the observing wavelength and the physical conditions in the active region. In Section III we review our V.L.A. observations of solar bursts, specifying the location of burst energy release and delineating the magnetic changes and preburst heating that precede solar bursts. The microwave bursts are themselves usually attributed to the gyrosynchrotron radiation of mildly relativistic electrons.

In Section IV we use the solar analogy to interpret the quiescent, or non-flaring, emission of nearby dwarf M flare stars. The stellar microwave emission is similar to that of solar active regions, with circularly polarized

radiation that is slowly varying on time scales of tens of minutes to hours. Thermal bremsstrahlung cannot explain the microwave emission from these stars. Gyroresonant radiation can explain the observed emission if the emitting region is about three times larger than the stellar photosphere. A smaller emitting region can occur if the radiation mechanism is the synchrotron emission of a relatively small number of energetic electrons. Microwave bursts from dwarf M flare stars are discussed in Section V. The stellar bursts are highly circularly polarized with durations of a few minutes, just as they are for the Sun. Bright, rapid, highly polarized spikes were observed during one microwave burst from AD Leo. The rise times of these spikes place stringent limits on the size of the emitting region, and indicate a coherent radiation mechanism like electron-cyclotron maser emission. Microwave bursts from the Sun also occasionally exhibit highly-polarized, millisecond fine structure that requires a coherent radiation mechanism. A summary of our observations of the microwave emission from solar active regions and nearby dwarf M flare stars is given in Section VI.

II. THE SLOWLY VARYING COMPONENT OF SOLAR MICROWAVE RADIATION

The radio emission from quiescent, or non-flaring, active regions has an intensity that is correlated with sunspot number and area. It arises at all levels within the solar atmosphere above active regions, from the chromosphere to the corona. Because this quiescent emission is only slowly varying over time scales of several hours, its detailed structure can be investigated using aperture synthesis techniques. These techniques have been employed at the Very Large Array, or V.L.A., to map different levels within the solar atmosphere with second-of-arc angular resolutions that are either better or comparable to those obtained from ground-based optical telescopes.

Synthesis maps at longer microwave wavelengths, λ, refer to higher levels within the solar atmosphere above active regions. For example, typical brightness temperatures T_B, range from $T_B \sim 10^4$ K at $\lambda = 2$ mm in the low chromosphere through $T_B \sim 10^5$ K at $\lambda = 2$ cm in the transition region to $T_B \sim 10^6$ K at $\lambda = 20$ cm in the low solar corona. At each wavelength, the synthesis maps of total intensity, I, describe the two-dimensional distribution of brightness temperature, while the synthesis maps of circular polarization, or Stokes parameter V, describe the two-dimensional structure of the magnetic field. The heights of the microwave structures can be inferred from their angular displacements from underlying photospheric features, and the two-dimensional maps at different microwave wavelengths can be combined to specify the three-dimensional structure of solar active regions.

The slowly varying component of solar microwave emission is thermal in nature, with brightness temperatures that do not normally exceed the local electron temperatures. The radiation at millimeter wavelengths is the thermal bremsstrahlung of hot, dense plasma in the chromosphere. At centimeter wavelengths the gyroresonant radiation of thermal electrons accelerated by magnetic fiel can compete with the bremsstrahlung of thermal electrons accelerated in the electric fields of ions. The dominant emission mechanism depends upon the wavelength and the physical conditions within the active regions.

The most intense emission from solar active regions at 6 cm wavelength originates in the legs of magnetic dipoles that have their footpoints in underlying sunspots. Coronal temperatures are inferred from the high brightness temperatures of $T_B \sim 10^6$ K, whereas heights h ~ 40,000 km are inferred from angular displacements from the underlying sunspots (see Figure 1 and Lang, Willson and Gaizauskas, 1983). The low electron density above

sunspots requires gyroresonance absorption if the bright 6 cm emission is to be explained (Alissandrakis, Kundu and Lantos, 1980; Pallavicini, Sakurai and Vaiana, 1980).

Gyroresonant emission in the legs of magnetic dipoles at 6 cm wavelength has been confirmed by the detection of circularly polarized horseshoe or ring shaped structures that lie above the curved magnetic fields of sunspot penumbrae (see Figure 2; Lang and Willson, 1982; and Alissandrakis and Kundu, 1982). The high degrees of circular polarization $\rho_c \sim 95\%$ of these horseshoes requires gyroresonant emission, and the structures were, in fact, predicted from the theory of gyroresonant emission of individual sunspots (Gel'freikh and Lubyshev, 1979). There is no detectable circular polarization above the central sunspot umbrae whose magnetic fields project radially upwards into the hot coronal regions. In contrast, the total intensity of the 6 cm radiation is often enhanced above the sunspot umbrae, with brightness temperatures $T_B \sim 10^6$ K.

A connection with intense magnetic fields is indicated by the high degrees of circular polarization of the microwave emission. These magnetic fields permeate every level of the solar atmosphere above active regions. In fact, magnetic loops that confine the hot coronal plasma are the dominant structural element in the solar corona. The microwave observations of circular polarization uniquely provide direct measurements of the strength and structure of these magnetic fields. Longitudinal magnetic field strengths of $H_\ell \sim 580$ Gauss are, for example, inferred from the 6 cm gyroemission that comes mainly from the third harmonic of the gyrofrequency. In fact, circular polarization maps at 6 cm wavelength act as coronal magnetograms, with the sense of circular polarization corresponding to the extraordinary mode of wave propagation (Kundu and Alissandrakis, 1975; Kundu et. al., 1977; Lang and Willson 1979, 1980). Observations of circular polarization at longer

wavelengths of λ = 12.6 cm and λ = 20 cm also act as coronal magnetograms that specify the strength and structure of the longitudinal component of the magnetic field in the low solar corona (Dulk and Gary, 1983; Lang and Willson, 1983a).

V.L.A. observations at 20 cm wavelength describe the magnetic, temperature and density structure of coronal loops. The ubiquitous coronal loops have previously only been detected during rare and expensive satellite observations at soft X-ray wavelengths (Vaiana and Rosner, 1978). Now, the loops can be routinely investigated using 20 cm V.L.A. observations (Lang, Willson and Rayrole, 1982; Lang and Willson, 1983b; McConnell and Kundu, 1983; Shevgaonkar and Kundu, 1984). The unique aspect of the 20 cm observations is that they can be used to specify the structure and strength of the magnetic field. This is not possible with any other techique, either at optical or X-ray wavelengths.

Much, if not all, of the 20 cm emission is due to the thermal bremsstrahlung of the same hot plasma that gives rise to the soft X-ray emission. Because the magnetic energy density dominates the thermal energy density in the low solar corona, this plasma usually remains trapped within the magnetic loops. Electron temperatures of T_e = 2 to 4 x 10^6 K, electron densities of N_e = 10^9 to 10^{10} cm^{-3} and loop extents L = 10^9 to 10^{10} cm are inferred from the 20 cm bremsstrahlung, while longitudinal magnetic field strenghts of H_ℓ ~ 50 Gauss are inferred from the circular polarization if it is due to propagation effects. Thermal gyroresonance emission may also play a role in the 20 cm coronal loops, and in this case stronger magnetic fields of H_ℓ ~ 200 Gauss are inferred from the polarization data.

III. MICROWAVE BURSTS FROM THE SUN - PRECURSORS AND LOCATION

Microwave bursts from the Sun are characterized by a compact (5" to 30"), circularly polarized (ρ_c = 10% to 90%) impulsive component with a brightness temperature of $T_B = 10^7$ to 10^{10} K lasting between 1 and 5 minutes. This is often followed by a larger, longer post-burst component with relatively low polarization and brightness temperature. The impulsive part of the microwave energy is usually released in the upper parts of coronal loops and between the flaring Hα kernels that mark the footpoints of magnetic loops (see Figure 5; Marsh and Hurford, 1980; Lang, Willson and Felli, 1981; Kundu and Vlahos, 1982). A nonthermal tail of electrons with energies greater than 100 KeV is created near the top of the coronal loop. Some of these electrons are trapped in the upper parts of the loop, producing the impulsive microwave bursts by synchrotron radiation. Other electrons stream down to the loop footpoints, producing hard X-ray bursts and the Hα kernels.

Changing magnetic fields within solar active regions must provide the energy source for solar bursts, or flares, and trigger their eruption (Gold and Hoyle, 1960). The location of these changes could not, however, be accurately specified from observations at optical wavelengths alone. This is because it is changes in the invisible coronal magnetic fields and temperature enhancements within coronal loops that seem to play the dominant role in the excitation of solar bursts. Theoretical considerations indicate, for example, that magnetic shear within coronal loops and interacting coronal loops can trigger solar bursts and supply their energy (Emslie, 1982; Heyvaerts, Priest and Rust, 1977; Priest, 1983; Somov and Syrovotskii, 1982; and Spicer, 1977, 1981).

Preburst activity is associated with increases in the intensity and the degree of circular polarization of the centimeter wavelength emission of solar active regions (Lang, 1974). These increases precede solar bursts on time

scales of tens of minutes to an hour. The high angular resolution provided by the V.L.A. on time intervals as short as 3.3 seconds has now shown that these increases are associated with changes in the coronal magnetic field and with preburst heating in coronal loops. (Kundu 1982, 1983; Willson, 1983, 1984; Willson and Lang, 1984).

Single coronal loops or arcades of loops often begin to heat up and change structure about fifteen minutes before the eruption of impulsive bursts. AS illustrated in Figure 7, a magnetic loop can heat up and twist in space. The magnetic shear produces a current sheet that triggers impulsive burst emission. The preburst heating shown in Figure 7 was also detected at soft X-ray wavelengths with the GOES satellite. A comparison of the X-ray and radio data (Willson, 1984) indicate a peak electron temperature of $T_e = 2.5 \times 10^7$ K and an average electron density of $N_e = 10^{10}$ cm^{-3} during the preburst heating. Preburst heating can also occur in coronal loops that are adjacent to, but spatially separated from, the sites of impulsive bursts. (Willson and Lang, 1984).

New bipolar loops can emerge and interact with preexisting ones, thereby triggering solar bursts. When the polarity of the new emerging flux differs from that of the preexisting flux, current sheets are produced that trigger the emission of bursts. A similar process can occur when preexisting adjacent loops undergo magnetic changes and trigger eruptions in nearby coronal loops.

Microwave bursts can be sequentially triggered within magnetically complex regions. As illustrated in Figure 8, successive intense bursts can be emitted from spatically separated coronal loops. Here the total intensity of the 20 cm burst emission is mapped. The polarization data indicate that the spatially separated structures are dipolar loops. In contrast to the intense bursts, the successive weaker bursts shown in the time profile were emitted from the same loop as the immediately preceding intense burst.

As illustrated in Figure 9, the ten second V.L.A. snapshot maps also reveal the apparent motion of plasma within coronal loops during solar bursts. Relatively rapid apparent velocities of about 2,000 kilometers per second are indicated. Although this speed is an order of magnitude higher than those detected spectroscopically during other bursts, it is comparable to an Alfven velocity or, perhaps, the speed of thermal conduction fronts that might excite plasma within the loop.

IV. THE SLOWLY VARYING COMPONENT OF MICROWAVE EMISSION FROM DWARF M FLARE STARS

Nearby main-sequence stars of late spectral type exhibit quiescent, or non-flaring, X-ray emission whose absolute luminosity may be as much as 100 times that of the Sun (Vaiana et. al., 1981). The X-ray radiation has generally been interpreted as the thermal bremsstrahlung of hot stellar coronae with electron temperatures $T_e \sim 10^7$ K, or an order of magnitude hotter than the Sun's corona. Because the absolute X-ray luminosity increases with stellar rotation speed (Pallavicini et. al., 1981), the brighter X-ray stars rotate faster than the Sun and could thereby generate stronger magnetic fields. In fact, surface magnetic fields of strength $H_\ell \sim 1{,}000$ Gauss covering as much as 60% of the stellar surface have been observed for several nearby main-sequence stars of late spectral type (Marcy, 1983). This suggests that these nearby stars may exhibit star spots and stellar loops that are detectable at radio wavelengths.

The solar analogy suggests that the magnetic fields and coronal plasma of other stars will be detected as slowly varying microwave emission. Nearby dwarf M stars of the UV Ceti type do, in fact, exhibit quiescent, or non-flaring, microwave emission that is slowly variable with time scales of tens of minutes to hours (Gary and Linsky, 1981; Linsky and Gary, 1983; Topka and

Marsh, 1982). The variation is not related to stellar rotation whose periods are on the order of 100 hours.

At the distance of the nearby dwarf M stars, the stellar disks have angular extents of about 10^{-3} seconds of arc. They therefore remain unresolved even with the V.L.A.; but the two components of the binary system EQ Pegasi have been detected (see Figure 10, Topka and Marsh, 1982). The slowly varying microwave emission of YZ Cmi is illustrated in Figure 11, while a summary of microwave detections is given in Table 1.

Table 1 Microwave emission from dwarf M flare stars at 6 cm wavelength

STAR	SPECTRAL TYPE	DISTANCE (parsecs)	RADIUS ($R_\odot$)	FLUX (mJy)	T_B* (°K)	Log L_x** (erg s^{-1})
χ^1 Ori	G0 + M4V	10.0	1.18	0.6	3×10^7	29.6
UV Cet	M5.6eV + M5.GeV	2.7	0.5	2.2	1×10^7	27.5
YY Gem	dM1e + dM1e	14.7	1.25	1.8	2×10^8	29.6
Wolf 630	dM4e + dM4e	6.4	0.68	1.5	1×10^8	29.3
EQ Peg	dM3.5e + dM4.5e	6.5	0.4	0.7	1×10^8	28.9
AD Leo	dM4.5e	4.9	0.5	1.5	1×10^8	29.0
YZ Cmi	dM4.5e	6.0	0.5	4.0	4×10^8	28.5

*Brightness temperature T_B assuming that the microwave emitter is equal in size to the visible stellar surface. For comparison, $T_B \sim 10^6$ K for the Sun's corona.

**The absolute X-ray luminosity is L_x. For comparison, the mean value for the Sun is $L_x = 10^{27.5}$ erg s^{-1}.

As illustrated in Table 1, brightness temperatures, $T_B \sim 10^7$ to 10^8 K are inferred if the microwave emitting source covers the entire visible surface of the star. Brightness temperatures comparable to that expected from the Sun ($T_B \sim 10^6$ K) or inferred from the absolute X-ray luminosity ($T_B \sim 10^7$ K), are obtained if the stellar emitting region is three times as large as the visible star. If this is the case, the slowly variable microwave radiation, which is often circularly polarized with $\rho_c \sim 30\%$, can be explained as the gyroresonant emission of thermal electrons spiralling in magnetic fields of strength $H_\ell \sim$ 300 Gauss. Alternatively, the gyrosynchrotron emission of a relatively small number of electrons from much smaller sources could explain the microwave emission (Linsky and Gary, 1983). Thermal bremsstrahlung is incidentally ruled out as a dominant microwave emitting mechanism, for the required electron temperatures are an order of magnitude higher than those inferred from the X-ray emission.

V. MICROWAVE BURSTS FROM DWARF M FLARE STARS

The nearby dwarf M stars of the UV Ceti type also emit X-ray flares in which the X-ray emission can increase by as much as a factor of thirty in a few minutes. This suggests that stellar active regions can undergo magnetic changes that trigger stellar microwave bursts. Microwave bursts have, in fact, been detected from nearby dwarf M stars by several observers (Spangler, et. al., 1974; Fisher and Gibson, 1982; Gary, Linsky and Dulk, 1982, and Lang et. al., 1983). The stellar microwave bursts are very similar to those emitted by the Sun, with high degrees of circular polarization $\rho_c \sim 100\%$ and relatively brief durations of a few minutes.

Recent observations of a 20 cm burst from the dwarf M star AD Leonis are of particular interest, for they indicate that the impulsive burst is emitted by a coherent radiation mechanism (Lang et. al., 1983). The highly polarized impulsive burst of a few minutes duration occurred druing the gradual rise of an

unpolarized burst that lasted about twenty minutes (see Figure 12). When the impulsive burst is examined with higher time resolution (Figure 13), a sequence of 100% left-hand circularly polarized spikes is detected. This situation is entirely analogous to the microwave bursts from solar active regions where the gradual event is interpreted as the bremsstrahlung of a high-temperature, thermal plasma and the circularly polarized impulsive emission is attributed to nonthermal radiation that typically occurs during the rise phase of a thermal burst.

The polarization did not change during the emission of successive spikes, suggesting that the magnetic field structure does not change during spike emission. A close examination of individual spikes (Figure 14) indicates that their rise times were less than the integration time of 200 milliseconds. An upper limit to the linear size, L, of the emitting region, estimated by the distance that light travels in 200 milliseconds, is $L \sim 6 \times 10^9$ cm. A more appropriate speed is the Alfven velocity of about 3,000 kilometers per second for a 300 Gauss magnetic field strength and an electron density of $N_e = 10^{14}$ cm^{-3}. If the microwave burst emission grows at the Alfven speed, then $L \sim 6 \times 10^7$ cm. A dM4.5e star like AD Leonis is expected to have a radius $R = 0.5R_\odot = 3.5 \times 10^{10}$ cm. The emitting region is therefore between 6 and 600 times smaller than the star's radius. Provided that the burst emitter is symmetric, it has an area that is between 3×10^{-6} and 3×10^{-2} of the stellar surface area, and a brightness temperature $T_B \sim 10^{13}$ to 10^{17} K.

The high brightness temperatures of the microwave spikes from AD Leonis require a coherent radiation mechanism similar to a maser. The high degrees of circular polarization $\rho_c = 100\%$ indicate that an intense magnetic field is involved in the emission process. Melrose and Dulk (1982) have attributed the high brightness temperatures and the high degrees of circular polarization of solar and stellar bursts to the masing action of electrons trapped within magnetic loops. Because radiation at the first harmonic of the gyrofrequency cannot escape from

such hot, dense plasmas, they attribute the bursts to masers operating at the second harmonic of the gyrofrequency. At our 20 cm observing wavelength, the second harmonic corresponds to a longitudinal magnetic field stregnth of H_ℓ = 250 Gauss.

We conclude this review of the solar-stellar connection by noticing that observational limitations may lead to incorrect interpretations of the microwave emission from the Sun and stars. For example, it was once thought that the quiescent microwave emission from solar active regions had a low degree of circular polarization with $\rho_c \lesssim 30\%$. This was due to beam dilution effects rather than an intrinsic property of the emitter. When the core microwave sources were eventually resolved using interferometers (Lang, 1974), it was realized that $\rho_c = 100\%$ was possible. A similar resolution problem may be occuring in the time domain, for most synthesis arrays and satellite equipment have integration times that are no shorter than a few seconds (for the V.L.A. it is 3.3 seconds). Such integration times preclude the detection of rapid, spiked emission of the AD Leonis type. They may also lead to serious underestimates of the burst flux density by averaging brief events over long time intervals.

As a matter of fact, impulsive microwave bursts from the Sun sometimes exhibit rapid, millisecond fine structure that is 100% circularly polarized (see Figures 15 and 16 and Slottje, 1978, 1980). Many of the solar spikes are shorter than the 20 millisecond integration time. If the emitting speed lies between the Alfven velocity and the velocity of light, then a 20 millisecond burst has a linear size $L = 6 \times 10^6$ to 6×10^8 cm, which is comparable to our estimates for the size of the AD Leonis microwave bursts. For the Sun, brightness temperatures of $T_B \sim 10^{15}$ K are inferred from these sizes and the observed flux densities. Coherent maser-like emission is therefore also indicated for the rapid bursts from the Sun.

VI. SUMMARY

Multiple wavelength V.L.A. observations of the Sun's slowly varying microwave emission are used to specify the three dimensional structure of solar active regions. The 6 cm radiation is emitted from the legs of magnetic dipoles, while the 20 cm radiation delineates the structure of the ubiquitous coronal loops. The microwave observations uniquely provide information on the strength and structure of the coronal magnetic field. The dominant radiation mechanism for the slowly varying microwave emission is either the gyroresonant emission of thermal electrons or thermal bremsstrahlung, depending upon the wavelength and the physical conditions in the solar active region.

V.L.A. observations of solar bursts indicate that the microwave energy is usually released near the apex of coronal loops. Preburst heating and magnetic changes precede burst emission on time scales of tens of minutes. Magnetic changes that may trigger the emission of solar bursts include magnetic shear within isolated coronal loops, emerging coronal loops, and interacting coronal loops.

Nearby dwarf M stars emit slowly varying microwave emission that is similar to that emitted by solar active regions. Brightness temperatures of $T_B \sim 10^7$ to 10^8 K are inferred if the stellar microwave emitter covers the entire visible surface of the star. The electron temperatures inferred from the stellar X-ray luminosities are an order of magnitude lower than these brightness temperatures. Gyroresonant emission from gigantic stellar loops or gyrosynchrotron emission from smaller star spots may explain the slowly varying microwave emission from dwarf M stars.

These stars also emit microwave bursts that are similar to their solar counterparts. The impulsive component of a burst from the dwarf M star AD Leonis consisted of rapid, highly polarized spikes that are attributed to an electron-cyclotron maser. Linear sizes of $L \sim 6 \times 10^7$ to 6×10^9 cm and brightness temperatures of $T_B \sim 10^{13}$ to 10^{17} K are inferred for the emitter. Very similar sizes and brightness temperatures have been inferred for millisecond fine structure

during some microwave bursts from the Sun. Observational constraints may lead to incorrect conclusions regarding the polarization, flux density and temperatures of solar and stellar bursts.

ACKNOWLEDGMENTS

The research leading up to this review was done in collaboration with Robert F. Willson at Tufts University. Radio astronomical studies of the Sun and other active stars at Tufts University are supported under grant AFOSR-83-0019-B with the Air Force Office of Scientific Research.

REFERENCES

Alissandrakis, C.E. and Kundu, M.R. 1982, Ap. J. (Letters), 253, L49.

Alissandrakis, C.E., Kundu, M.R., and Lantos, P. 1980, Astr. Ap., 82, 30.

Dulk, G.A., and Gary, D.E. 1983, Astr. Ap., 124, 103.

Emslie, A.G. 1982, Ap. Lett. 22, 41.

Fisher, P.L., and Gibson, D.M. 1982, in Second Cambridge Workshop on Cool Stars, Stellar Systems and the Sun, ed. M.S. Giampapa and L. Golub (Smithsonian Observatory Special Report No. 392), pp. 109-114.

Gary, D.E., and Linsky, J.L. 1981, Ap. J., 250, 284.

Gary, D.E., Linsky, J.L., and Dulk, G.A. 1982, Ap. J. (Letters), 263, L79.

Gel'freikh, G.B., and Lubyshev, B.I. 1979, Soviet Astr. - A.J., 23, 316.

Gold, T., and Hoyle, F. 1960, M.N.R.A.S., 120, 89.

Heyvaerts, J., Priest, E.R., and Rust, D.M. 1977, Ap. J., 216, 123.

Kundu, M.R. 1982, Rep. Prog. Phys., 45, 1435.

Kundu, M.R. 1983, Solar Phys., 86, 205.

Kundu, M.R., and Alissandrakis, C.E. 1975, Nature, 257, 465.

Kundu, M.R., et. al. 1977, Ap. J., 213, 278.

Kundu, M.R., and Vlahos, L. 1982, Space Sci. Rev., 32, 405.

Lang, K.R. 1974, Solar Phys., 36, 351.

Lang, K.R., and Willson, R.F. 1979, Nature, 278, 24.

Lang, K.R., and Willson, R.F. 1980, in I.A.U. Symposium 86, Radio Physics of the Sun, ed. M.R. Kundu and T.E. Gergely (Dordrecht: Reidel), p. 109.

Lang, K.R., and Willson, R.F. 1982, Ap. J. (Letters), 255, L111.

Lang, K.R., and Willson, R.F. 1983a, Astr. Ap., 127, 135.

Lang, K.R., and Willson, R.F. 1983b, in Adv. Space Res. Proc. XXIV COSPAR (Pergamon: London), p. 91-100.

Lang, K.R., Willson, R.F., and Gaizauskas, V. 1983, Ap. J., 267, 455.

Lang, K.R., Willson, R.F., and Felli, M. 1981, Ap. J., 247, 338.

Lang, K.R., Willson, R.F., and Rayrole, J. 1982, Ap. J., 258, 384.

Lang, K.R., Bookbinder, J., Golub, L. and Davis, M.M. 1983, Ap. J. (Letters), 272, L15.

Linsky, J.L., and Gary, D.E. 1983, Ap. J., 274, 776.

Marcy, G.W. 1983, in I.A.U. Symposium 102, Solar and Stellar Magnetic Fields: Origins and Coronal Effects, ed. J.O. Stenflo (Dordrecht: Reidel).

Marsh, K., and Hurford, G.J. 1980, Ap. J. (Letters), 240, L111.

McConnell, D., and Kundu, M.R. 1983, Ap. J. 269, 698.

Melrose, D.B., and Dulk, G.A. 1982, Ap. J., 259, 844.

Pallavicini, R., Sakurai, T., and Vaiana, G.S. 1981, Astr. Ap., 98, 316.

Pallavicini, R. et. al. 1981, Ap. J., 248, 279.

Priest, E.R. 1983, Solar Phys., 86, 33.

Shevgaonkar, R.K., and Kundu, M.R., 1984, Ap. J. 283, 413.

Spangler, S.R., Rankin, J.M. and Shawhan, S.D. 1974, Ap. J. (Letters), 194, L43.

Somov, B.V., and Syrovotskii, S.I. 1982, Solar Phys., 75, 237.

Spicer, D.S. 1977, Solar Phys., 53, 305.

Spicer, D.S. 1981, Solar Phys., 70, 149.

Topka, K., and Marsh, K.A. 1982, Ap. J., 254, 641.

Vaiana, G.S., and Rosner, R. 1978, Ann. Rev. Astr. Ap., 16, 393.

Vaiana, G.S., et. al. 1981, Ap. J., 244, 163.

Willson, R.F. 1983, Solar Phys., 83, 285.

Willson, R.F. 1984, Solar Phys., to be published.

Willson, R.F. and Lang, K.R. 1984, Ap. J., 279, 427.

FIGURE LEGENDS

Fig. 1. A V.L.A. synthesis map of the total intensity, I, of the 6 cm radiation superimposed upon an off-band Hα photograph of the same active region taken at the Ottawa River Solar Observatory on the same day. The largest component of 6 cm emission has an angular extent of about 60". The two components of 6 cm emission are displaced inward away from the oppositely polarized sunspots as would be expected if they originate in the higher-lying legs of the magnetic loops that join the sunspots. An inward displacement of 25" corresponds to a height of h ~ 40,000 km above the sunspots. The peak brightness temperature of the two 6 cm sources is $T_B \sim 10^6$ K, which occurs above the sunspot umbrae.

Fig. 2. a V.L.A. synthesis map of circular polarization, V, of the 6 cm radiation superimposed upon an off-band Hα photograph of the same active region taken at the Big Bear Solar Observatory on the same day. The angular scale is denoted by the 60" spacing between the fiducial marks on the axes. There is no detectable circular polarization above the sunspot umbrae where the magnetic fields are strong and nearly vertical. The polarized emission is concentrated above the penumbrae, where the magnetic field lines are curved with a sharp gradient. The contours of the V map mark levels of equal brightness temperature corresponding to 0.3, 0.4, ...0.9 times the maximum brightness temperatures of $+3.0 \times 10^5$ K and -2.8×10^5 K.

Fig. 3. A V.L.A. synthesis map of the total intensity, I, of the 20 cm radiation from a coronal loop that joins sunspots of opposite magnetic polarity. The active region was located 20 degrees across the solar surface from the east limb, thereby accounting for the eastward (left) projection of the loop. Here the contours mark levels of equal brightness temperature corresponding to 0.2, 0.4, ...1.0 times the maximum brightness temperature of $T_B = 2 \times 10^6$ K.

Fig. 4. A V.L.A. synthesis map of the total intensity, I, of the 20 cm emission from a coronal loop. The contours mark levels of equal brightness temperature corresponding to 0.2, 0.4, ...1.0 times the maximum brightness temperature of $T_B = 2 \times 10^6$ °K. A schematic portrayal of the 6 cm emission, which comes from the legs of the magnetic loops, has been added together with the underlying sunspots that are detected at optical wavelengths.

Fig. 5. A ten second V.L.A. synthesis map of a solar burst at 6 cm wavelength superimposed upon an Hα photograph taken at the same time at the Big Bear Solar Observatory. The contours mark levels of equal brightness temperature corresponding to 5.5×10^6, 1.1×10^7, ...3.8×10^7 K. The microwave energy is released in a large part of the top of the dipolar loop, while the Hα kernels are emitted at the footpoints of the loop.

Fig. 6. The ten second V.L.A. synthesis maps of the impulsive phase of two solar bursts at 20 cm wavelength superimposed on Hα photographs of the optical flares taken at the same time at the Big Bear Solar Observatory. The 20 cm bursts originate near the tops of coronal loops that are about 40,000 km above the flaring region seen at optical wavelengths. The western solar limb is visible in both photographs.

Fig. 7. The time profile of a solar burst at 20 cm wavelength illustrates heating within a coronal loop prior to the emission of two impulsive bursts. The 20 cm V.L.A. synthesis maps for ten second intervals are given below. The angular scale can be inferred from the 60" spacing between fiducial marks on the axes. The maps show that the coronal loop twisted in space, producing magnetic shear that led to impulsive burst emission from the same loop. This emission triggered a second burst from an adjacent source.

Fig. 8. The time profile of successive impulsive bursts at 20 cm wavelength is compared with ten second V.L.A. synthesis maps at the same wavelength. Here the countour intervals are in steps of 1.0×10^7 K and the angular scale can be inferred from the 30" spacing between fiducial marks on the axes.

Fig. 9. A series of ten second snapshot maps of the total intensity, I, of an impulsive burst at 20 cm wavelength. The outermost contour and the contour interval are both equal to 1.3×10^6 K. The angular scale is determined by the 30" spacing between the fiducial marks on the axes.

Fig. 10. A V.L.A. synthesis map of the total intensity, I, of the 6 cm emission from the binary star system EQ Pegasi. Both components of the binary are dwarf M stars. The optical positions are indicated by the dots, and the synthesized beam is shown in the lower lefthand corner (adopted from Topka and Marsh, 1982).

Fig. 11. The total flux density and circular polarization at 6 cm wavelength for a three hour observation of the dwarf M flare star YZ Cmi. This data was obtained by adding the signals from all of the interferometric baselines of the V.L.A.. It shows that YZ Cmi has showly varying emission over time scales of tens of minutes. A relatively brief, highly circularly polarized, impulsive burst was detected near the beginning of this observation.

Fig. 12. The 20 cm radiation detected with two independent circularly polarized receivers, while tracking the dwarf M flare star AD Leo at the Arecibo Observatory. The slow decline in signal that is continued with a dashed line is due to a reduction in ground radiation as the line feed nears the center of the dish. A left circularly polarized impulsive burst is superimposed upon an unpolarized gradual burst of greater duration. The impulsive burst is shown in greater detail in Fig. 13.

Fig. 13. The impulsive burst shown in Fig. 12 on a greatly expanded time scale. It is composed of a sequence of rapid spikes which are all 100% left-hand circularly polarized. The time profiles of the spikes denoted by the numbers 1, 2 and 3 are given in Fig. 14.

Fig. 14. Time profiles of the spikes marked 1, 2 and 3 in Fig. 13. The digital sampling rate was 100 milliseconds, the integration time was 200 milliseconds, and the distance between fiducial marks on the time axis is 500 milliseconds.

Fig. 15. Rapid, spiked emission with millisecond fine structure is superimposed on this longer solar burst at 11.3 cm wavelength. The rapid structure is shown in greater detail in Fig. 16 (adapted from Slottje, 1980).

Fig. 16. A sequence of rapid spikes during a solar burst at 11.3 cm wavelength. They are all 100% left-hand circularly polarized, and have durations of 50 milliseconds or less (adapted from Slottje, 1980).

Fig. 1

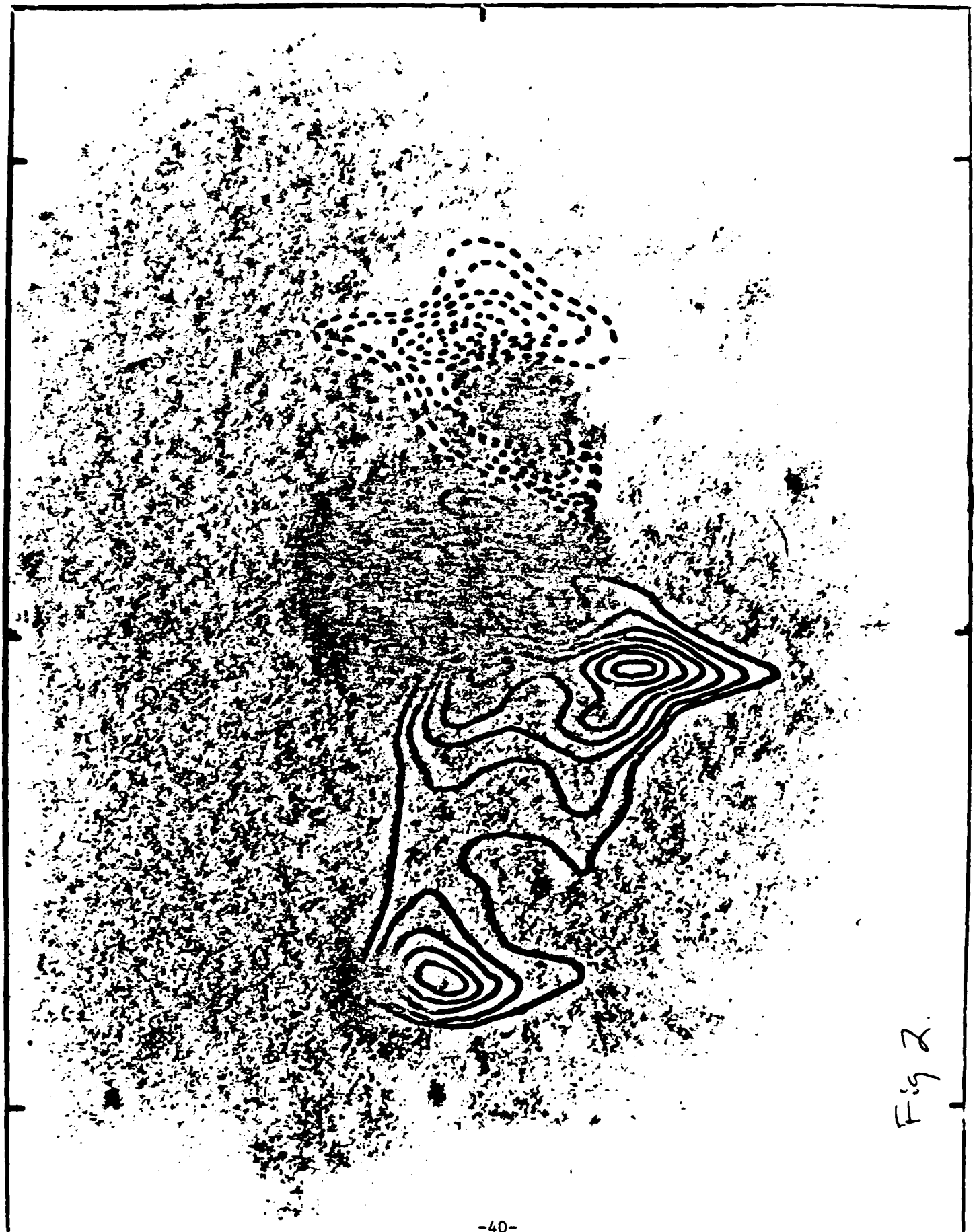

Fig 2.

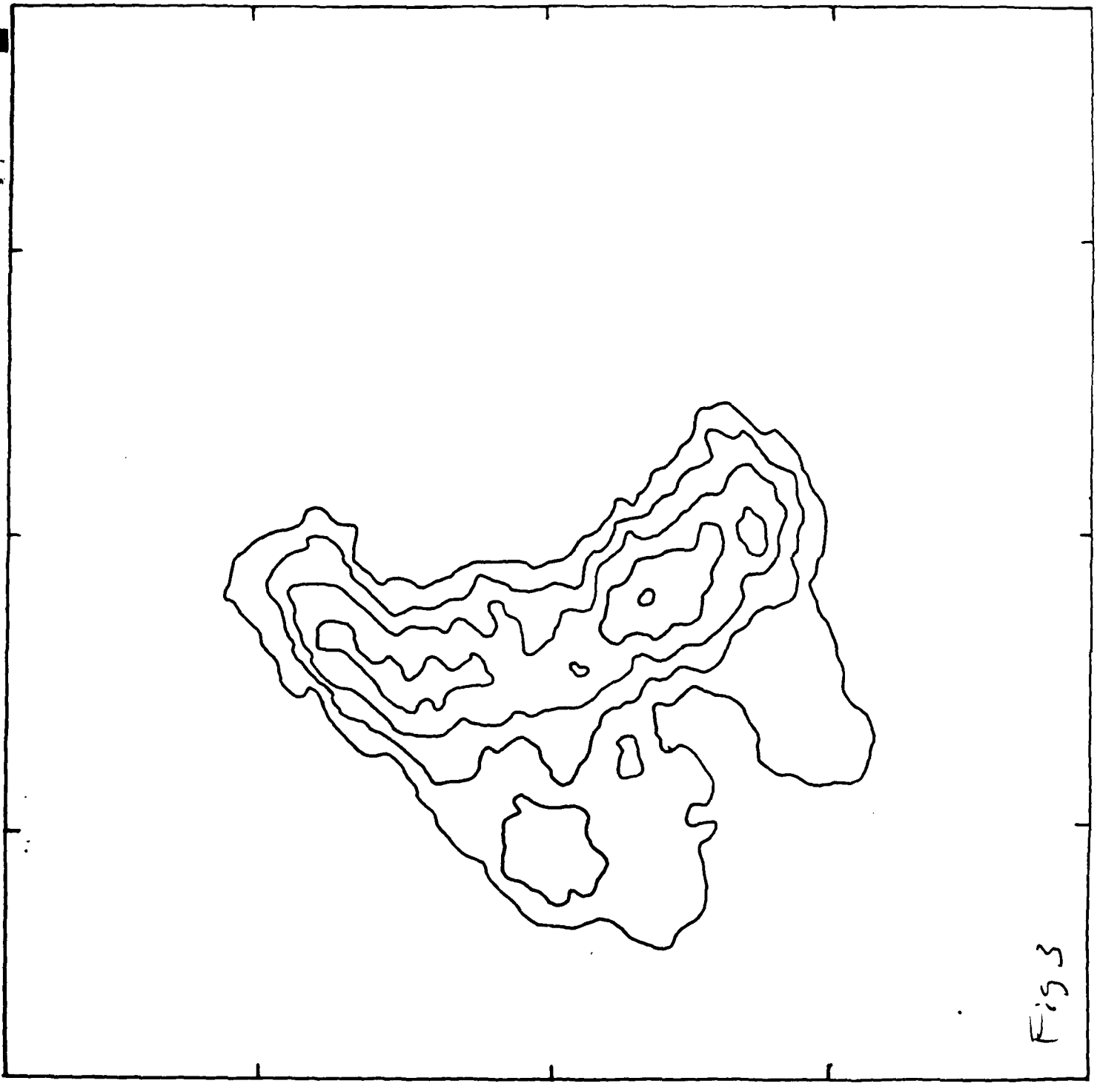

Fig 3

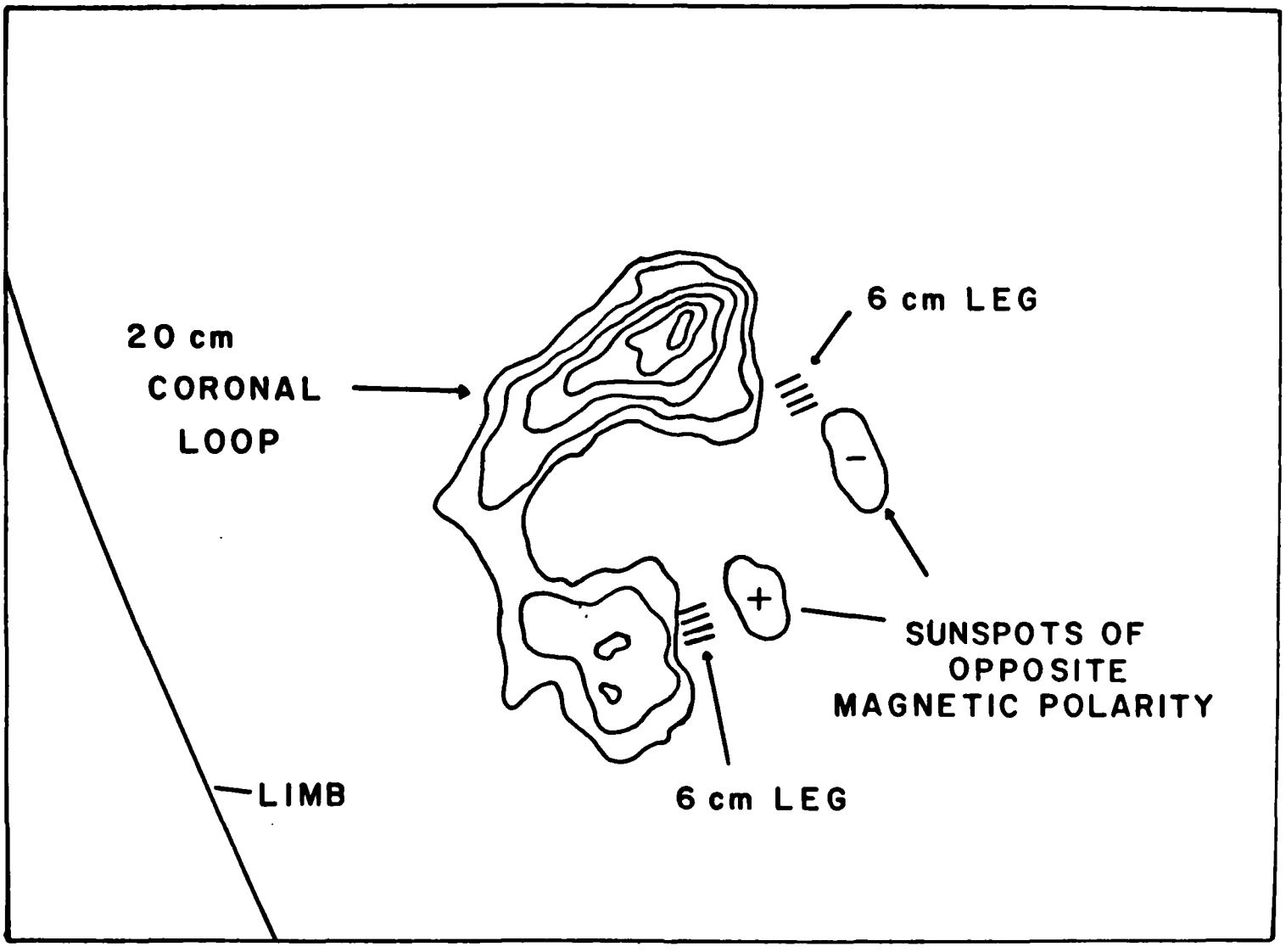
20 cm
CORONAL
LOOP
6 cm LEG
−
+
SUNSPOTS OF
OPPOSITE
MAGNETIC POLARITY
LIMB
6 cm LEG

Fig 4

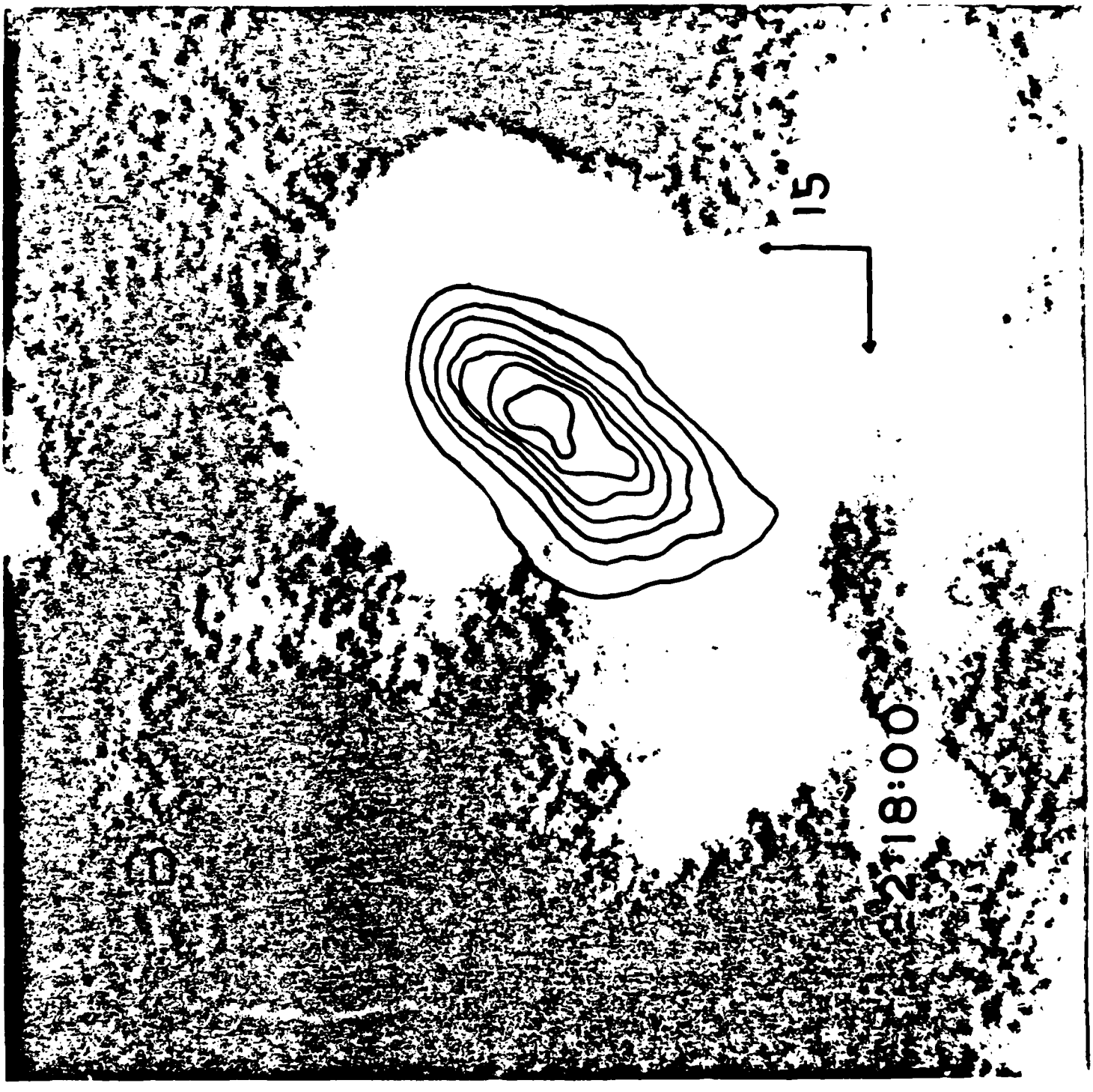

Fig 7

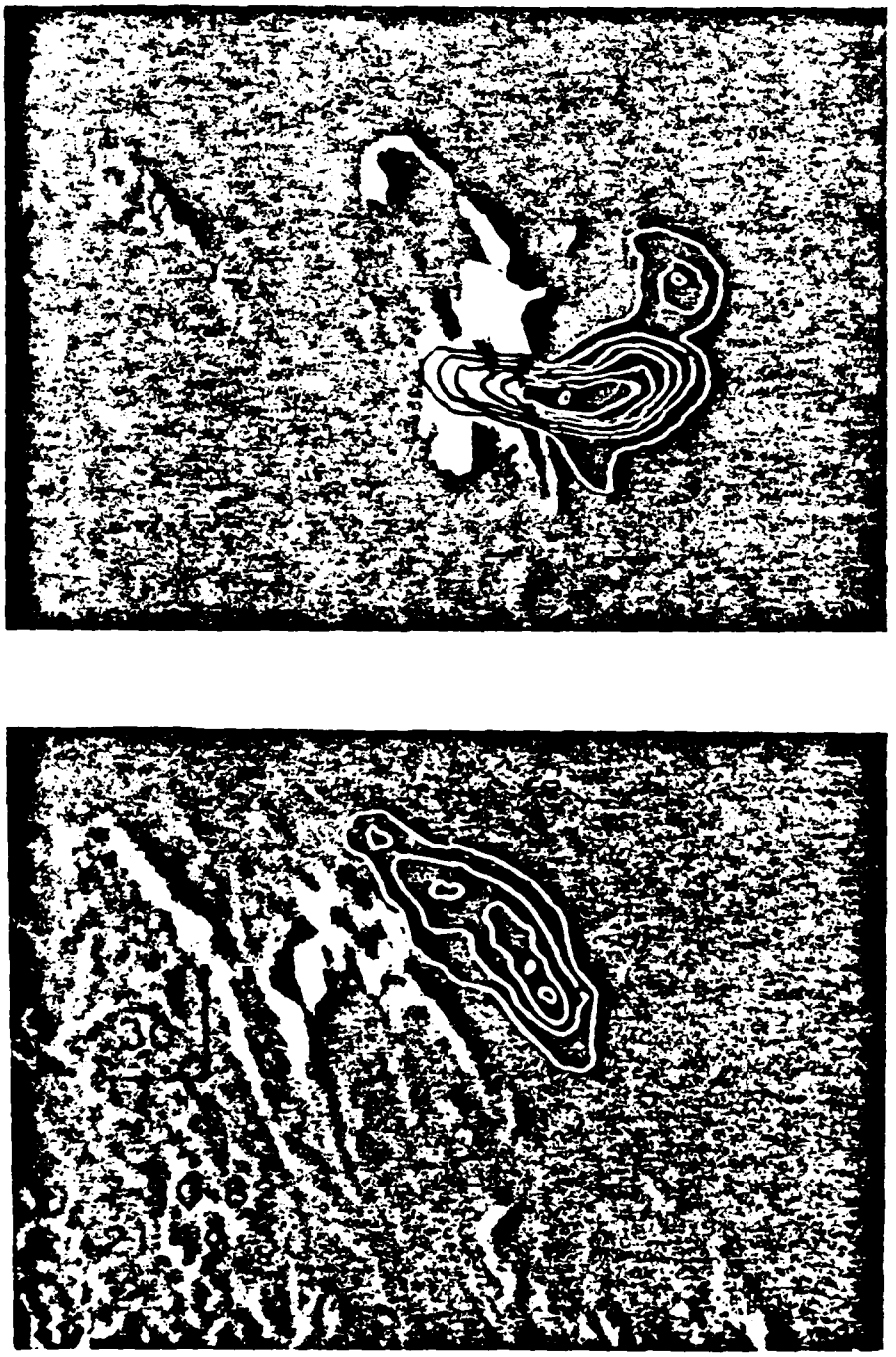

Fig. 6.

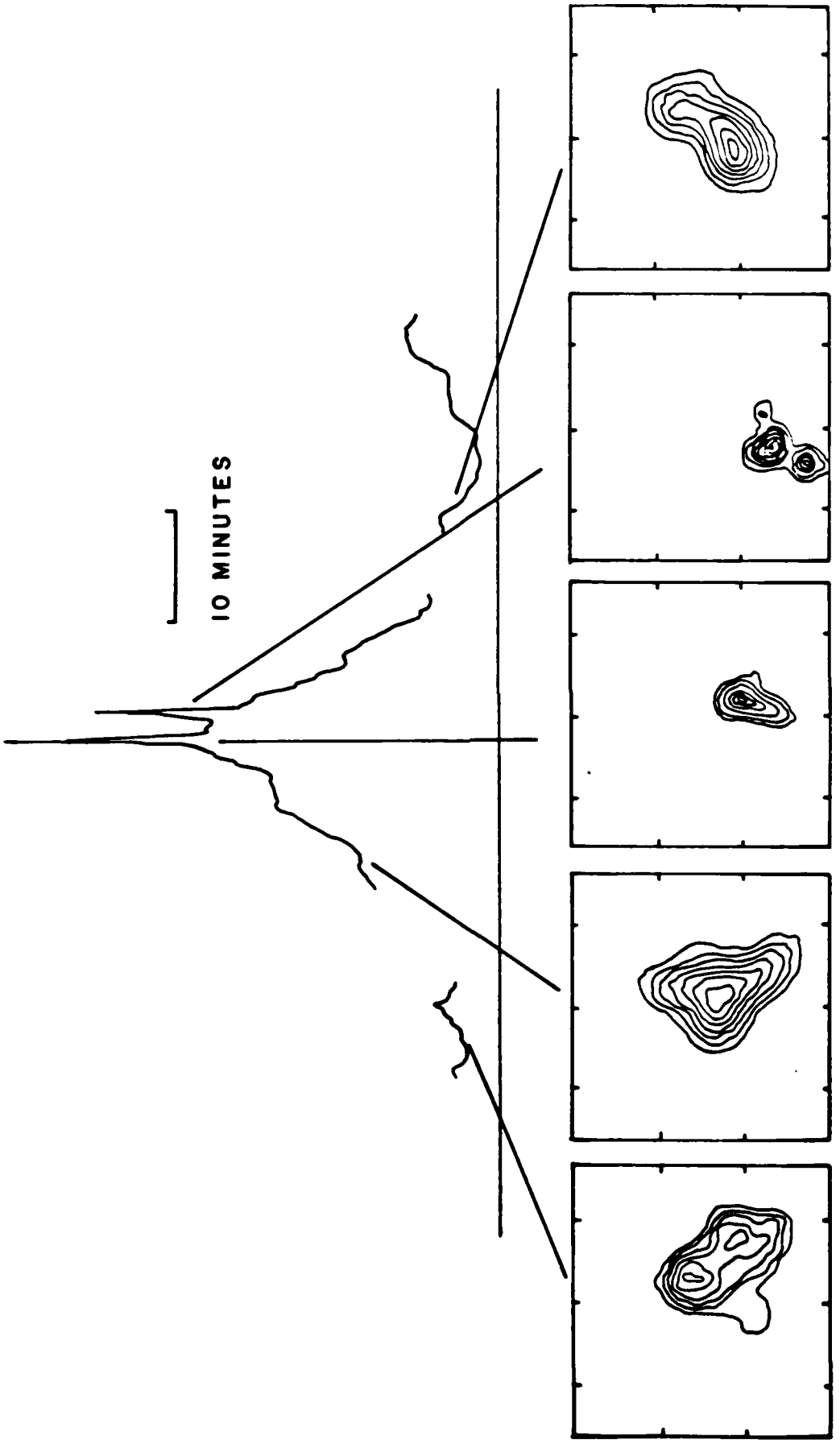

Fig 7

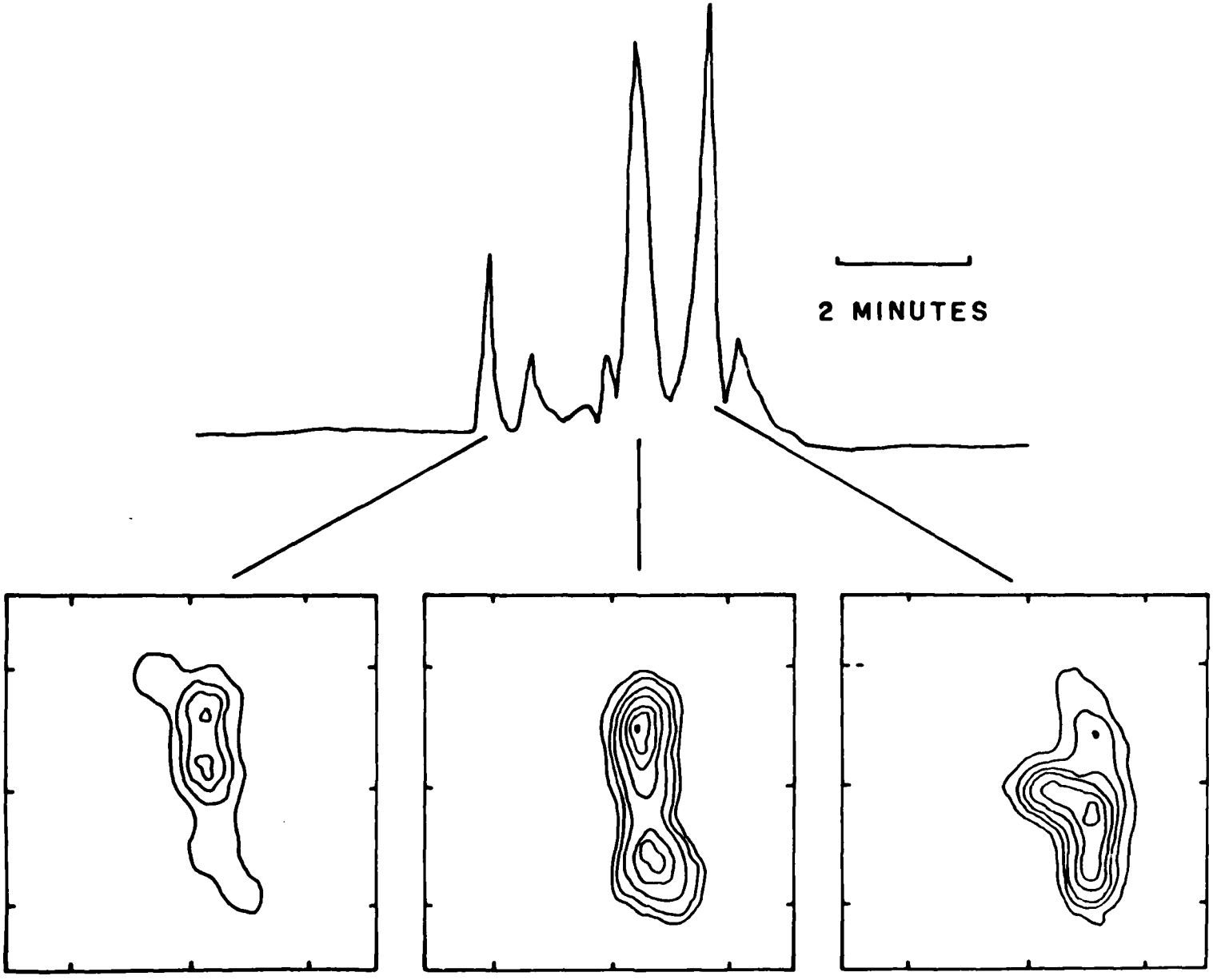

Fig 8

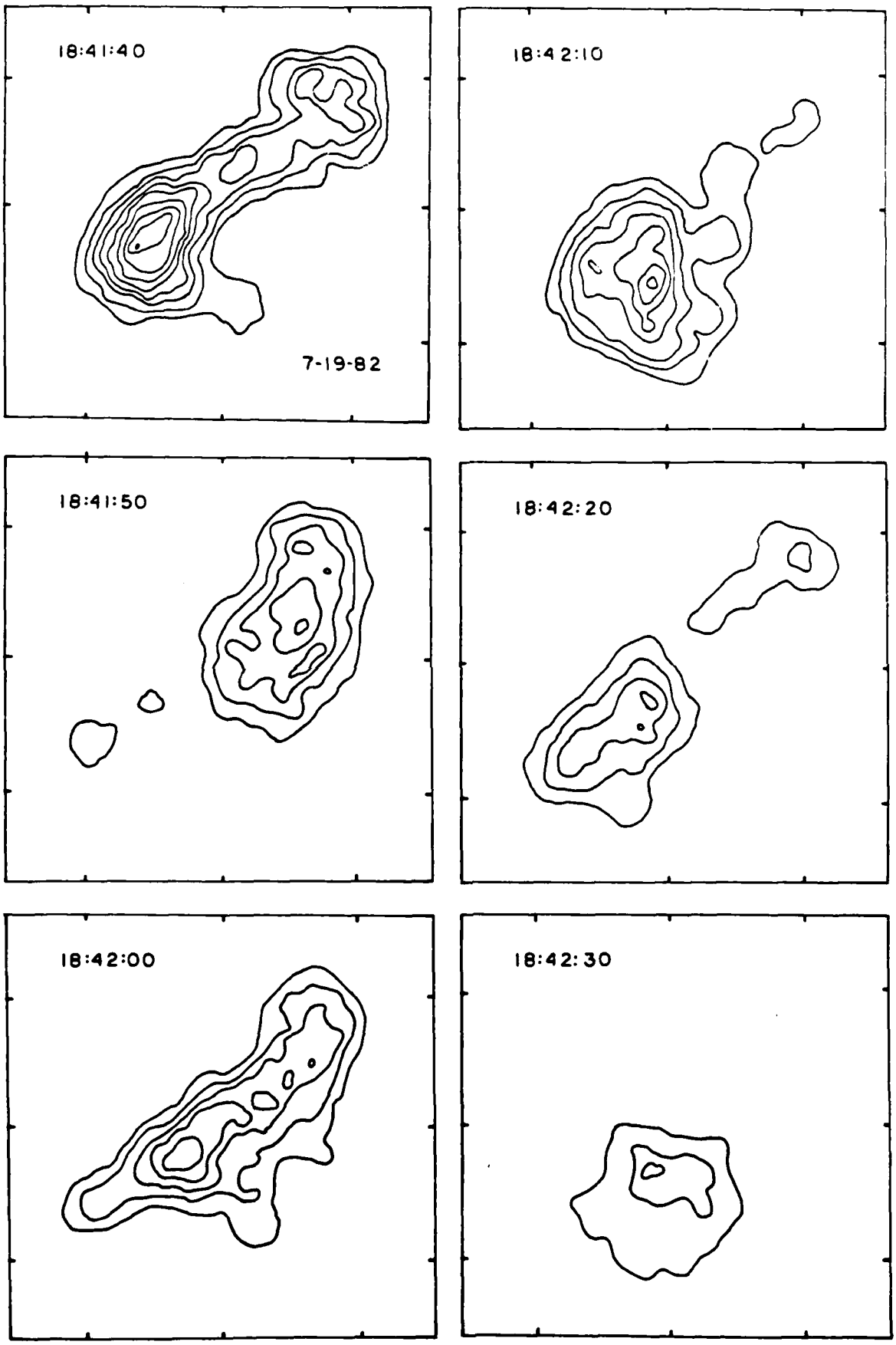

Fig 9

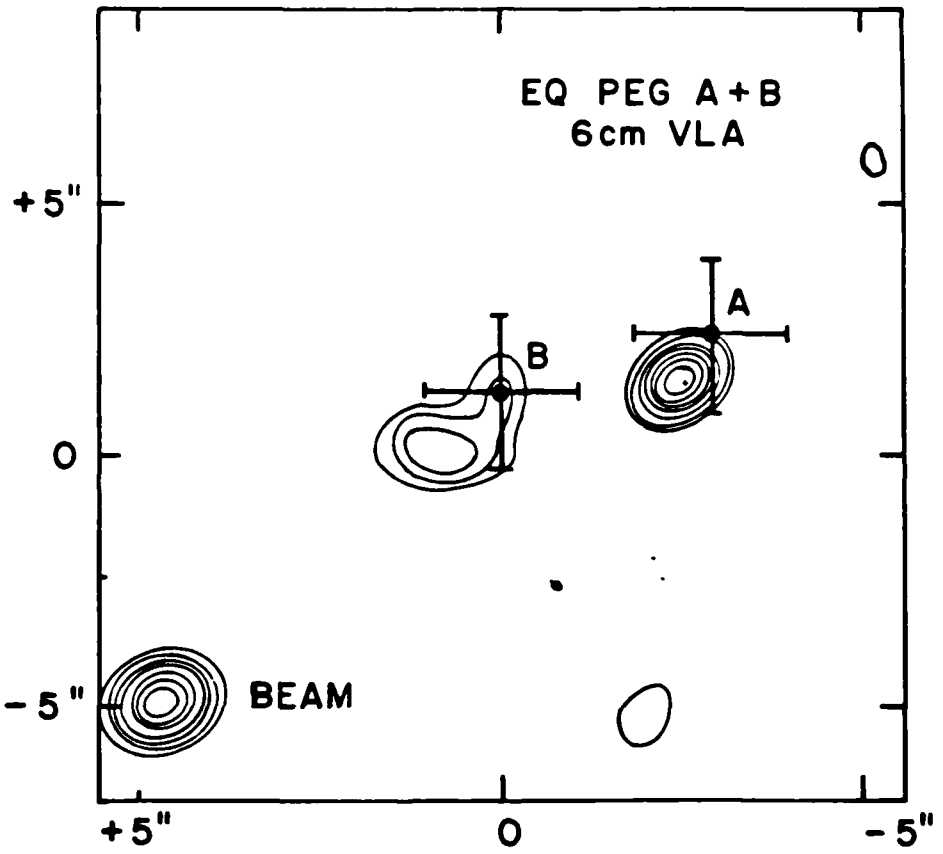

Fig. 10

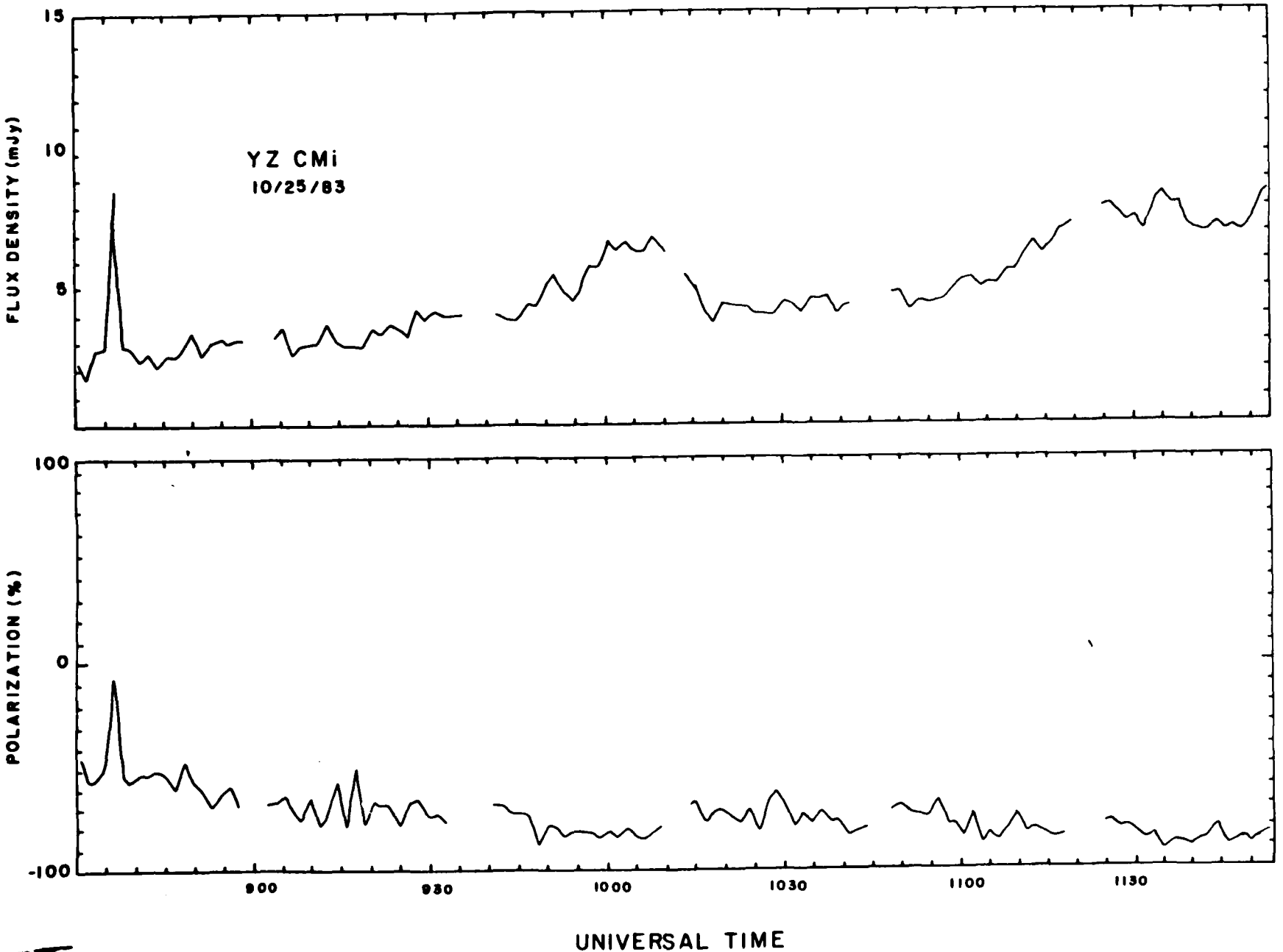
YZ CMi
10/25/83
FLUX DENSITY (mJy)
15
10
5
POLARIZATION (%)
100
0
-100
900
930
1000
1030
1100
1130
UNIVERSAL TIME

Fig. 11

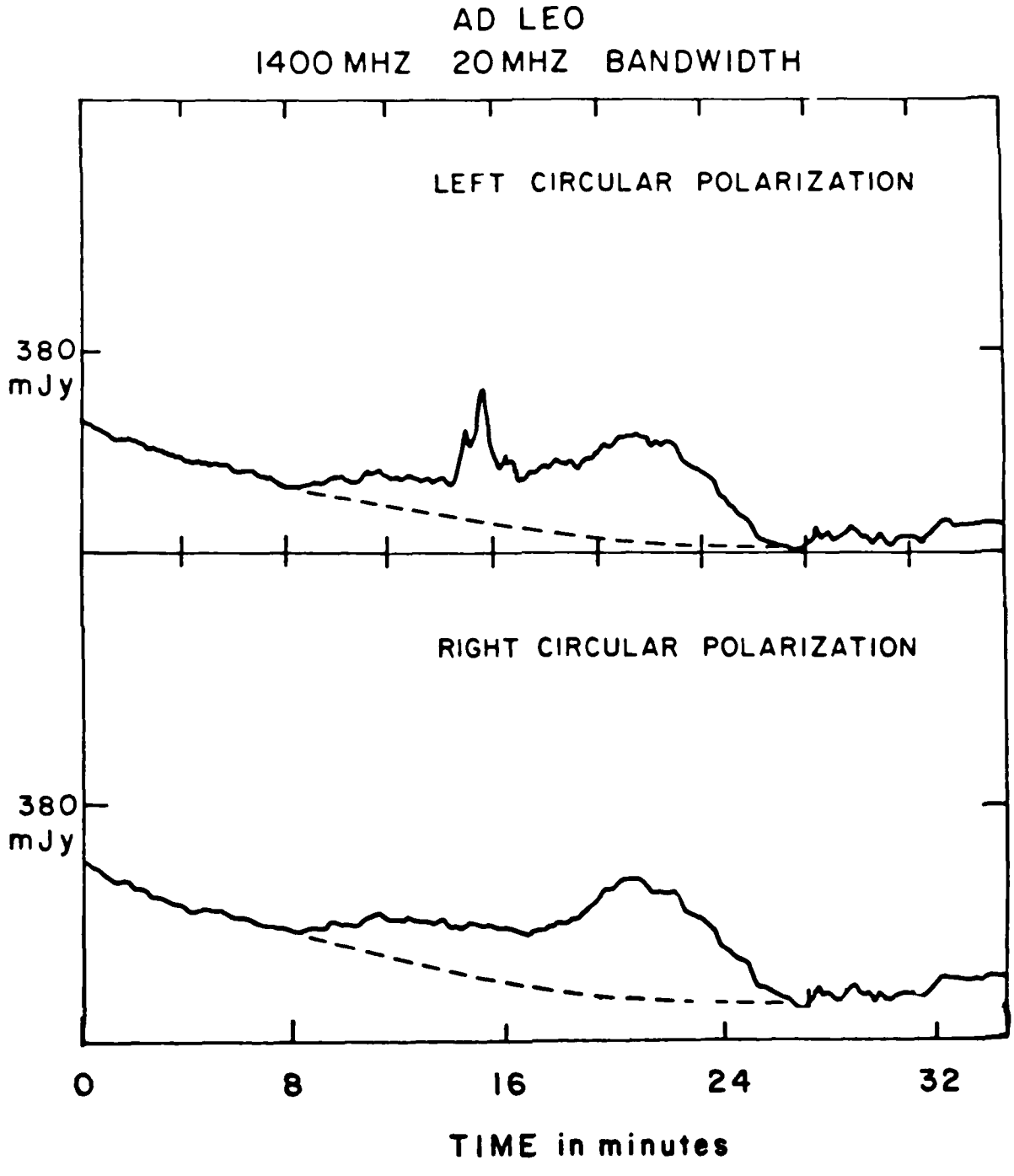
AD LEO
1400 MHZ 20 MHZ BANDWIDTH
LEFT CIRCULAR POLARIZATION
380
mJy
RIGHT CIRCULAR POLARIZATION
380
mJy
0
8
16
24
32
TIME in minutes

Fig. ~~12~~ 12

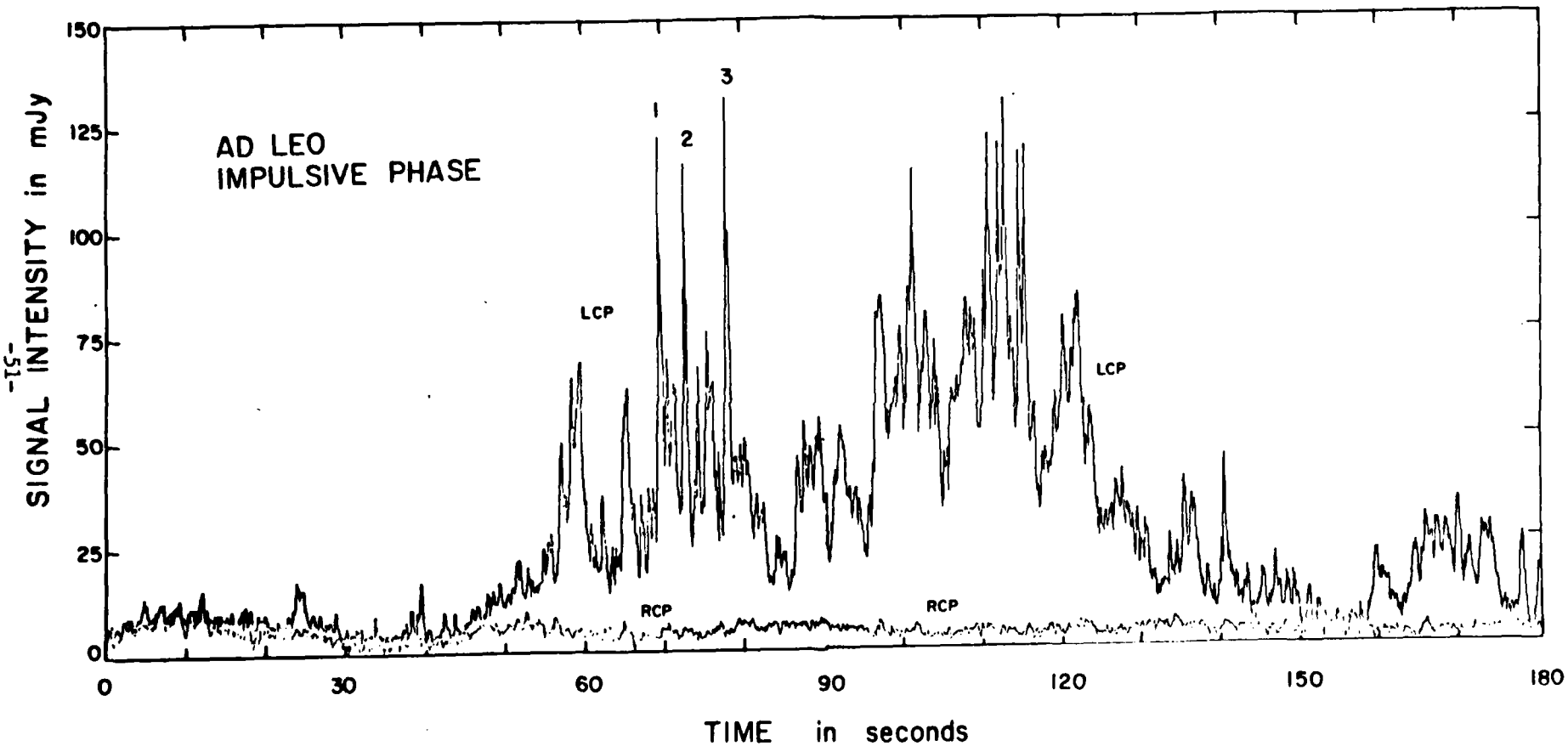
AD LEO
IMPULSIVE PHASE
SIGNAL INTENSITY in mJy
-51-
150
125
100
75
50
25
0
1
2
3
LCP
LCP
RCP
RCP
0
30
60
90
120
150
180
TIME in seconds

Fig 1&3

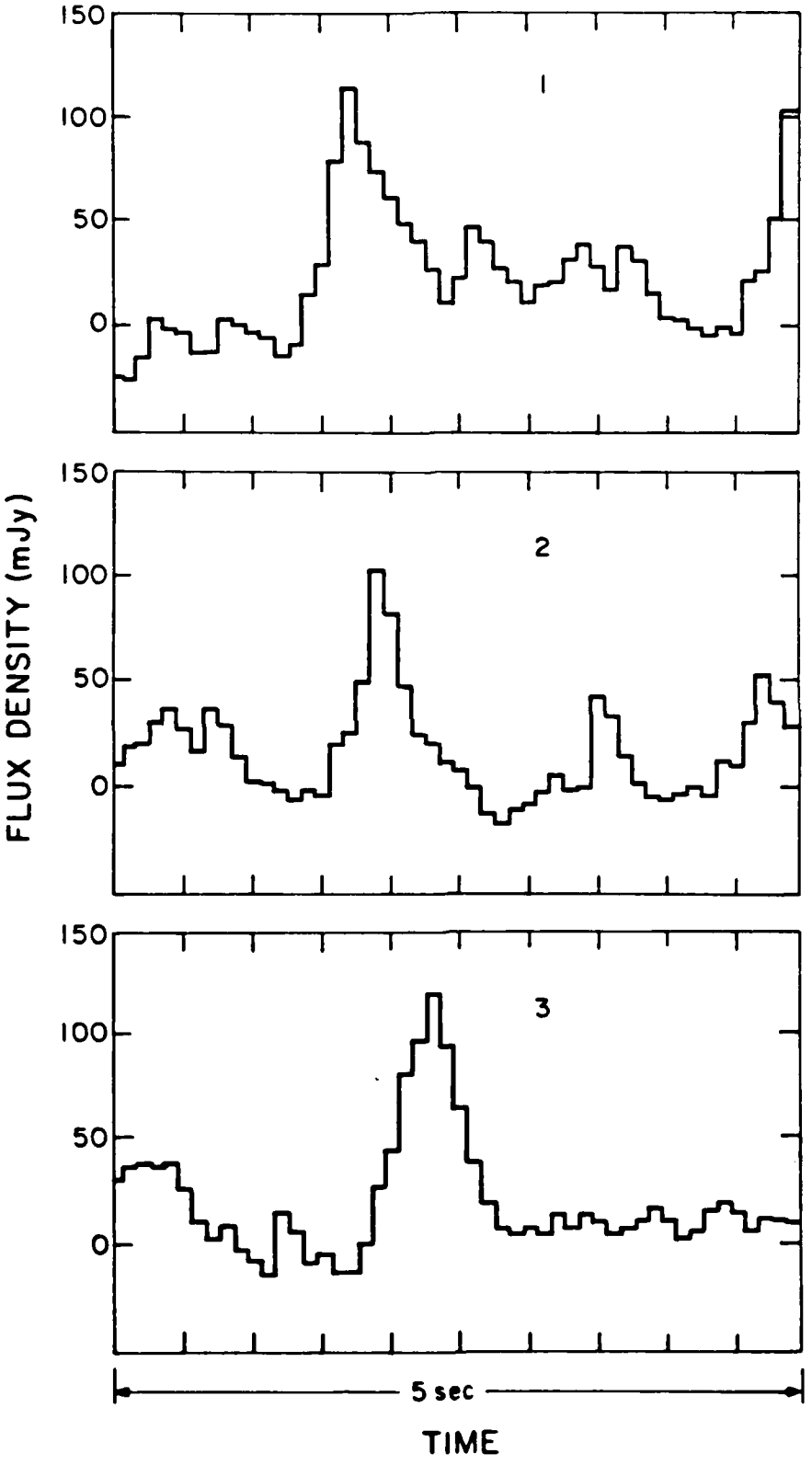

Fig. 15

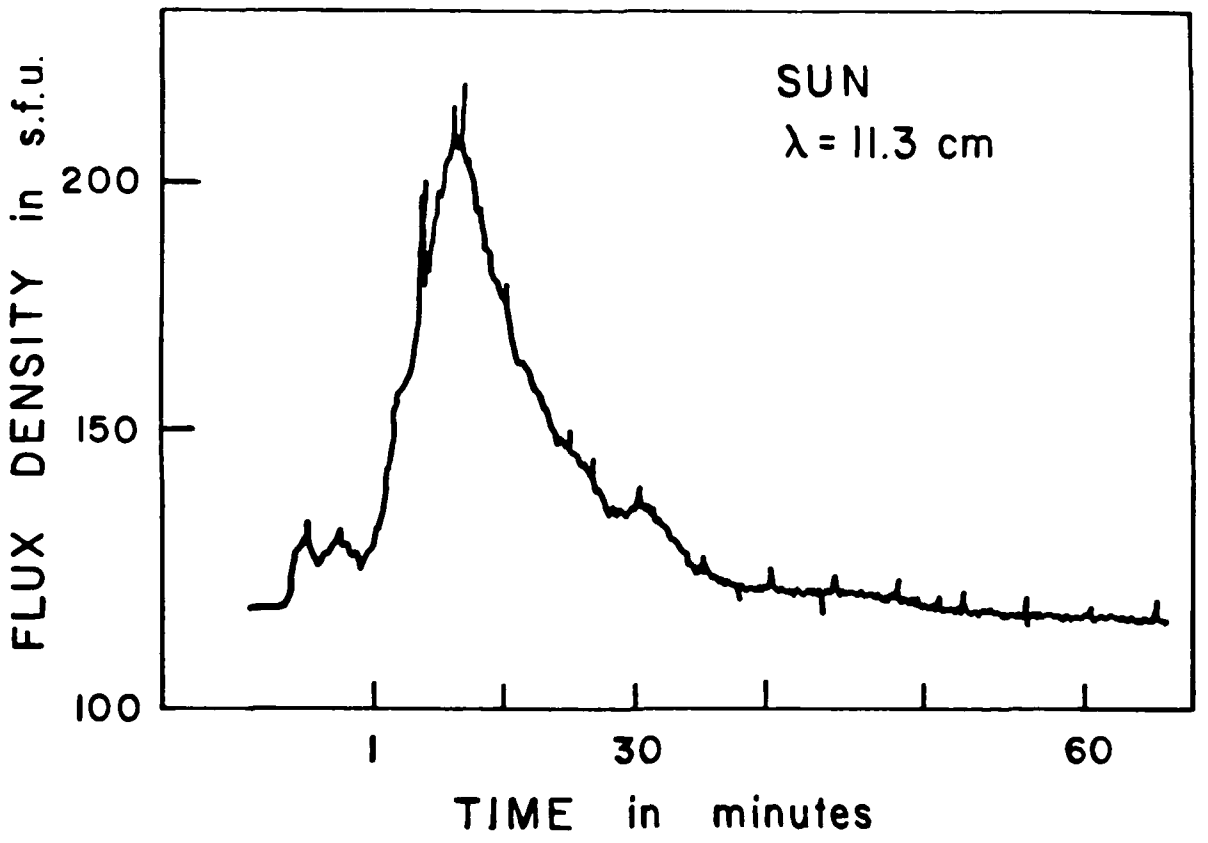
SUN
λ = 11.3 cm
FLUX DENSITY in s.f.u.
200
150
100
1
30
60
TIME in minutes

Fig. 15

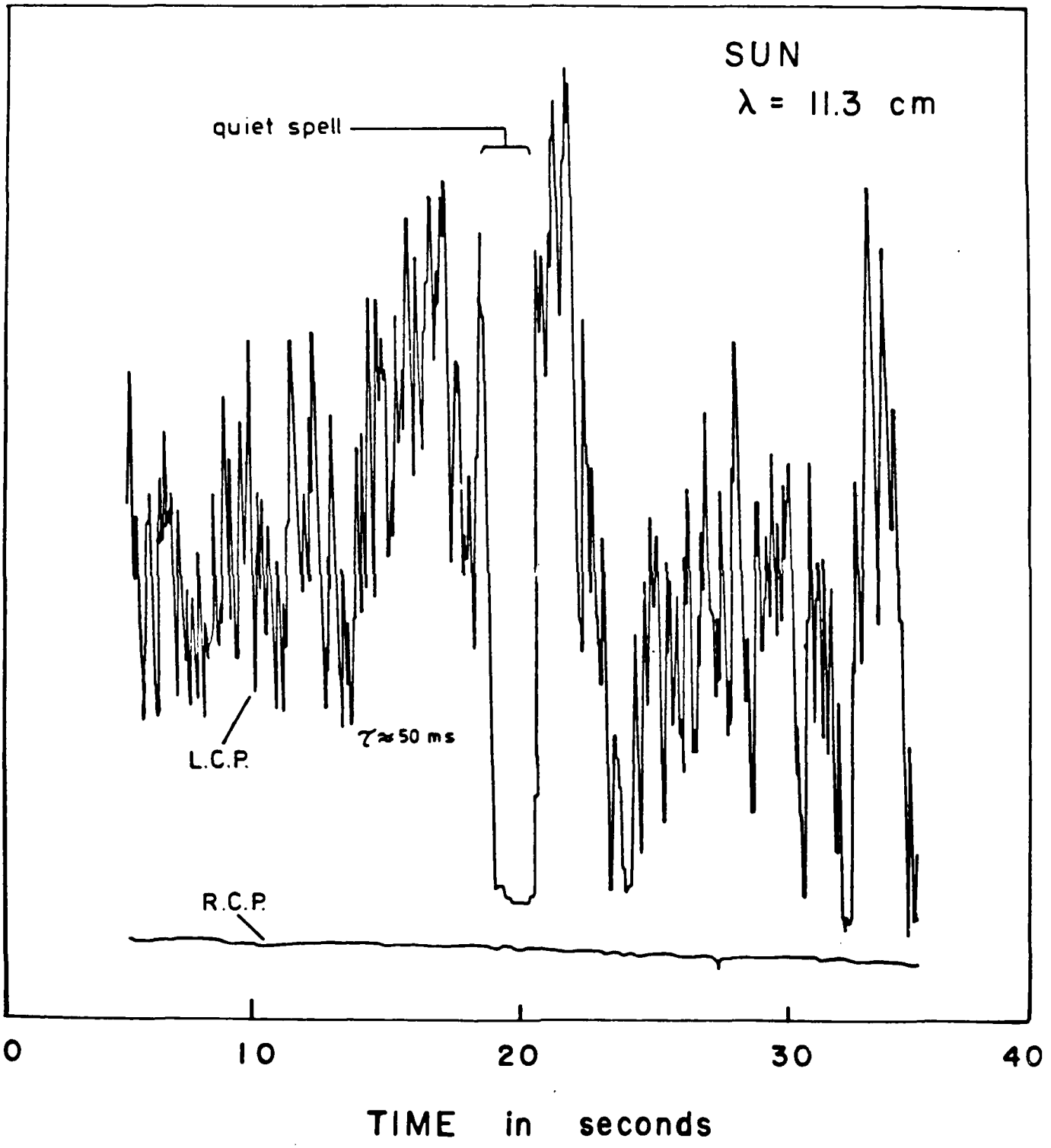
SUN
λ = 11.3 cm
quiet spell
L.C.P.
τ≈50 ms
R.C.P.
0
10
20
30
40
TIME in seconds

Fig VI

B. OBSERVATIONS OF PREBURST HEATING AND MAGNETIC FIELD CHANGES IN A CORONAL LOOP AT 20 cm WAVELENGTH

ROBERT F. WILLSON

Department of Physics, Tufts University, Medford, MA 02155, U.S.A.

(Received 12 December, 1983; in revised form 27 February, 1984)

Abstract. The Very Large Array (VLA) has been used at 20 cm wavelength to study the evolution of a burst loop with 4″ resolution on timescales as short as 10 s. The VLA observations show that the coronal loop began to heat up and change its structure about 15 min before the eruption of two impulsive bursts. The first of these bursts occurred near the top of the loop that underwent preburst heating, while the second burst probably occurred along the legs of an adjacent loop. These observations evoke flare models in which coronal loops twist, develop magnetic instabilities and then erupt. We also combine the VLA observations with GOES X-ray data to derive a peak electron temperature of $T_e = 2.5 \times 10^7$ K and an average electron density of $N_e \approx 1 \times 10^{10}$ cm^{-3} in the coronal loop during the preburst heating phase.

1. Introduction

High resolution VLA observations of centimeter radio bursts have recently provided a wealth of new information about the flare emission process. Of special interest are the changes in both intensity and circular polarization which are sometimes observed on timescales of minutes to tens of minutes before the onset of the impulsive phase. These changes are thought to be related to preburst heating and the reorientation or emergence of magnetic flux in coronal loops. Willson (1983), for example, recently observed a coronal loop that began to heat up about 2 min before the eruption of one 6 cm burst. By comparing the preburst VLA snapshot maps with the locations of the Hα flare kernels, he argued that the loop was heated in the legs, rather than at the top where the impulsive energy release took place. Kundu *et al.* (1982) have also observed an active region in which a quadruple magnetic loop structure may have emerged a few tens of seconds before a 6 cm burst, and which they believe may be related to the impulsive energy release. More recent 21 cm VLA observations by Willson and Lang (1984) showed evidence for preburst heating and magnetic field changes in burst sources that were spatially separated from the sites of the impulsive sources. These radio wavelength results are similar to those that have been detected at X-ray wavelengths in which adjacent loops brighten and perhaps trigger the eruption of other bursts (Vorpahl *et al.*, 1975; Kahler *et al.*, 1975; Kahler *et al.*, 1976). It is unclear however, that preburst heating is a general property of all solar bursts, for Kahler (1979) and Wolfson (1982) have found that soft X-ray bursts of weak to moderate strength ($\leq 1.5 \times 10^{25}$ erg s^{-1}, a C5 level in the Solrad and GOES classification schemes) are typically not preceded by an enhancement in the X-ray flux. Nevertheless, many theoretical models of solar flares include a preflare phase in which the coronal loop is heated, becomes unstable

Solar Physics **92** (1984) 189–198. 0038-0938/84/0921-0189$01.50.

and then erupts, giving rise to the impulsive phase (Heyvaerts *et al.*, 1977; Spicer, 1981; Somov and Syrovatskii, 1982). High resolution observations of the preburst evolution of coronal loops may therefore place useful constraints on these models as well as allow comparisons with other preflare phenomena, such as filament eruption, preflare vortical structure, Hα and X-ray brightening and coronal transients, for which direct association with flares has been implied (cf. Martin, 1980).

In this paper we present 20 cm VLA observations of an active region that underwent significant structural changes before the eruption phase of two spikelike bursts. The radio observations are compared with simultaneous X-ray and Hα observations which also show evidence for preburst activity. We also discuss these results in light of theoretical models that have been proposed for the preburst heating of coronal loops and the triggering of bursts. Finally, we combine the radio and X-ray data to estimate the kinetic temperature and electron density in the coronal loop that underwent these preburst changes.

2. Observations

The Very Large Array (B configuration) was used to observe the active region AR 3806 on July 13, 1982. The location of AR 3806 at 13 : 00 UT on this day was S 23, E 06. The entire VLA, consisting of 27 antennas was used to observe for successive 15 min periods at wavelengths of 21.7 and 17.6 cm (1377 MHz and 1698 MHz). At these wavelengths, the half power beamwidth of the individual 25 m antennas is $\sim 31'$ and the synthesized beamwidth is $\sim 3'' \times 4''$. Each 15 min solar observation was followed by a 2 min observation of the calibrator source OI 318 whose flux was assumed to be 1.7 Jy. The data were calibrated according to the procedure given by Lang and Willson (1979). These data were then used to produce synthesis maps of the total intensity I = (RCP + LCP)/2 and circular polarization, V = (RCP − LCP)/2, (where RCP and LCP denote the right and left handed circularly polarized signals) of the preburst, impulsive and postburst phases at intervals as short as 10 s. Finally, these maps were cleaned to produce microwave images with a dynamic range of about 10 : 1.

Figure 1 shows the time profile of the radio burst together with the profiles of X-ray emission in the 1.6–12.5 keV and 3.1–25 keV energy bands as observed by the GOES X-ray satellite. This burst was classified as a type M1.1 event by *Solar Geophysical Data*. The X-ray profiles are similar for the two bands; both show a rapid increase beginning $\sim$21 : 40 UT with a peak near 21 : 50 UT followed by a more gradual decrease lasting nearly half an hour. This X-ray burst was also accompanied by Hα brightenings which also began $\sim$21 : 40 UT (see below).

The radio burst profile has a different structure with two impulsive spikes of less than 10 s in duration at 21 : 58 : 10 UT and 22 : 00 : 50 UT. These spikes, which do not have X-ray counterparts, are also superimposed on a more gradual intensity increase that may also have begun as early as 21 : 40 UT.

In Figure 2 we show a series of VLA snapshot maps of both I and V which depict the evolution of the active region about 30 min before the first impulsive radio burst.

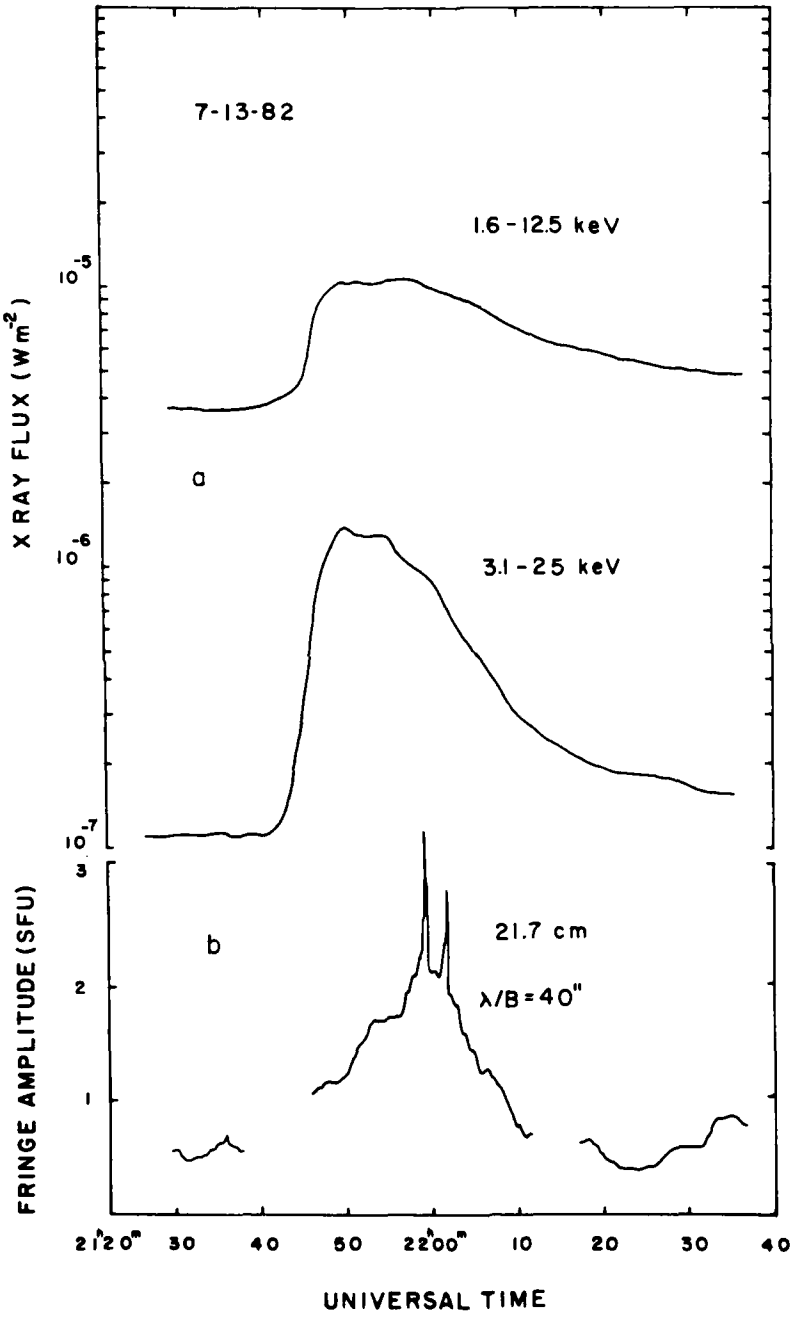

Fig. 1. (a) Time profiles in the 1.6–12.5 keV and 3.1–25 keV energy bands of X-rays as observed by the GOES satellite during the burst on July 13, 1982. (b) The fringe amplitude, versus time, of the total intensity I, for the burst detected at 20 cm wavelength at the VLA on a baseline of 40" fringe spacing.

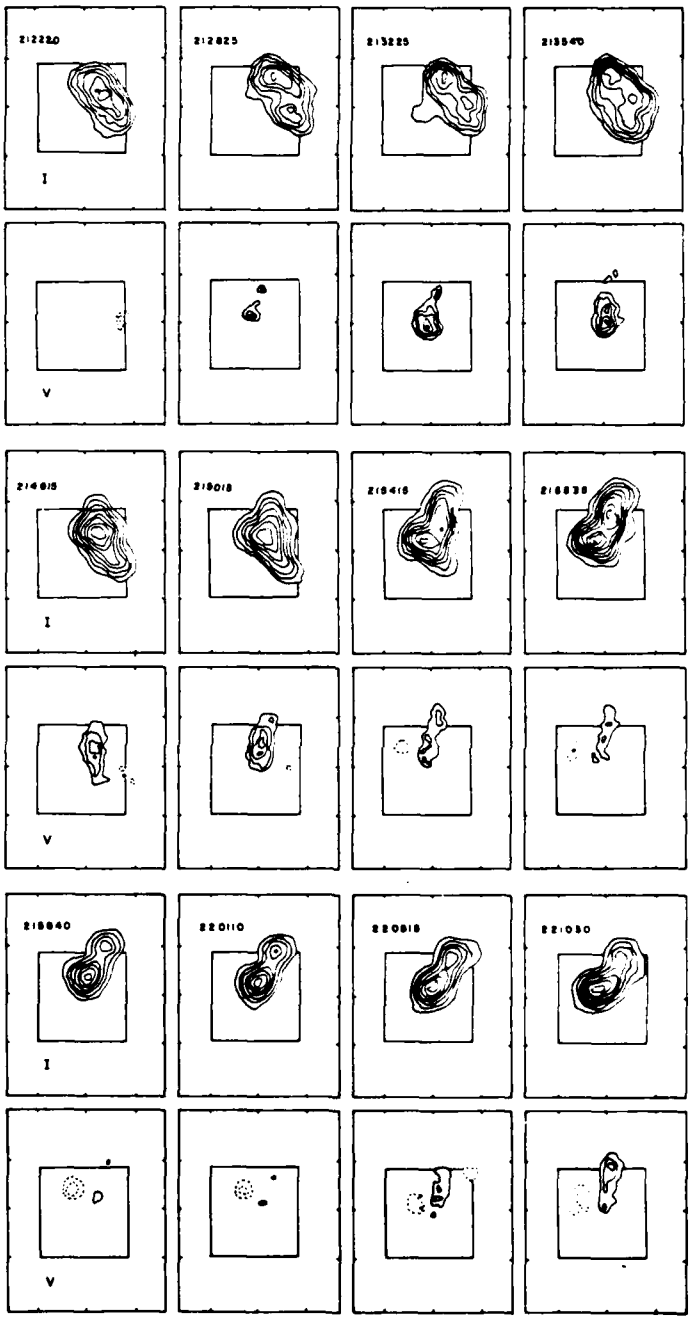

Fig. 2. A series of VLA maps of total intensity I, and circular polarization V, for the burst shown in Figure 1. Each map was made from 2 min of data beginning at the time indicated. Here north is up and east is to the left. The contours of both sets of maps mark levels of equal brightness temperature and the solid and dashed line, of the V maps denote positive and negative values of V, respectively. The outermost contour and the contour interval of the I maps are both equal to 4×10^5 K. The outermost contour and contour interval of the V maps are equal to 4×10^5 K and 2×10^5 K, respectively. The angular scale is determined from the 60″ spacing between the fiducial marks on the axes. The area within the boxes corresponds to the field of view of the 10 s snapshot maps of the two impulsive sources which are shown in Figure 4.

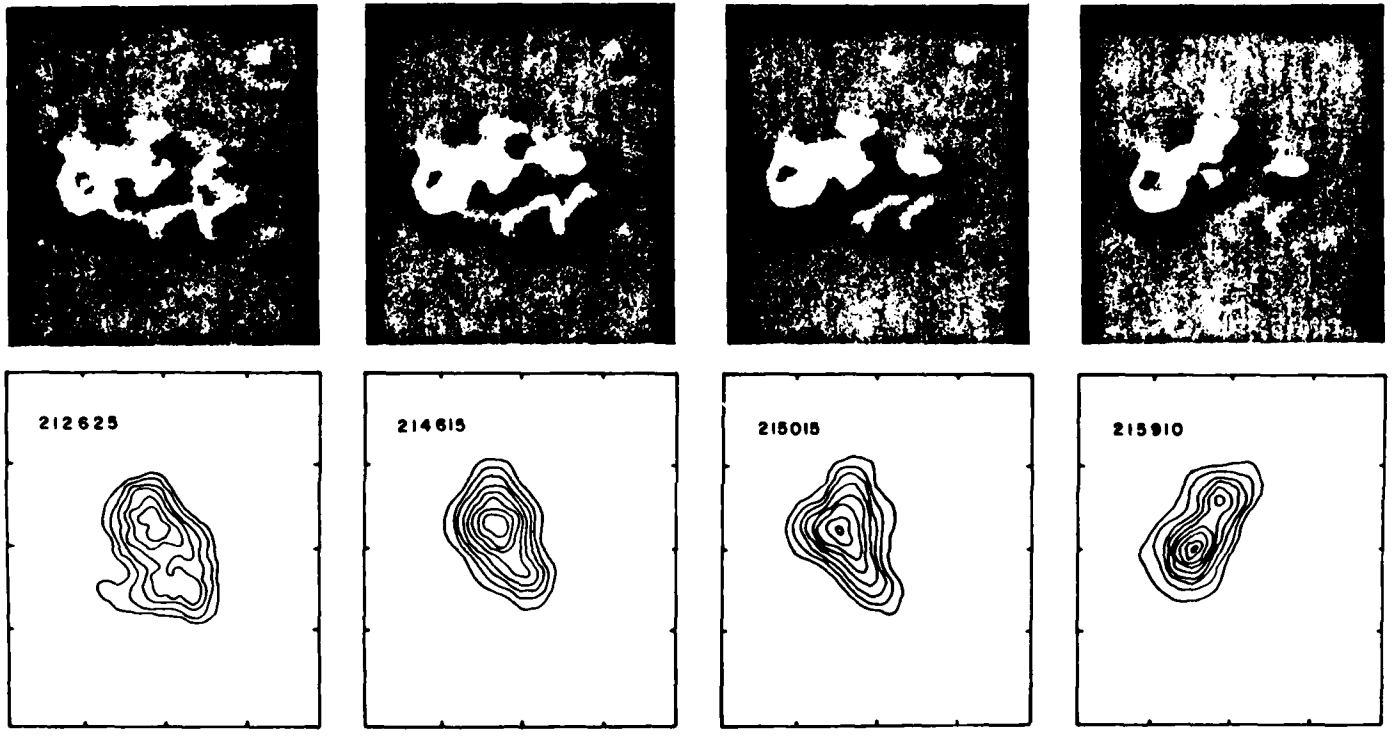

Fig. 3. Simultaneous Hα photographs (top) and VLA synthesis maps (bottom) of total intensity during the gradual phase of the burst shown in Figure 1. The contour of the radio maps are the same as those given in Figure 2. The Hα photographs were taken at the Big Bear Solar Observatory (courtesy of Frances Tang). The angular scales of both sets of pictures can be determined from the 60″ spacing between the fiducial marks on the radio maps. Note that both the optical and radio data indicate significant changes during the gradual phase of the burst.

Each map was made from 2 min of data beginning at the time indicated. Between 21 : 22 and 21 : 50 UT the radio emission is contained within a looplike structure of about 1.5′ in length with a NE–SW orientation. During this time interval, the peak brightness temperature gradually increased from $\sim 2 \times 10^6$ K to 3.5×10^6 K, while the circular polarization increased from $\leq 20\%$ to $\sim 60\%$. A comparison with a Kitt Peak magnetogram taken at 13 : 50 : 26 UT indicated that the source bridges regions of opposite magnetic polarity, suggesting a magnetically confined coronal loop. At ~21 : 50 UT, and well after the start of the X-ray burst, the loop began to twist in a clockwise direction, developed a second intensity peak, and finally became oriented in a NW–SE direction. Maps of the post-impulsive phase also show a looplike structure, oriented

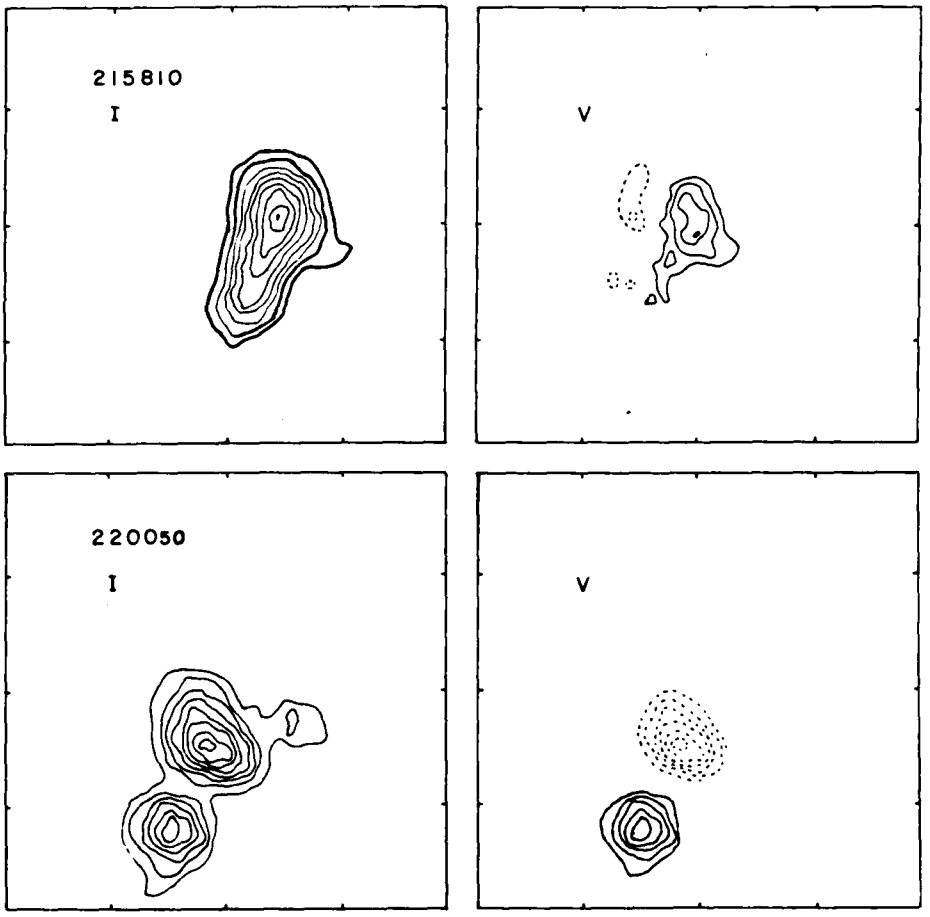

Fig. 4. VLA 10 s snapshot maps of the total intensity I, and circular polarization V, for the two impulsive bursts shown in Figure 1. The outermost contour and contour interval of the I maps are both equal to 3.5×10^6 K and 1.7×10^6 K, respectively. The angular scale is determined by the 30″ spacing between the fiducial marks on the axes.

NW–SE, whose peak brightness temperature decreased steadily from $\sim 2.5 \times 10^6$ K at 22 : 05 UT to $\sim 1.5 \times 10^6$ K at 22 : 20 UT.

The GOES X-ray data are spatially unresolved and thus it is impossible to compare the morphologies of the radio and X-ray sources. We have, however, made a comparison between the radio maps and simultaneous Big Bear Solar Observatory Hα data (courtesy of Frances Tang) which also show evidence for preflare changes. This comparison is shown in Figure 3 where the uncertainty in alignment between the radio and optical images is $\sim \pm 5''$. The first panel, at 21 : 20 UT, shows the preflare Hα emission in which the plage is concentrated mainly in the eastern half of the region. The next three panels show that the Hα brightenings occurred primarily in the plage, with a fainter brightening near the large spot in the west. In contrast, the radio emission was most intense $\sim 10''$–$20''$ to the west of the strongest Hα brightenings. This shift in position of the radio emission with respect to the underlying Hα emission suggests that the radio wavelength heating occurred in the upper regions of a coronal loop that connects the large spot and the bright plage.

In Figure 4 we show maps of the two impulsive bursts. These 10 s snapshot maps cover the smaller field of view contained within the boxes shown in Figure 2. The first impulsive spike at 21 : 58 : 10 UT has a peak brightness temperature of 3.1×10^7 K and a looplike structure of $\sim 30''$ in size which is nearly spatially coincident with the most intense peak of the preburst loop. The second, less intense, burst at 22 : 00 : 50 UT is shifted $\sim 30''$ to the south of the first and consists of two compact ($\theta \sim 10''$–$15''$) oppositely polarized sources (pc $\sim 100\%$) with peak brightness temperatures of $\sim 2.5 \times 10^7$ K. The bipolar structure of these sources as well as their separation from the preburst emission suggests that they are located near the footpoints of an adjacent loop that may have become activated by the eruption of the larger loop to the north. A similar pattern of multiple burst emission has been observed at 20 cm by Willson and Lang (1984) in which sequential triggering of burst loops may have occurred in a magnetically complicated region.

3. Discussion

Our observations show that the active region underwent significant changes before the eruption of the two impulsive bursts. In this case a large ($L \sim 6 \times 10^9$ cm) 20 cm loop began to twist and heat up about 15 min before these bursts occurred. These dramatic structural changes were also accompanied by changes in circular polarization suggesting the reorientation or emergence of magnetic fields in the loop. An interesting feature of these changes is their large physical scale. Other high resolution radio studies of the preburst state of active regions have, for example, revealed changes in both intensity and circular polarization (Kundu *et al.*, 1982; Willson and Lang, 1984) but these changes appear to have occurred on angular scales of a few to tens of arc seconds ($L \sim 10^8$–10^9 cm) and therefore involved changes in much smaller loops.

The changes seen in this loop are reminiscent of flare models in which coronal loops twist and develop kinks in response to motions in the photospheric footprints (Priest,

1983). In these models, the loop slowly heats up and remains stable until the twist exceeds a critical value (Raadu, 1972; Giachetti *et al.*, 1977; Hood and Priest, 1979) after which the loop is heated explosively (Spicer, 1977). The fact that the first of the impulsive bursts occurred within the loop that appeared to twist and heat up lends support to these models. Unfortunately, there are no simultaneous optical wavelength magnetograms that would allow us to check for the presence of such motions in the photosphere.

On the other hand, the fact that the second impulsive burst appears to have occurred in an adjacent loop lends support to the interacting loop model developed by Emslie (1982) in which an energy release in one loop triggers, through a magnetohydrodynamic disturbance, an energy release in a neighboring loop. In this case, the second loop did not show a gradual heating phase, and in fact was invisible on the 20 cm maps before and after it erupted.

The bipolar structure of this burst also provides evidence that microwave sources do not always lie at the top of loops as has been observed, for example, at 1.3 and 2.0 cm by Marsh and Hurford (1980) and 6 and 20 cm by Willson (1983) but they may also occur along the legs or near the footpoints as has been observed at 6 cm by Kundu *et al.* (1982). Petrosian (1982) has shown, for example, that if the magnetic field strength increases very rapidly from the top of the loop to the footpoints, or if the accelerated particles injected in the loop have an anisotropic distribution of pitch angles, then the microwave brightness can be greatest near the footpoints, as in the case for this burst.

Our observations of preburst heating were also accompanied by an enhancement of the soft X-ray flux. This is not surprising since theoretical investigations by Mätzler (1978) and Dulk *et al.* (1979) indicate that X-ray and radio bursts may arise from the same population of thermal or non-thermal electrons. In this case, it is possible to estimate the temperature and density of the loop by combining the radio and X-ray data. Marsh *et al.* (1981) and Hoyng *et al.* (1983) have analyzed several bursts and concluded that the microwave and *hard* X-rays are probably *not* produced by a common population of either thermal or non-thermal electrons. However, Hoyng *et al.* (1981) and Duijveman and Hoyng (1983) have found that the soft (3.5–5.5 keV) and hard (16–30 keV) X-rays originate in different parts of the flare loop, with the former originating at the top of the loop and the latter near the footpoints. In the following analysis, we therefore assume that the soft X-ray enhancement, which represents the thermal phase of the burst, occurred in the 20 cm loop and that the X-ray and microwave sources therefore share a common temperature and density. This assumption is probably not valid for the two impulsive bursts which do not have soft X-ray counterparts and which therefore likely arise from a different population of electrons.

A recently shown by Schmahl (1984 and personal communication) the kinetic temperature of the X-ray emitting plasma can be estimated directly from the ratio of the flares in the two GOES energy channels. His technique uses the spectra of Raymond and Smith (1977) and Mewe and Gronenschild (1981). Near the peak of the X-ray enhancement at 21 : 50 UT the ratio $I(1\text{–}8\ \text{Å})/I(0.5\text{–}4\ \text{Å}) \sim 6.1$ corresponds to a temperature of $\sim 1 \times 10^7$ K. By 22 : 10 UT, this ratio had decreased to ~ 20, corresponding to a

lower temperature of $\sim 5 \times 10^7$ K. Because these temperatures are higher than the 20 cm brightness temperatures of between 1.5×10^6 and 3.5×10^6 K, we infer that the radio emission is optically thin. Comparing the X-ray and radio brightness temperatures throughout the gradual burst, we find that the 20 cm optical depth increased from 0.32 at 21 : 50 UT to 0.65 at 22 : 10 UT. These results are consistent with the relatively high degree of circular polarization which also requires that the 20 cm loop be optically thin. Finally, assuming that the loop geometry is a cylinder of length $L \approx 6.5 \times 10^9$ cm and radius $R \sim 1 \times 10^9$ cm, we derive an average electron density of $N_e \sim 9.0 \times 10^9$ cm^{-3}, consistent with the densities typically found in pre-impulsive X-ray burst loops (Dere *et al.*, 1977; McKenzie *et al.*, 1980; Moore *et al.*, 1980).

Acknowledgements

Solar radio astronomy at Tufts University is supported under grant AFOSR-83-0019 with the Air Force Office of Scientific Research. The author is grateful to Frances Tang of the Big Bear Solar Observatory for providing the Hα photographs. He also thanks Kenneth Lang for useful discussions. The Very Large Array is operated by Associated Universities, Inc., under contract with the National Science Foundation.

References

Dere, K. P., Horan, M., and Kreplin, R. W.: 1977, *Astrophys. J.* **217**, 976.
Duijveman, A. and Hoyng, P.: 1983, *Solar Phys.* **86**, 279.
Dulk, G. A., Melrose, D. B., and White, S. M.: 1979, *Astrophys. J.* **234**, 1137.
Giachetti, R., Van Hoven, G., and Chivderi, C.: 1977, *Solar Phys.* **55**, 371.
Heyvaerts, J., Priest, E. R., and Rust, D. M.: 1977, *Astrophys. J.* **216**, 123.
Hood, A. W. and Priest, E. R.: 1979, *Solar Phys.* **64**, 303.
Hoyng, P. *et al.*: 1981, *Astrophys. J. Letters* **244**, L153.
Hoyng, P., Marsh, K. A., Zirin, H., and Dennis, B. R.: 1983, *Astrophys. J.* **268**, 865.
Kahler, S. W.: 1979, *Solar Phys.* **62**, 347.
Kahler, S. W., Krieger, A. S., and Vaina, G. S.: 1975, *Astrophys. J. Letters* **199**, L57.
Kahler, S. W., Petrasso, R. D., and Kane, S. R.: 1976, *Solar Phys.* **50**, 179.
Kundu, M. R., Schmahl, E. J., Velusamy, T., and Vlahos, L.: 1982, *Astron. Astrophys.* **108**, 188.
Landini, M. and Monsignori-Fossi, B. C.: 1979, *Astron. Astrophys.* **72**, 171.
Marsh, K. A., Hurford, G. J., Zirin, H., Dulk, G. A., Dennis, B. R., Frost, K. J., and Orwig, L. E.: 1981, *Astrophys. J.* **251**, 797.
Martin, S.: 1980, *Solar Phys.* **68**, 217.
Mätzler, C.: 1978, *Astron. Astrophys.* **70**, 181.
McKenzie, D. L., Broussard, R. M., Landecker, P. B., Rugge, H. R., and Young, R. M.: 1980, *Astrophys. J. Letters* **238**, L43.
Mewe, R. and Gronenschild, E. H. B. M.: 1981: *Astron. Astrophys. Suppl. Ser.* **45**, 11.
Moore, R., McKenzie, D. L., Švestka, Z., Widing, K. G., and 12 co-authors: 1980, in P. A. Sturrock (ed.), *Solar Flares*, Colorado Associated University Press, p. 341.
Priest, E. R.: 1983, *Solar Phys.* **86**, 33.
Raadu, M. A.: 1972, *Solar Phys.* **22**, 425.
Raymond, J. C. and Smith, B. W.: 1977, *Astrophys. J. Suppl. Ser.* **35**, 419.
Schmahl, E. J.: 1984, *Bull. Am. Astron. Soc.* (Jan. 1984 meeting).
Somov, B. V. and Syrovatskii, S. I.: 1982, *Solar Phys.* **75**, 237.

Spicer, D. S.: 1977, *Solar Phys.* **53**, 305.
Spicer, D. S.: 1981, *Solar Phys.* **70**, 149.
Willson, R. F.: 1983, *Solar Phys.* **83**, 285.
Willson, R. F. and Lang, K. R.: 1984, *Astrophys. J.* (to be published).
Wolfson, C. J.: 1982, *Solar Phys.* **76**, 377.

C. POSSIBLE DETECTION OF THERMAL CYCLOTRON LINES FROM SMALL SOURCES WITHIN SOLAR ACTIVE REGIONS

ROBERT F. WILLSON

Department of Physics, Tufts University, Medford, MA 02155, U.S.A.

(Received 31 May; in revised form 21 July, 1983)

Abstract. Theoretical spectra of thermal cyclotron line emission from solar active regions are presented for two frequency bands available at the Very Large Array (VLA). VLA synthesis maps of three active regions at 1380, 1540, and 1705 MHz are then presented. The maps of two of these regions show significant changes in the brightness temperature within these narrow frequency ranges. We show that these changes may be attributed to thermal cyclotron line emission in small regions (θ = 10" to 30") where the magnetic field is relatively constant with H = 125–180 G. An alternative interpretation, involving height-dependent variations in the physical conditions may also explain the changes in one of these regions. The potential to study coronal magnetic fields using VLA observations of cyclotron lines is also discussed.

1. Introduction

It was realized more than two decades ago that the cyclotron radiation (or gyroemission) of thermal electrons accelerated in solar magnetic fields may compete with the bremsstrahlung of thermal electrons accelerated in the electric fields of coronal ions (Stepanov, 1959; Ginzburg and Zheleznyakov, 1959). At the time, peculiarities in the frequency spectrum and polarization of solar active regions at radio wavelengths were interpreted in terms of the combined effects of cyclotron radiation and bremsstrahlung (Zheleznyakov, 1962; Kakinuma and Swarup, 1962). The observations used in support of this interpretation were, however, made with relatively small antennas whose large beamwidths could not resolve the individual sources within active regions. Interferometric observations at centimeter wavelengths indicated that beam dilution effects had, in fact, previously prevented the detection of small, intense sources which were very highly circularly polarized (Kundu, 1959; Enome *et al.*, 1969; Lang, 1974). This high polarization could only be attributed to cyclotron radiation. Early observations of solar active regions with the Very Large Array (VLA) at 6 cm wavelength then revealed unusually hot ($\approx 10^6$ K) and highly circulated polarized (up to 95%) radiation above sunspots (Lang and Willson, 1979; Kundu *et al.*, 1981). This radiation was attributed to the cyclotron radiation of coronal electrons trapped within the legs of magnetic dipoles whose feet are found in lower lying sunspots (Alissandrakis *et al.*, 1980; Lang *et al.*, 1983). In the meantime, observations at X-ray wavelengths had indicated that magnetic loops are the dominant structural features of the corona, but that the X-ray emission is most intense in the regions which lie between sunspots. The relatively weak X-ray radiation above sunspots implied low electron densities in these regions and this meant that bremsstrahlung could not account for the 6 cm emission above sunspots

Solar Physics **89** (1983) 103–113. 0038–0938/83/0891–0103$01.65.

(Pallavicini *et al.*, 1981). Additional opacity due to gyroresonant absorption was required to explain the high brightness temperatures at radio wavelengths. The presence of cyclotron radiation in the coronal atmosphere above sunspots was then confirmed by accurate polarization measurements at 6 cm wavelength using the Westerbork Synthesis Radio Telescope (WSRT) (Lang and Willson, 1982). The observations indicated that highly polarized (up to 100%) horseshoe structures overlie sunspot penumbrae. These structures can only be explained by cyclotron radiation, and they had, in fact actually been predicted by the theory of gyroresonant absorption above individual sunspots (Gel'freikh and Lubyshev, 1979).

The theory of cyclotron absorption indicates that observations at a given frequency, ν, refer to a narrow layer in the solar atmosphere at which $\nu = s\nu_H$, where $s = 2, 3, 4 \ldots$ is the harmonic, the gyrofrequency $\nu_H = 2.8 \times 10^6 H$ Hz, and H is the magnetic field strength in gauss. Because the magnetic field strength of dipolar loops decreases systematically with height above the solar photosphere, it was thought that the individual cyclotron lines would be superimposed to give a continuum spectrum, but that observations at longer wavelengths would refer to higher altitudes above the photosphere. Nevertheless, theoretical work predicted that individual cyclotron lines might be detected if the radiation was confined to a fixed altitude where the magnetic field is relatively constant. This might, for example, occur when neutral current sheets develop and subsequently rupture, thereby giving rise to solar bursts (Syrovatskii and Kuznetsov, 1980; Kuznetsov and Syrovatskii, 1981). The cyclotron radiation is able to escape only from a thin edge of the current sheet where the magnetic field is practically homogeneous. It was therefore imagined that thermal cyclotron lines might be detected during the temperature enhancements that occur before and during solar flares or bursts (Zheleznyakov and Zlotnik, 1980a; Zheleznyakov and Tikhomorov, 1980). Zheleznyakov and Zlotnik (1980b) have pointed out that cyclotron lines might also be detected from quiescent active regions if the loop geometry allowed observations of relatively constant magnetic field. Kaverin *et al.* (1980) have, in fact, detected narrow band structures at centimeter wavelengths from several active regions. They suggested that these structures may be attributed to cyclotron line emission from small sources within these regions where the magnetic field is nearly uniform.

The optical depths, τ_{s_e} and τ_{s_o}, for the extraordinary and ordinary modes for an individual cyclotron line at harmonic s are given by (Zheleznyakov and Zlotnik, 1980; Zheleznyakov, 1970):

$$\tau_{s_{o,e}} = 3.93 \frac{\nu}{c}\left(\frac{\nu_p}{\nu}\right)^2 \frac{s^{2s}}{2^s s!} \beta_T^{2s-3} L_H F(\alpha) \exp(-z^2), \tag{1}$$

where

$$F(\alpha) = (1 \pm \cos\alpha)^2 \frac{\sin\alpha^{2s-2}}{|\cos\alpha|}$$

and

$$z = \frac{\nu - s\nu_H}{\sqrt{2}\nu\beta_T \cos\alpha} .$$

Here, the frequency $\nu = s\nu_H$, the gyrofrequency is $\nu_H = 2.8 \times 10^6 H$, the velocity of light is c, the plasma frequency $\nu_p = 8.9 \times 10^3 N_e^{1/2}$ for an electron density of N_e, the factor $\beta_T = V_{th}/c = 3.89 \times 10^5 T_e^{1/2}/c$ for an electron thermal velocity V_{th} and an electron temperature of T_e, and L_H is the scale length of the magnetic field. The function $F(\alpha)$ depends on the angle α, between the magnetic field and the line of sight and the + and − signs denote the extraordinary and ordinary modes of wave propagation. The gaussian function $\exp(-z^2)$ describes a Doppler broadened line with a peak value of unity at $\nu = s\nu_H$ and a full width to half maximum of $\Delta\nu_D = 2.335\beta_T\nu$.

In addition to cyclotron emission, thermal bremsstrahlung can also contribute to the opacity above active regions. The optical depths τ_{B_e} and τ_{B_o}, of the extraordinary and ordinary modes due to thermal bremsstrahlung are given by

$$\tau_{B_e} = \frac{\tau_B}{\left[1 - \frac{\nu_H \cos\alpha}{\nu}\right]^2} ,$$

$$\tau_{B_o} = \frac{\tau_B}{\left[1 + \frac{\nu_H}{\nu}\cos\alpha\right]^2} , \qquad (2)$$

where

$$\tau_B = \frac{9.78 \times 10^{-3} N_e^2 L}{\nu^2 T_e^{3/2}} \ln[4.7 \times 10^{10} T_e/\nu]$$

is the classical expression for the bremsstrahlung optical depth in the absence of a magnetic field. The brightness temperatures $T_{B_{e,o}} = [1 - \exp(-\tau_{e,o})]T_e$, where $\tau_{e,o} = \tau_{s_{e,o}} + \tau_{B_{e,o}}$. We have calculated the brightness temperature $T_B = (T_{B_e} + T_{B_o})/2$ and the degree of circular polarization $\rho_c = [T_{B_e} + T_{B_o}]/[T_{B_e} - T_{B_o}]$ as a function of frequency for the harmonics 2, 3, 4, and 5 and a number of different values of the magnetic field strength, temperature, density, scale length, and angle. The results of our calculations for two frequency bands between 1000 and 2000 MHz and 4000–5000 MHz are shown in Figures 1 and 2. These frequency ranges were chosen because they are centered on two of the frequency bands available at the VLA. As illustrated in these figures, we obtain thermal cyclotron lines of half-width $\Delta\nu_D$ = 50–150 MHz, superimposed upon optically thin bremsstrahlung. Because τ_s depends strongly on the harmonic s, the cyclotron lines become optically thick at s = 2, 3, and 4 with flat tops and broad widths which refer to the lower, truncated parts of the gaussian function $\exp(-z^2)$. Because $\Delta\nu_D/\nu$ is a constant, the lines between 4 and

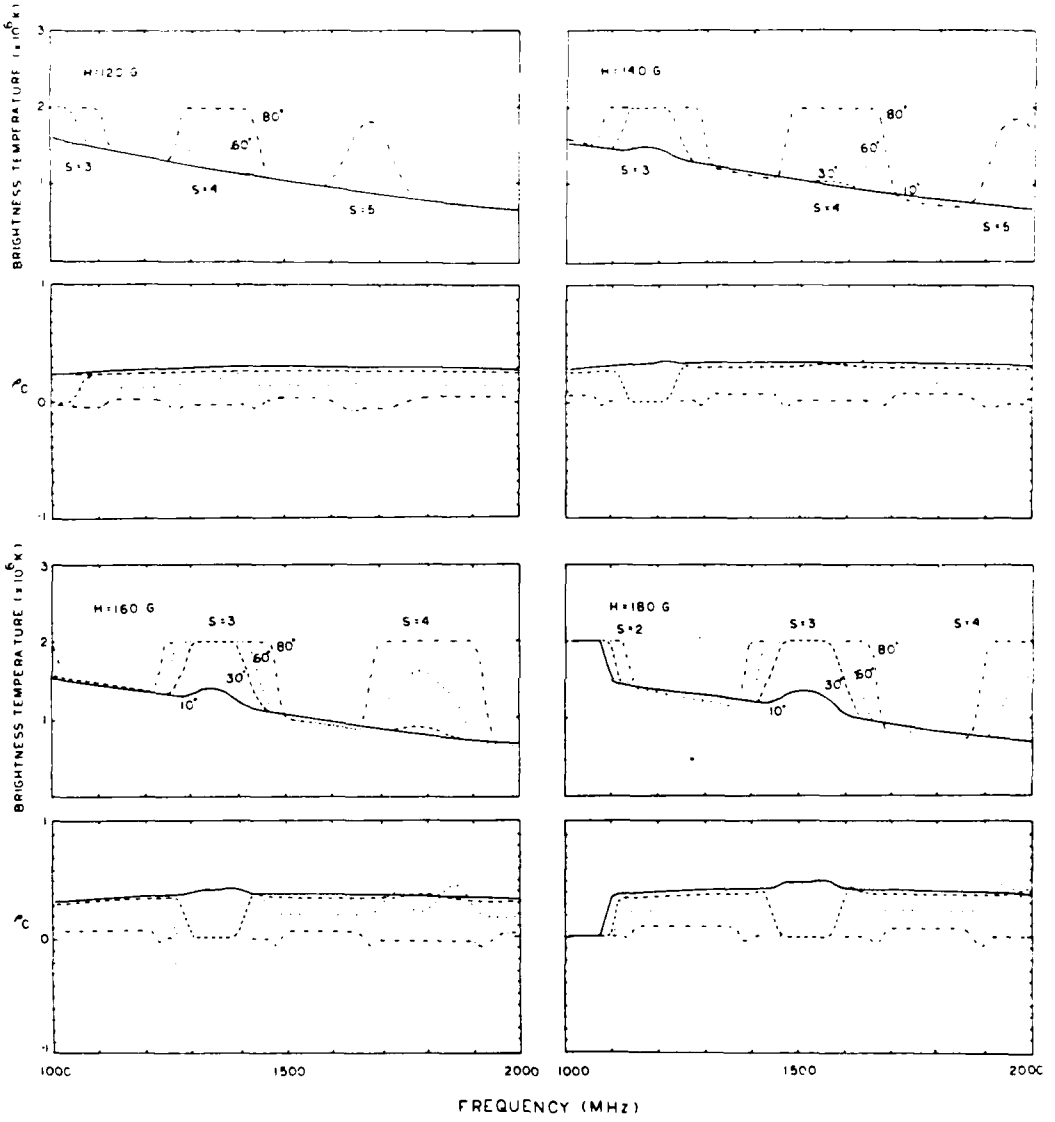

Fig. 1. Theoretical plots of the brightness temperature, T_B, and degree of circular polarization, ρ_c, of thermal cyclotron lines at different harmonics $S = 2$, 3, 4, and 5 for magnetic field strengths $H = 120$, 140, 160, and 180 G, and angles, α, of 10°, 30°, 60°, and 80°. These curves were generated using an electron temperature $T_e = 2 \times 10^6$ K, an electron density $N_e = 5 \times 10^9$ cm^{-3} and a path length $L = L_H = 1 \times 10^9$ cm.

5 GHz are about a factor of 3 wider than those between 1 and 2 GHz. Thus, under favorable conditions, observations of active regions at closely spaced frequencies may show jumps or more complicated variations in both the total intensity and circular

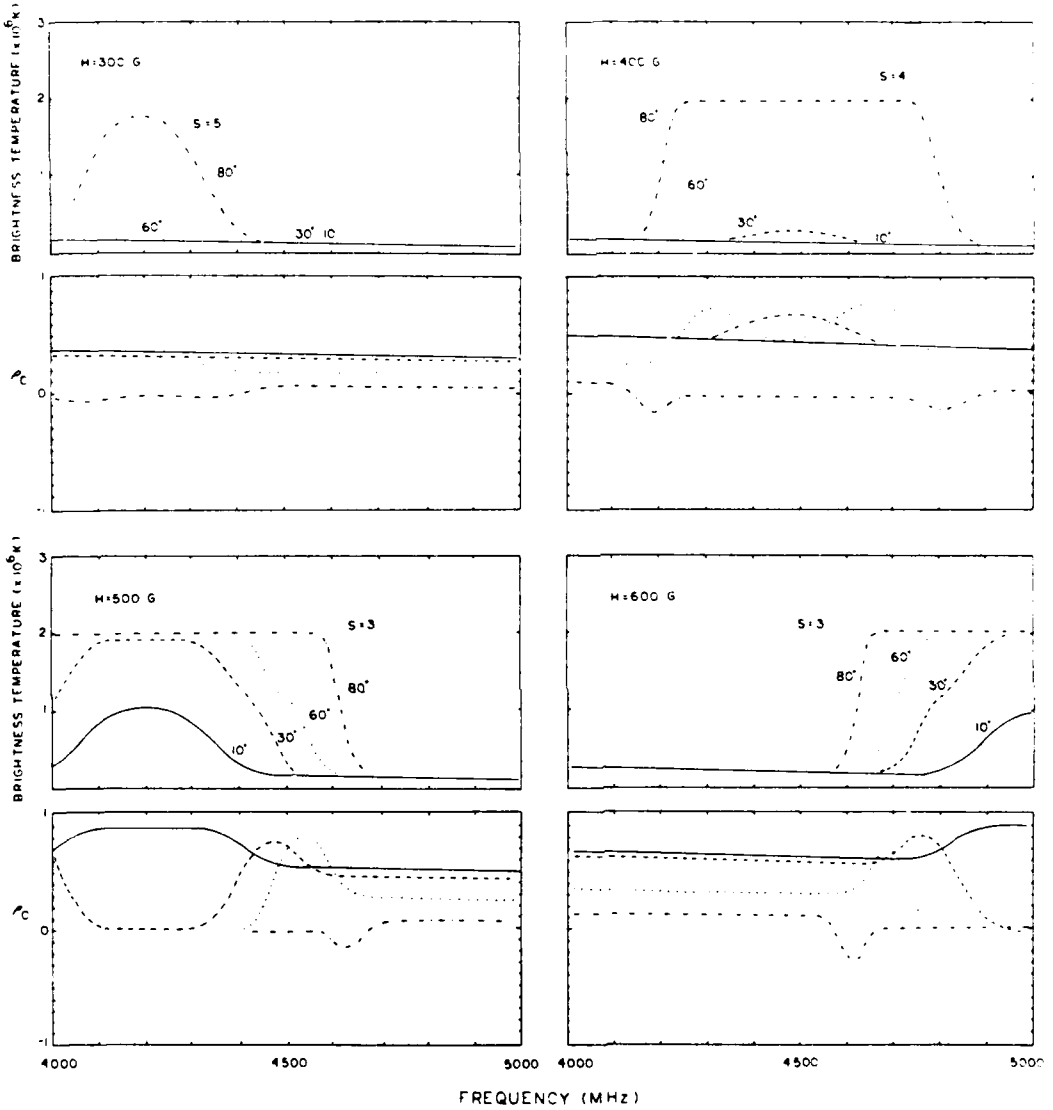

Fig. 2. Theoretical plots of the brightness temperature, T_B, and degree of circular polarization, ρ_c, of thermal cyclotron lines at different harmonics $S = 3, 4$, and 5 for magnetic field strengths $H = 300, 400, 500$, and 600 G, and angles, α, of 10°, 30°, 60°, and 80°. These curves were generated using an electron temperature $T_e = 2 \times 10^6$ K, an electron density $N_e = 5 \times 10^9$ cm^{-3} and a path length $L = L_H = 1 \times 10^9$ cm.

polarization. In the next section, we describe observations of two active regions which, in fact, show such changes, and which may be attributed to thermal cyclotron line emission.

2. Possible Detection of Thermal Cyclotron Lines

It has been shown that VLA observations of quiescent active regions at centimeter wavelengths delineate the ubiquitous coronal loops that were previously detected at X-ray wavelengths (Kundu and Velusamy, 1980; Lang *et al.*, 1982). The brightness temperatures of $T_B \approx 2 \times 10^6$ K suggested that the radio emission was due to the optically thick bremsstrahlung of a hot plasma trapped within the magnetic loops. Under this interpretation an electron density of $N_e \approx 5 \times 10^9$ cm^{-3} and a line-of-sight thickness of $L \approx 10^9$ cm are inferred. The classical expression for the bremsstrahlung optical depth, τ_B, (Equation (2)) indicates that it is very close to unity at an observing frequency of $\nu \approx 1400$ MHz under these conditions. We therefore planned observations at three frequencies near 1400 MHz with the hope of detecting optically thin bremsstrahlung ($\tau_B < 1$). Because the observations at these frequencies refer to the upper parts of coronal loops, the magnetic field strength may be relatively constant. There was therefore the additional hope that thermal cyclotron lines might be detected as emission that is enhanced above the optically thin bremsstrahlung.

The active regions AR 3804 and AR 3828 were observed on 19 and 28 July, 1982, respectively, with the entire VLA (*B* configuration) at 1380 MHz, 1540 MHz, and 1705 MHz. The position of AR 3804 was N 09 W 64 at 13:00 UT on 19 July and the position of AR 3828 was N 06 E 27 at 13:00 UT on 28 July. The active regions were successively observed for 10 min periods at the three frequencies, and this was followed by successive 2 min observations of the calibrator source O1 318. The entire 36 min sequence was repeated for an eight hour period centered on local noon. At these frequencies, the half-power beamwidth of the individual antennas is $\approx 31'$ and the synthesized beamwidth is $\approx 3'' \times 4''$. In all cases the bandwidth was 12.5 MHz. The average correlated flux of 356 interferometer pairs was sampled every 10 s for both the left hand circularly polarized (LCP) and right hand circularly polarized (RCP) signals. The data were then calibrated according to the procedure described by Lang and Willson (1979) together with a correction for the difference in the signal from high temperature noise sources detected in each polarization channel. The assumed fluxes of the calibrator source O1 318 at 1380, 1540, and 1705 MHz were 1.73 Jy, 1.65 Jy, respectively. At these frequencies the temperatures of the calibration noise sources are the same to within $\pm 15\%$. The calibrated data were then edited and used together with the standard CLEAN procedure to make the synthesis maps shown in Figures 3 and 4.

These maps show dramatic changes in the structure of the active regions at the three closely spaced frequencies. In Table I we give the brightness temperatures at several locations within the active regions where these temperature differences are particularly striking. The intensity within both the northern and southern components of AR 3804 (Figure 3) varies by as much as a factor of 5 at some locations at the three frequencies. AR 3828 exhibits an enhancement in only one component of the active region (*A*, Figure 4) where the brightness temperature at 1540 MHz is about a factor of 2.5 greater than at 1380 MHz and 1705 MHz. The *V* maps shown in Figure 4 indicate that the

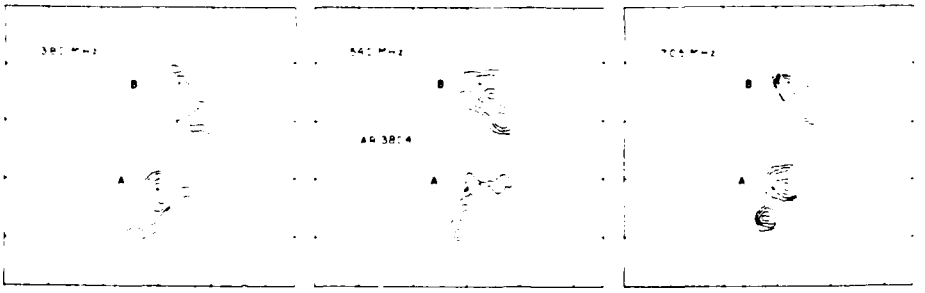

Fig. 3. VLA synthesis maps of the total intensity, I, of AR 3804 at three closely spaced frequencies using data obtained during an eight hour period on 19 July, 1982. The synthesized beamwidth is $\theta \approx 3'' \times 4''$. The contours of the map mark levels of equal brightness temperature. The outermost contour and the contour level are equal to 3.2×10^5 and 1.6×10^5 K, respectively. The positions of components A and B, referred to in the text and Table I, are marked with a cross. The angular scale can be determined from the 60″ spacing between the fiducial marks on the axes.

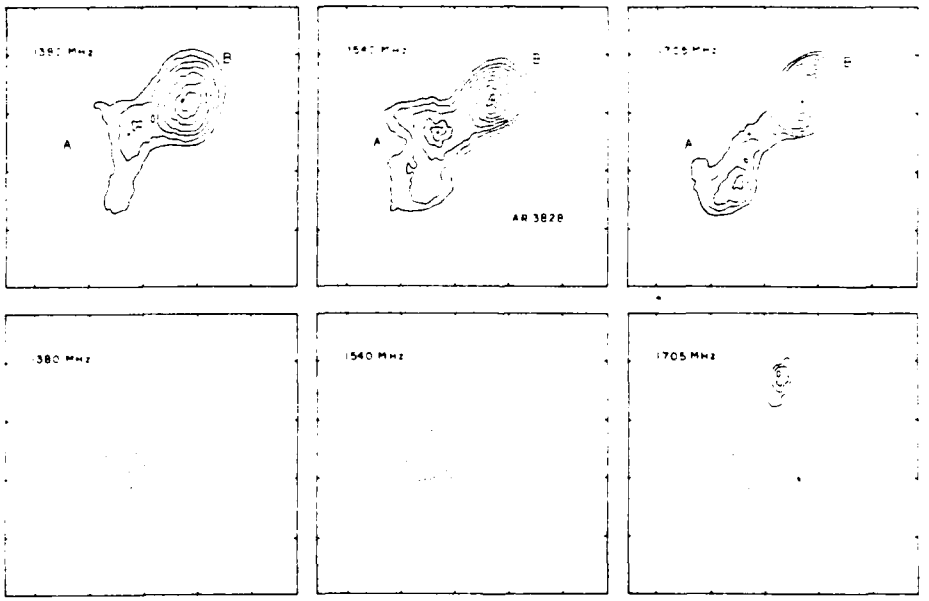

Fig. 4. VLA synthesis maps of the total intensity, I (top), and circular polarization, V (bottom) of AR 3828 at three closely spaced frequencies using data obtained during an eight our period on 28 July, 1982. The synthesized beamwidth is $\theta \approx 3'' \times 4''$. The contours of the maps mark levels of equal brightness temperature, and the solid and dashed contours of the V maps denote positive and negative values of V, respectively. The outermost contour and the contour level of the I maps are equal to 4.3×10^5 and 2.2×10^5 K, respectively. The contours of the V maps are drawn at -3.6×10^5, -3.2×10^5, $-2.8 \times 10^5 \ldots 2.1 \times 10^5$ K. The positions of components A and B, referred to in the text and Table I, are marked with a cross. The maximum degree of circular polarization, ρ_c, is $\approx 35\%$ at each of the three frequencies in component A. The angular scale can be determined from the 30″ spacing between the fiducial marks on the axes.

TABLE I

Maximum brightness temperatures, T_b (max), of components within AR 3804, AR 3828, and AR 3828 NW at different frequencies

Component T_b		1380 MHz (K)	1540 MHz (K)	1705 MHz (K)
AR 3804	A	1.3×10^6	4.6×10^5	5.3×10^5
	B	3.1×10^5	4.7×10^5	1.5×10^6
AR 3828	A	6.2×10^5	1.5×10^6	6.5×10^5
	B	1.9×10^6	1.9×10^6	2.1×10^6
AR 3828 NW	A	1.2×10^6	1.4×10^6	1.4×10^6

circularly polarized emission is also enhanced in the same part of the active region where the total intensity is the highest. We were unable to detect any polarized emission from AR 3804 to a limit of $< 10\%$.

These striking changes in source structure cannot be due to an artifact of the cleaning process, as they were also visible in the uncleaned, or 'dirty' maps. If these changes were due to a systematic error in calibration or to the confusion from neighboring sources located on the Sun, then we would expect similar variations in all of the sources located within the antenna beam. For comparison, in Figure 5 we show synthesis maps of an active region located $\approx 3.2'$ W and $\approx 2.5'$ N of AR 3828 (AR 3828 NW) on 28 July. These maps of total intensity indicate that the source structure and peak brightness temperature at the three frequencies are the same to within $\approx 15\%$.

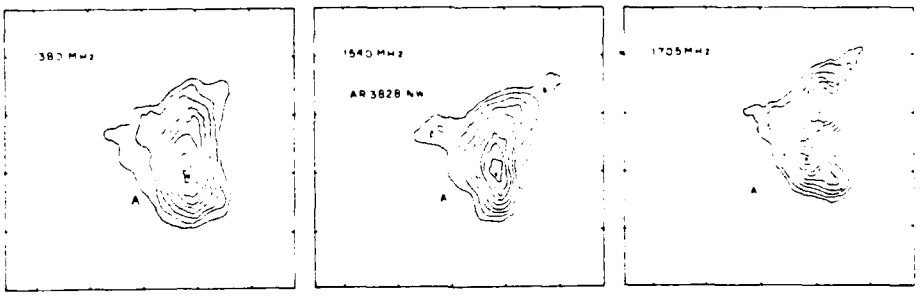

Fig. 5. VLA synthesis maps of the total intensity, I, of an active region, AR 3828 NW, located $\approx 5'$ NW of AR 3828 on 28 July, 1982. The contours of the maps mark levels of equal brightness temperature, where the outermost contour and the contour interval are equal to 2.9×10^5 and 1.4×10^5 K, respectively. The position of maximum intensity is marked with a cross. The angular scale can be determined from the 30″ spacing between the fiducial marks on the axes.

3. Discussion

The changes in source structure are difficult to explain by the conventional radiation mechanisms of gyroemission or thermal bremsstrahlung which predict gradual changes

in brightness temperature and polarization over the observed frequency range. In the optically thick regime, the brightness temperature of a uniform source due to the bremsstrahlung and gyro-emission vary as ν^{-2} and ν^{-1}, respectively, where ν is the observing frequency. Our observations however indicate much more rapid brightness temperature variations, with $T_b \sim \nu^{\pm 5}$ for some components (see Table I). These abrupt changes in brightness temperature can, however, be explained by cyclotron line emission.

The maximum brightness temperatures as a function of frequency of components *A* and *B* of AR 3804 and component *A* of AR 3828 NW have been plotted in Figure 6 with

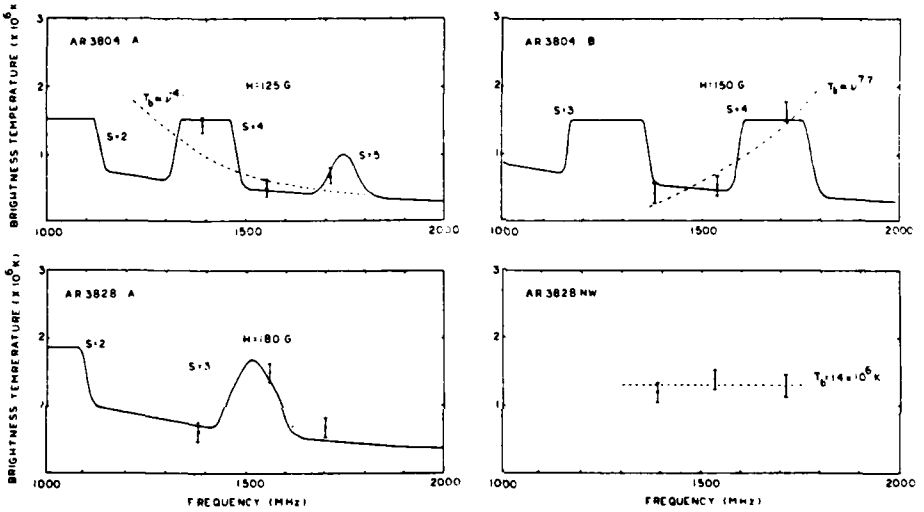

Fig. 6. Theoretical plots of the brightness temperature of thermal cyclotron lines at different harmonics $S = 2$, 3, 4, and 5 for magnetic field strengths of $H = 125$, 150, and 180 G. The maximum brightness temperatures observed for components *A* and *B* of AR 3804 and components *A* of AR 3828 and AR 3828 NW are also plotted with error bars corresponding to the peak-to-peak fluctuations in the background temperature of the synthesis maps. The theoretical curves for AR 3804 were calculated assuming an electron temperature of $T_e = 1.5 \times 10^6$ K, an electron density $N_e = 3 \times 10^9$ cm^{-3}, a path length $L = L_H = 1 \times 10^9$ cm, and an angle $\alpha = 80°$. The curves for AR 3828 were calculated with the same values of electron density and path length but with $T_e = 1.8 \times 10^6$ K, and $\alpha = 20°$. The dashed lines refer to power-law fits to the observed brightness temperatures. The data for AR 3828 NW are fit by optically thick thermal bremsstrahlung with $T_b = T_e = 1.4 \times 10^6$ K.

conservative error bars corresponding to the peak-to-peak fluctuations in the background noise temperature of the synthesis maps. We also show the brightness temperature of theoretical curves of cyclotron line emission for the harmonics $s = 3$, 4, and 5 and a number of different values of the magnetic field strength, temperature, density, scale length and angle. We find that thermal cyclotron lines can explain the observed total intensity and polarization of AR 3804 and AR 3828 with plausible physical parameters $H = 125$–180 G, an electron density $N_e = 3 \times 10^9$ cm^{-3}, an electron temperature $T_e = 1.5 \times 10^6$ K, and a scale length $L = L_H = 1 \times 10^9$ cm. The

observations of AR 3828 NW, can, however, be explained as either optically thick bremsstrahlung or gyro-emission with $T_b = T_e = 1.4 \times 10^6$ K. The polarization data constrain the angle α to be $\geq 80^\circ$ for AR 3804 and $\approx 20^\circ$ for AR 3828. Under the assumption that the magnetic field projects radially outward from the surface of the Sun into the corona, these angles are also plausible, as AR 3804 and AR 3828 were, respectively, near the solar limb and near central meridian, at the time of observation. These model curves are not unique, however, as the parameters can be adjusted to give acceptible agreement with the data.

There may also be alternative explanations of our data. One possibility is that the emission at each frequency originates at a different height above the active region where the physical conditions are also different. Observations at successively lower frequencies refer to successively higher levels in the solar atmosphere where the electron temperature and density and magnetic field systematically increase and decrease, respectively. The brightness temperature of optically thick emission ($T_b = T_e$) can therefore only decrease with increasing frequency, whereas the brightness temperature of optically thin emission ($T_b \approx T_e \tau$) may increase with increasing frequency. In Figure 6 we show power law fits to the brightness temperatures of components *A* and *B* of AR 3804. For component *A*, $T_b \sim \nu^{-4.1}$ so that the decrease in brightness temperatures might be attributed to an optically thick source in which the temperature systematically decreases with decreasing height. For component *B*, $T_b \sim \nu^{+7.7}$, suggesting an optically thin source in which the temperature or the density or both change with height. This alternative explanation however, cannot explain the observations of AR 3828 which show neither a systematic increase or decrease of the brightness temperature with frequency. Because thermal cyclotron lines can explain the observed data with plausible physical parameters while conventional radiation mechanisms cannot, we believe that we have a possible detection of cyclotron lines. This has important implications for the combined measurements of bremsstrahlung and cyclotron lines provide a sensitive probe of the physical properties of coronal loops. For instance, it is known that the electron temperature of quiescent coronal loops have a narrow range of temperature between 1 and 3×10^6 K. A measurement of the electron temperature, say using the Solar Maximum Mission X-ray instruments (when it is repaired in 1984) combined with VLA observations of the radio brightness temperature and bremsstrahlung optical depth will give a reliable measurement of the emission measure. As illustrated in Figures 1, 2, and 6, the central frequencies of the cyclotron lines provide a sensitive measurement of the magnetic field strength, for a change of only 20 G produces a 170 MHz shift in the central frequency of the line. Carefully calibrated, high resolution maps of the total intensity and circular polarization of active regions at uniformly spaced frequencies over a frequency range of ≈ 1 GHz may provide a detailed description of the magnetic field, temperature and density of the active region. Measurements of these effects can probably best be made with the VLA which provides sufficient angular resolution to resolve the different sources of cyclotron lines. The poorer angular resolution of single antennas would combine the signals from different sources, and the cyclotron lines might be lost in the superposition of the different sources which radiate at different frequencies.

Acknowledgements

The author wishes to thank Kenneth R. Lang for helpful discussions. Radio interferometric studies at Tufts University are supported under grant AFOSR-83-0019 with the Air Force Office of Scientific Research. The VLA is operated by Associated Universities, Inc., under contract with the National Science Foundation.

References

Alissandrakis, C. E., Kundu, M. R., and Lantos, P.: 1980, *Astron. Astrophys.* **82**, 30.
Enome, S., Kakinuma, T., and Tanaka, H.: 1969, *Solar Phys.* **6**, 428.
Gel'freikh, G. B. and Lubyshev, B. I.: 1979, *Soviet Astron. A.J.* **23**, 316.
Ginzburg, V. L. and Zheleznyakov, V. V.: 1959, *Soviet Astron. A.J.* **3**, 235.
Kakinuma, T. and Swarup, G.: 1962, *Astrophys. J.* **136**, 975.
Kaverin, N. S., Kobrin, M. M., Kovshunov, A. I., and Sushunov, V. V.: 1980, *Soviet Astron. A.J.* **24**, 442.
Kundu, M. R.: 1959, *Ann. Astrophys.* **22**, 1.
Kundu, M. R. and Velusamy, T.: 1980, *Astrophys. J. Letters* **240**, L63.
Kundu, M. R., Schmahl, E. J., and Rao, A. P.: 1981, *Astron. Astrophys.* **94**, 72.
Kuznetsov, V. D. and Syrovatskii, S. I.: 1981, *Solar Phys.* **69**, 361.
Lang, K. R.: 1974, *Solar Phys.* **36**, 351.
Lang, K. R. and Willson, R. F.: 1979, *Nature* **278**, 24.
Lang, K. R. and Willson, R. F.: 1982, *Astrophys. J. Letters* **255**, L111.
Lang, K. R., Willson, R. F., and Rayrole, J.: 1982, *Astrophys. J.* **258**, 384.
Lang, K. R., Willson, R. F., and Gaizauskas, V.: 1983, *Astrophys. J.* **267**, 455.
Pallavicini, R., Sakurai, T., and Vaiana, G. S.: 1981, *Astron. Astrophys.* **98**, 316.
Stepanov, K. N.: 1959, *Soviet Phys. JETP* **8**, 195.
Syrovatskii, S. I. and Kuznetsov, V. D.: 1980, in M. R. Kundu and T. E. Gergely (eds.), 'Radio Physics of the Sun', *IAU Symp.* **86**, 109.
Zheleznyakov, V. V.: 1962, *Soviet Astron. A.J.* **6**, 3.
Zheleznyakov, V. V.: 1970, in *Radio Physics of the Sun and Planets*, New York, Pergamon Press.
Zheleznyakov, V. V. and Tikhomorov, Yu. V.: 1982, *Solar Phys.* **81**, 121.
Zheleznyakov, V. V. and Zlotnik, E. Ya.: 1980a, *Solar Phys.* **68**, 317.
Zheleznyakov, V. V. and Zlotnik, E. Ya.: 1980b, *Soviet Astron. A.J.* **24**, 448.

THE ASTROPHYSICAL JOURNAL, 279:427–437, 1984 April 1

D. VERY LARGE ARRAY OBSERVATIONS OF SOLAR ACTIVE REGIONS. IV. STRUCTURE AND EVOLUTION OF RADIO BURSTS FROM 20 CENTIMETER LOOPS

ROBERT F. WILLSON AND KENNETH R. LANG
Department of Physics, Tufts University
Received 1983 April 18; accepted 1983 September 19

ABSTRACT

The Very Large Array (VLA) has been used to study the structure and evolution of six solar bursts near 20 cm wavelength. In most cases the burst emission has been resolved into looplike structures with total lengths, $L \sim 3 \times 10^9$ cm, brightness temperatures $T_B \sim 10^7$–10^8 K, and degrees of circular polarization $\rho_c \lesssim 90\%$. Changes in the total intensity and circular polarization of the bursts occur on time scales as short as 10 s. The individual peaks of one multiple-component burst originated in different locations within a magnetically complicated region. Preburst heating occurred minutes before the onset of the impulsive phase of one burst, and circular polarization changes occurred minutes before the onset of the impulsive phase of another burst. In one case, a loop system emerged in the vicinity of the impulsive source, and two adjacent loop systems may have emerged and triggered the burst.

Subject headings: interferometry — polarization — Sun: radio radiation

I. INTRODUCTION

Centimeter wavelength ($\lambda = 2$ cm or 6 cm) observations with the Very Large Array (VLA) at high angular resolution ($\theta \geq 1''$) and moderate time resolution ($\tau \approx 10$ s) have provided new insights into the physics of solar radio bursts. The radio bursts are usually located above magnetic neutral lines rather than sunspots, while the Hα flares often occur near the sunspots (Alissandrakis and Kundu 1978; Marsh, Zirin, and Hurford 1979; Marsh and Hurford 1980; Lang, Willson, and Felli 1981; Willson 1983). The total intensity and circular polarization of the radio emission often change before the bursts, suggesting that they are triggered by preburst heating or by magnetic changes. Variations in the distribution of circular polarization also reflect changes in the magnetic field configuration during solar bursts (Kundu, Bobrowsky, and Velusamy 1982; Velusamy and Kundu 1982; Willson 1983). The observations at $\lambda = 2$ cm and 6 cm therefore suggest that radio bursts are emitted near the apices of magnetic loops, rather than at their feet and that either preburst heating within loops or emerging loops trigger burst emission.

There have been comparatively few VLA observations of solar bursts at the longer 20 cm wavelength. Observations of the quiescent emission from solar active regions at $\lambda = 20$ cm delineate looplike structures which are the radio wavelength counterpart of the ubiquitous coronal loops detected at soft X-ray wavelengths (Lang, Willson, and Rayrole 1982). Velusamy and Kundu (1981) have reported the detection of a postflare loop at $\lambda = 20$ cm, and Lang, Willson, and Felli (1981) have shown that some 20 cm bursts have small angular sizes $\theta \sim 3''$–$5''$ and brightness temperatures $T_B \sim 2 \times 10^7$ K that are similar to those of hard X-ray kernels and soft X-ray bursts. The 20 cm data are nevertheless meager, and in this paper we therefore present a VLA analysis of six bursts from 20 cm loops. In § II we present time profiles and 10 s snapshot maps that describe the evolution of the 20 cm bursts, preburst heating, and changes in magnetic structure before and during the bursts. The angular sizes $\theta \sim 20''$–$60''$, total linear extents $L \sim (0.7$–$5) \times 10^9$ cm and brightness temperatures $T_B \sim (2$–$20) \times 10^7$ K of the 20 cm bursts are similar to those observed at soft X-ray wavelengths. In § III we discuss the implications of our observations and place them within the framework of other observational and theoretical work.

II. OBSERVATIONS OF RADIO BURSTS FROM 20 CENTIMETER LOOPS

The Very Large Array (B configuration) was used to observe the active region AR 3804 on 1982 July 12–20 at 1380 MHz, 1540 MHz, or 1705 MHz (or wavelengths $\lambda = 21.7$, 19.4, and 17.6 cm). On July 12 the active region was observed for successive 10 minute periods at 1380 MHz and 1705 MHz, while on July 19 and 20 the region was observed at all three frequencies for successive 10 minute intervals. At these

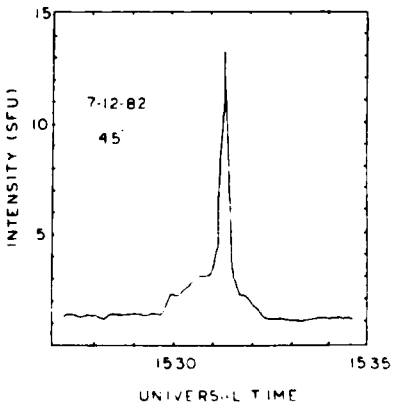

FIG. 1.—The fringe amplitude and total intensity, I, vs. time for a spikelike burst detected at 20 cm wavelength with an interferometer pair with angular resolution $\theta = 45''$ on 1982 July 12.

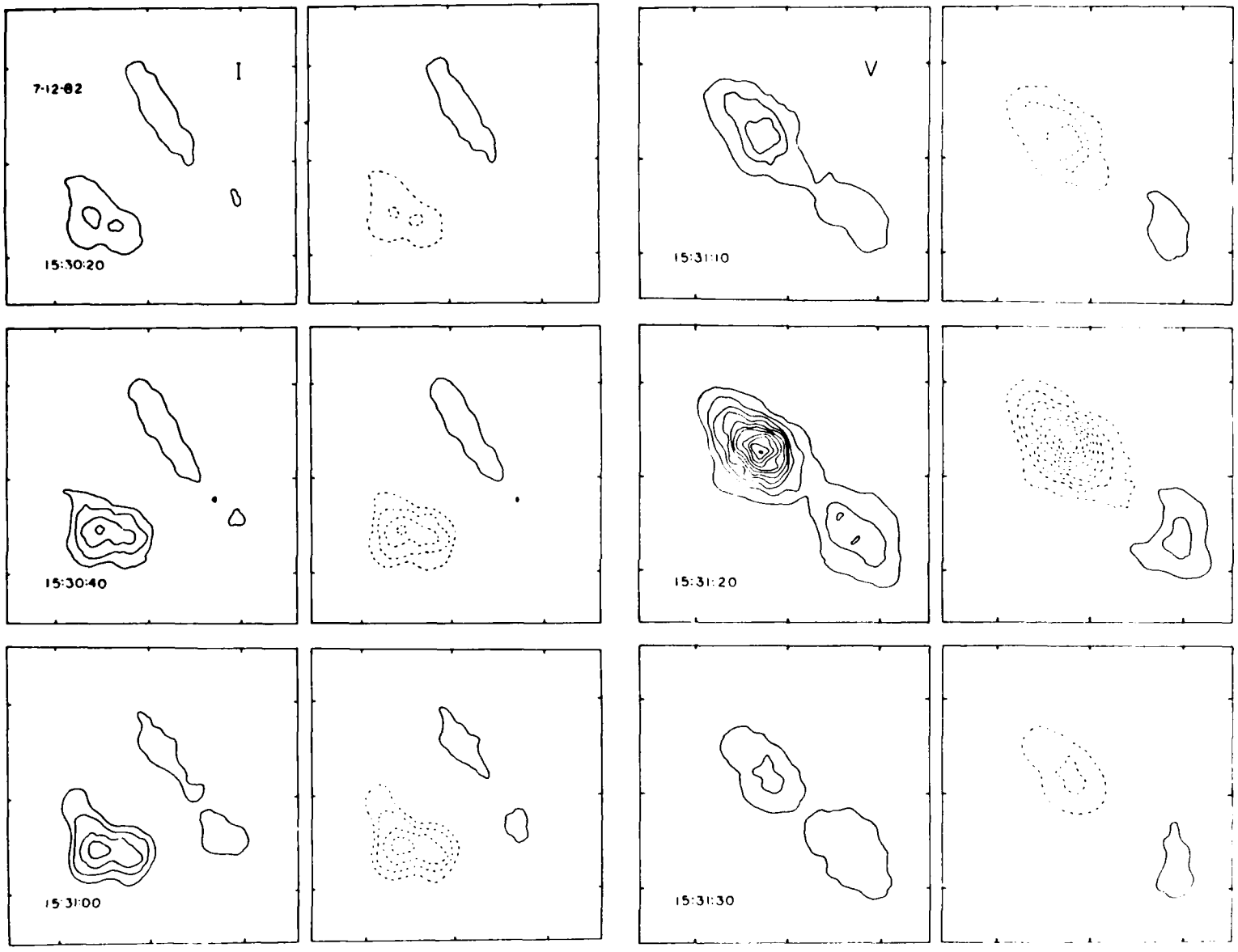

FIG. 2. A series of 10 s snapshot maps of the total intensity, I, and circular polarization, V, for the burst shown in Fig. 1. The contours of the map mark levels of equal brightness temperature, and the solid and dashed contours of the V maps denote positive and negative values of V, respectively. The development of the gradual burst emission is shown on the left-hand side. Maps of the impulsive phase are shown on the right-hand side. The outermost contour level and the contour interval of the gradual component maps are 2.4×10^6 K and 1.2×10^6 K, respectively. The outermost contour and contour interval of the impulsive phase maps are both equal to 7.2×10^6 K. The angular scale can be determined from the 30″ spacing between the fiducial marks on the axes.

TABLE 1

OBSERVED PARAMETERS OF SOLAR BURSTS NEAR 20 CENTIMETER WAVELENGTH

Date	Time (UT)	Wavelength (cm)	Maximum Brightness Temperature (K)	Maximum Circular Polarization (percent)	Angular Size (arcsec)
1982 Jul 12	15:31 15:32	21.7	1.5×10^8	~90	~45
1982 Jul 12	19:05 19:09	17.6	1.4×10^8	~70	~30
1982 Jul 12	20:03 20:07	21.7	2.0×10^7	~20	~40
1982 Jul 19	18:41 18:43	19.4	1.2×10^7	~40	~60
1982 Jul 20	21:49 21:51	19.4	1.3×10^7	~60	~60
1982 Jul 20	23:10 23:12	17.6	4.9×10^7	~25	~45

frequencies the half-power beamwidth of the individual antenna is ~31′ and the synthesized beamwidth was 3″ × 4″. Each 10 minute observation was followed by a 2 minute observation of the calibrator source OI 318. In all cases the bandwidth was 12.5 MHz, and the assumed calibrator flux was 1.7 Jy. The average correlated flux of 356 interferometer pairs was sampled every 10 s for both the left-hand circularly polarized (LCP) and right-hand circularly polarized (RCP) signals. The amplitude and phase of the correlated signal were then calibrated according to the procedure described by Lang and Willson (1979) together with a correction for the difference in the signal from high temperature noise sources detected in each polarization channel. These data were then edited and used to produce synthesis maps of both the total intensity, $I = (\mathrm{RCP} + \mathrm{LCP})/2$ and circular polarization $V = (\mathrm{RCP} - \mathrm{LCP})/2$ of the burst emission at intervals of 10 s. The CLEAN procedure developed by Clark (1980) was then used to produce synthesis maps with a dynamic range of about 10:1.

The date, time, observing wavelength, maximum brightness temperature and maximum degree of circular polarization, and angular size for six bursts are given in Table 1. In Figure 1 we show the time profile of the spikelike burst on July 12. The rapid impulsive spike lasting ~60 s is superposed on a more gradual component lasting about 2 minutes. In Figure 2 we present 10 s snapshot maps of both the total intensity, I, and circular polarization, V, for both of these components. The impulsive spike consists of two components of unequal intensity and size that are separated by about 45″ and which are nearly 100% oppositely circularly polarized. These two components are also connected by a bridge of weaker, unpolarized emission. The gradual component, which began about 1 minute before the impulsive spike, is contained within an adjacent source having a peak brightness temperature of $T_B \sim 6 \times 10^6$ K and a polarization of about 100%, suggesting that preburst heating in an adjacent part of the active region triggered the impulsive spike. An alternative explanation is that this component represents heating in an adjacent loop which was unrelated to the triggering of the burst. The impulsive emission occurred mainly along the legs of a magnetic loop. Kundu and Vlahos (1979) have shown that if the magnetic field strengths at the feet of a loop are different or if unequal numbers of particles are injected downward along each leg, then both the intensity and degree of circular polarization of the two microwave sources will be different, as is the case here. The bipolar structure of this burst is nevertheless uncommon, for the impulsive component of most microwave bursts occurs at the apices of coronal loops, rather than along their legs.

Figure 3 shows the time profile of a multiple-spike burst on July 12. The fourth and fifth spikes were associated with an Hα flare. Snapshot maps coinciding with the peaks of the spikes (Fig. 4) show that the most intense peaks (1, 4, and 5 in Fig. 3) arise from spatially separated structures having peak brightness temperatures between 2×10^7 K and 1.5×10^8 K and angular extents between 20″ and 50″ [linear extents

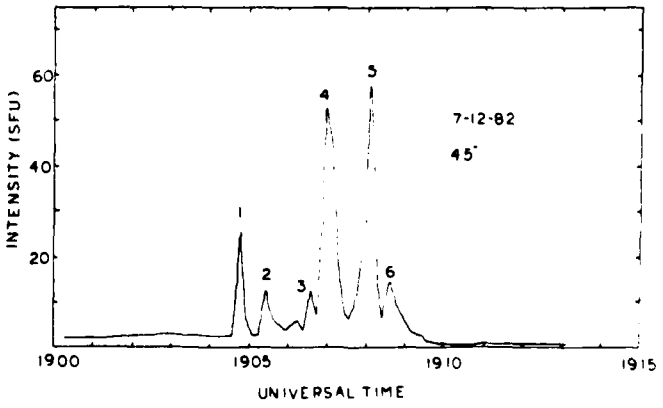

FIG. 3.—The time profile of a multiple-spike burst detected at 20 cm wavelength with an interferometer pair with angular resolution $\theta = 45''$ on 1982 July 12

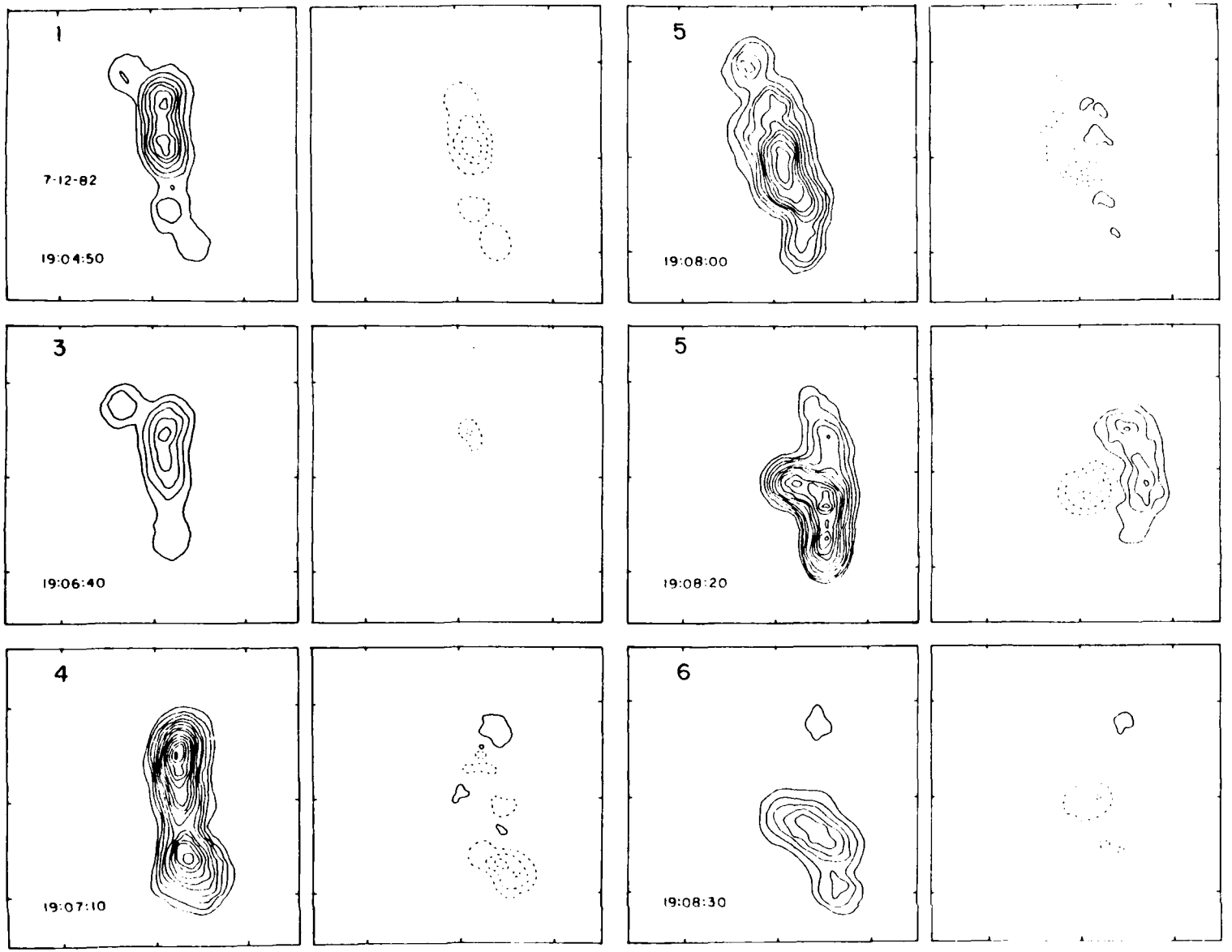

FIG. 4.—A series of 10 s snapshot maps made at the most intense peaks (1, 4, and 5) of the impulsive spikes of the complex burst whose time profile is shown in Fig. 3. The contours of the maps mark levels of equal brightness temperature and the solid and dashed contours of the I maps denote positive and negative values of I, respectively. For both sets of maps the outermost contour and the contour interval are both equal to 1.0×10^7 K. The angular scale can be determined from the 30″ spacing between the fiducial marks on the axes.

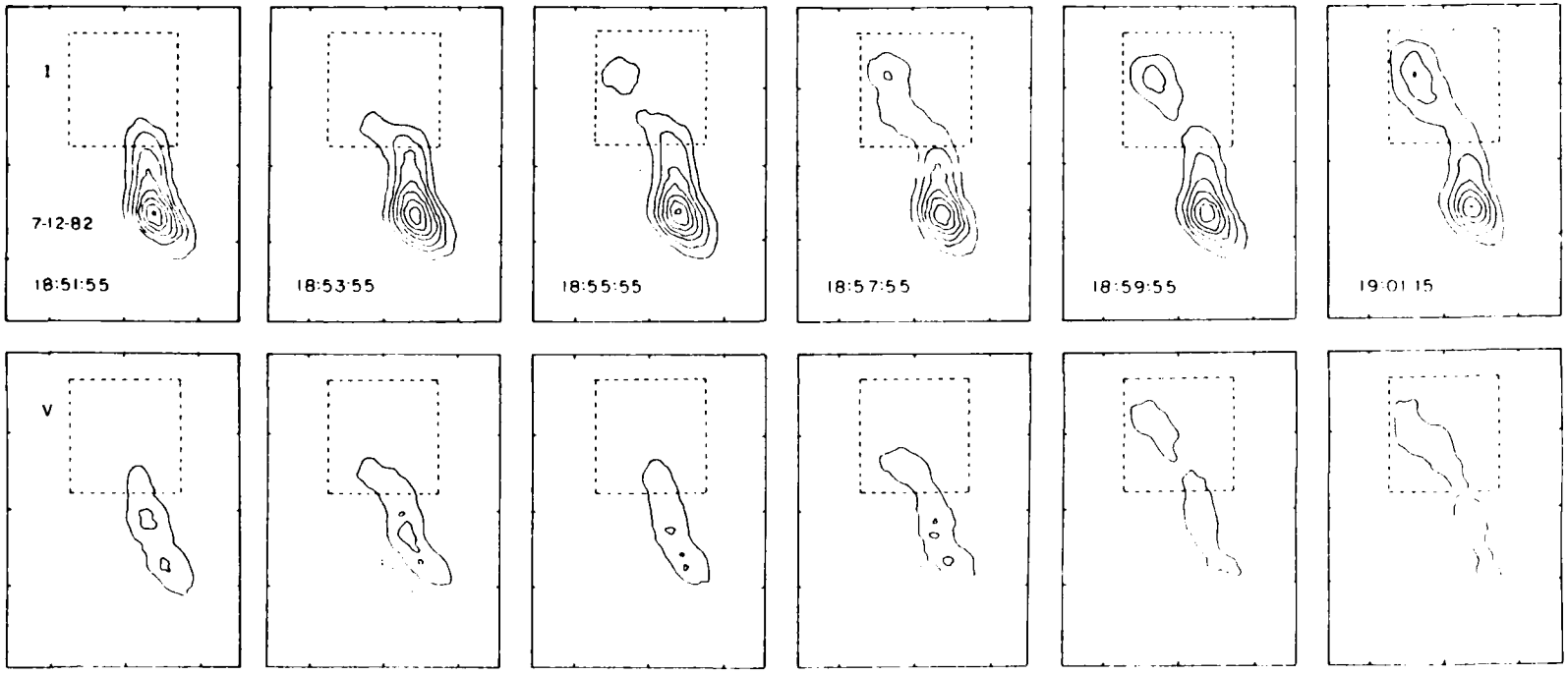

FIG. 5.—A series of VLA maps showing the development of the active region AR 3804 before the complex burst shown in Fig. 3. Each map of total intensity, I (*top*), and circular polarization, V (*bottom*), was made from 2 minutes of data beginning at the time indicated. The contours of both sets of maps mark levels of equal brightness temperature, and the solid and dashed lines of the V maps denote positive and negative values of V, respectively. For both sets of maps the outermost contour level and the contour interval are equal to 1.7×10^6 K. The angular scale can be determined from the 60" spacing between the fiducial marks on the axes. The arc within the dashed boxes corresponds to the field of view of the 10 s snapshot maps which are shown in Figure 4.

$L = (1.4\ 3.5) \times 10^9$ cm] The weaker spikes (2, 3, and 6 in Fig. 3) that followed a more intense spike were, however, located in the same source as the intense one. Thus, successive weak spikes seem to be emitted in the same loop, while successive intense spikes are emitted from different loops. This last conjecture is supported by the circular polarization changes that reflect different magnetic structures at the times of successive intense spikes.

In Figure 5 we show VLA synthesis maps of the preburst emission made during a 15 minute interval before the start of the first impulsive spike shown in Figure 3. Each map was made from 2 minutes of data beginning at the time indicated. Here the dashed boxes refer to the field of view of the 10 s snapshot maps of the impulsive spikes shown in Figure 4. Both the total intensity and circular polarization increased and changed in an adjacent source during the 15 minutes preceding the first spike. At 18:51:55 UT the peak brightness temperature of this adjacent source was $T_B \sim 7 \times 10^6$ K, about a factor of 3 to 4 above the brightness temperature typically observed in coronal radio loop structures (Kundu *et al.* 1977; Felli, Lang, and Willson 1981; Lang, Willson, and Rayrole 1982). The adjacent source began to heat up about 30 minutes before the onset of the impulsive spikes and remained at $T_B \sim 7 \times 10^6$ K until 5 minutes before the first impulsive spike. At this time the region of spiked emission began to heat up, while the adjacent source cooled to $T_B \sim 4 \times 10^6$ K. This newly heated region of spiked emission was about 60% right circularly polarized, suggesting that it occurred in one leg of a coronal loop.

In Figure 6 we show the time profile of the July 19 burst whose evolution is shown in Figures 7*a* and 7*b*. This event consists of two components, whose combined duration was 70 s. The burst structure at first consists of two sources separated by a bridge of weaker emission. The polarization maps (Fig. 7*b*) indicate that these two sources were oppositely circularly polarized ($\rho_c \approx 20\%$–30%) and that they therefore probably mark the legs of magnetic loops. One interpretation of the burst structure in total intensity (Fig. 7*a*) is that mass motions are occurring within the coronal loop. Craig and McClymont (1970) and Antiochos and Sturrock (1982) have pointed out that mass motions may play a role in the cooling of flare loops.

In Figure 8 we show the time profile of the July 20 burst, whose evolution is shown in Figure 9. A looplike structure having a peak brightness temperature of $\sim 5 \times 10^6$ K corresponds to the peak precursor, shown in Figure 8. Rapid polarization changes occurred before the main burst (see Fig. 9). The dipolar loop A-B either brightened or emerged at 23:09:50 UT, while the dipolar loop C-D brightened or emerged at 23:10:00 UT. There was also a brightening of A-B at 23:10:10 UT and a diming of B and C at 23:10:20 UT. All of these changes occurred before the main burst that was emitted at 23:10:40 UT. This impulsive peak is contained within a looplike structure, but it is oriented perpendicular to the present loop. The impulsive peak is also located nearly between the oppositely polarized sources A and B and may have been triggered by the brightening or emergence of this loop. The impulsive source apparently moved by $\sim 10''$ to the west during this time interval. This limbward displacement could be explained as an outward motion of the burst source or as the brightening of progressively higher lying loops. If the burst is moving radially outward from the surface of the Sun, then the inferred velocity is ~ 370 km s^{-1}. For comparison, the velocities of moving type IV bursts typically range between 250 and 1200 km s^{-1} (Pick and Trottet 1978; Robinson 1978; Kai 1978) while outward motions of 250–400 km s^{-1} have been detected in coronal X-ray burst loops (Poland *et al.* 1982; Antonucci *et al.* 1982).

In Figure 10 we compare the impulsive phase of this burst as well as that of another burst which began on the same day with simultaneous Hα photographs showing the underlying optical flares. Here the uncertainty in the alignment between the radio and optical pictures is $\pm 5''$. The figure shows that the centroids of both radio images are displaced limbward by $\sim 30''$–$40''$ with respect to the Hα kernels. This displacement can be attributed as a radial, limbward displacement caused by the greater height of the 20 cm emission, indicating a height $h = (2\text{–}3 \pm 0.4) \times 10^9$ cm above the solar photosphere. These values are consistent with the height $h \sim (3\text{–}4) \times 10^9$ cm for quiescent loops (Lang, Willson, and Gaizauskas 1983).

III. DISCUSSION

The observations presented here provide new insight into the evolution of solar microwave bursts and the physical

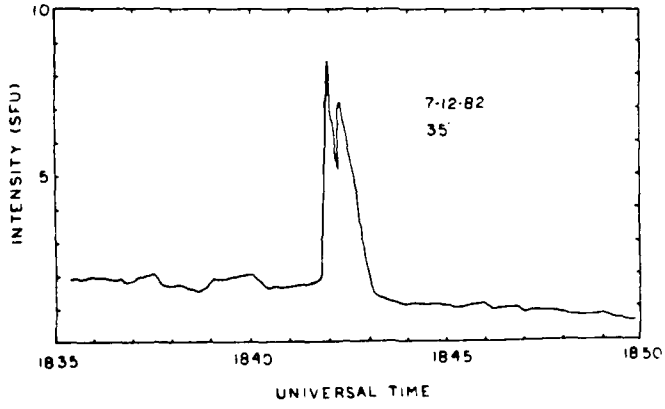

FIG. 6.—The fringe amplitude of the total intensity, I, vs. time for a burst detected at 20 cm wavelength with an interferometer pair with an angular resolution $\theta = 35''$ on 1982 July 19.

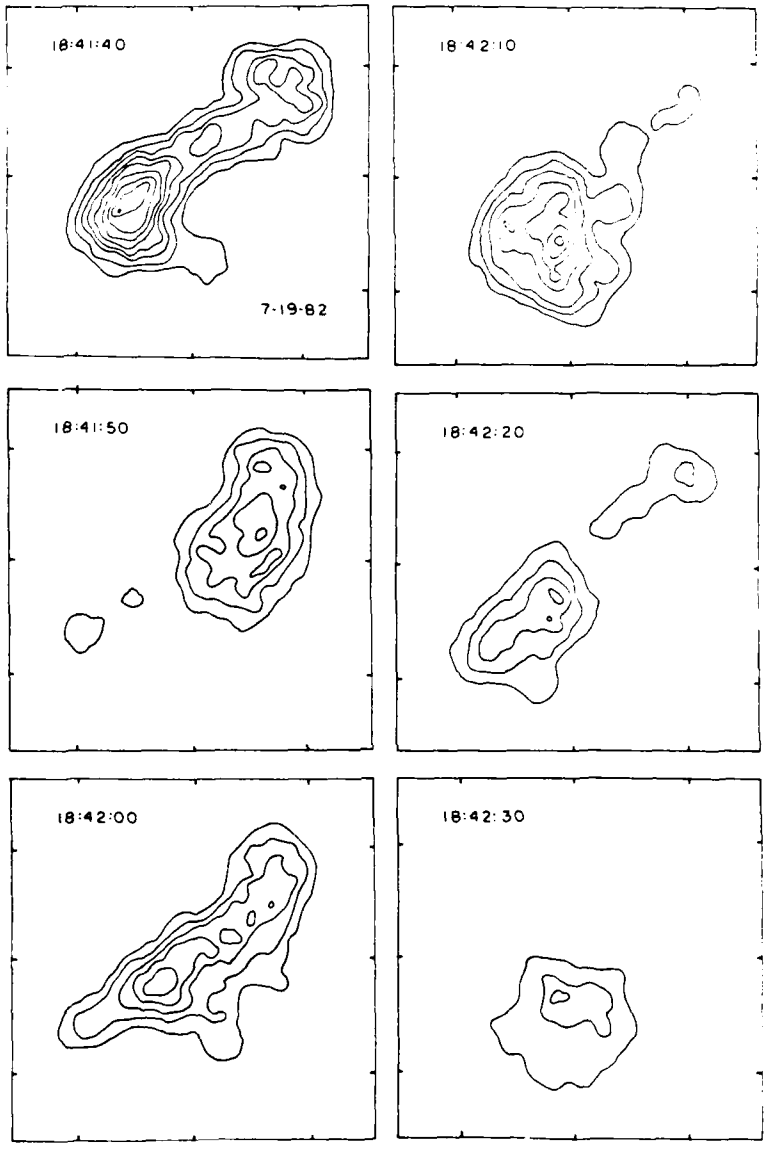

FIG. 7a

FIG. 7.—A series of 10 s snapshot maps of the total intensity, I (Fig. 7*a*), and circular polarization, V (Fig. 7*b*), for the burst shown in Fig. 6. The outermost contour and the contour interval of the I maps are both equal to 1.3×10^6 K. The outermost contour and the contour interval of the V maps are equal to 1.3×10^6 K and 6.5×10^5 K, respectively. The angular scale is determined by the 30" spacing between the fiducial marks on the axes.

processes which may trigger them. In one case, the intense components of multiple bursts originated in different sources, suggesting that a number of loops may have become successively activated like some complex X-ray bursts (Vorpahl *et al.* 1975; Kahler, Krieger, and Vaiana 1975). There is evidence for different magnetic field strengths at different times in the evolution of these X-ray bursts (Karpen, Crannell, and Frost 1979). Because only a small percentage of the magnetic energy is expected to be converted to particle energy during the impulsive phase (Baum and Bratenahl 1976), both the radio and X-ray results suggest that the components of intense multiple bursts originate in separate locations within an active region. On the other hand, this does not always occur, for Kundu, Bobrowsky, and Velusamy (1982) and Lang, Willson, and Felli (1981) found that the positions of the individual peaks of multiple component microwave bursts were at the same location to within a few seconds of arc, and we also found that weaker successive components originate in the same source.

We also found evidence for both preburst heating and magnetic changes that may have triggered the impulsive energy release in the loops. (Also see Lang 1974; Syrovotskii and

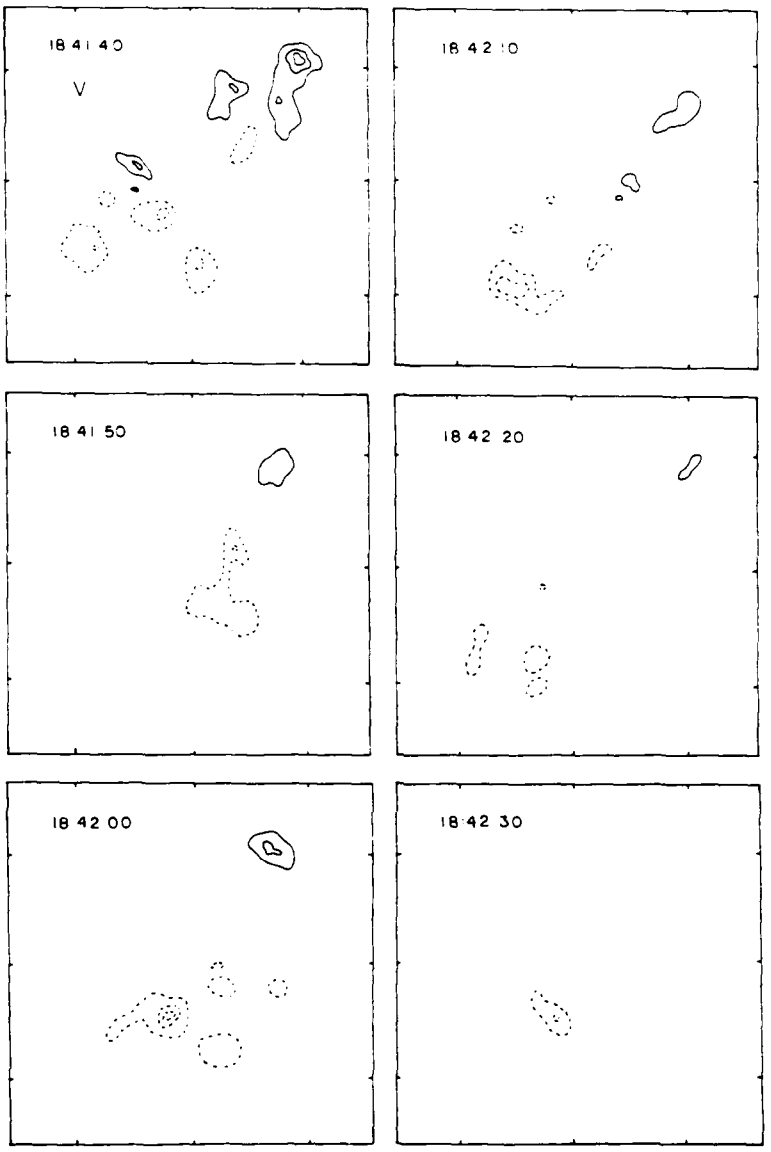

FIG. 7b

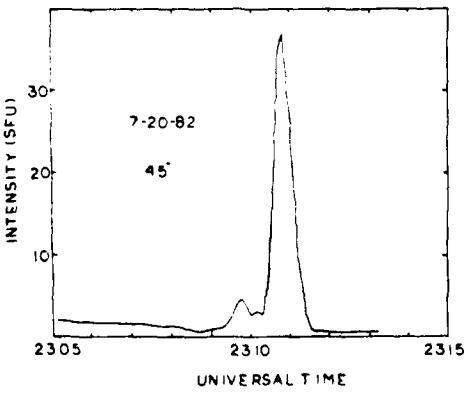

The fringe amplitude, I, vs. time for a burst detected at 20 cm wavelength with an interferometer pair whose angular resolution $\theta = 45''$ on

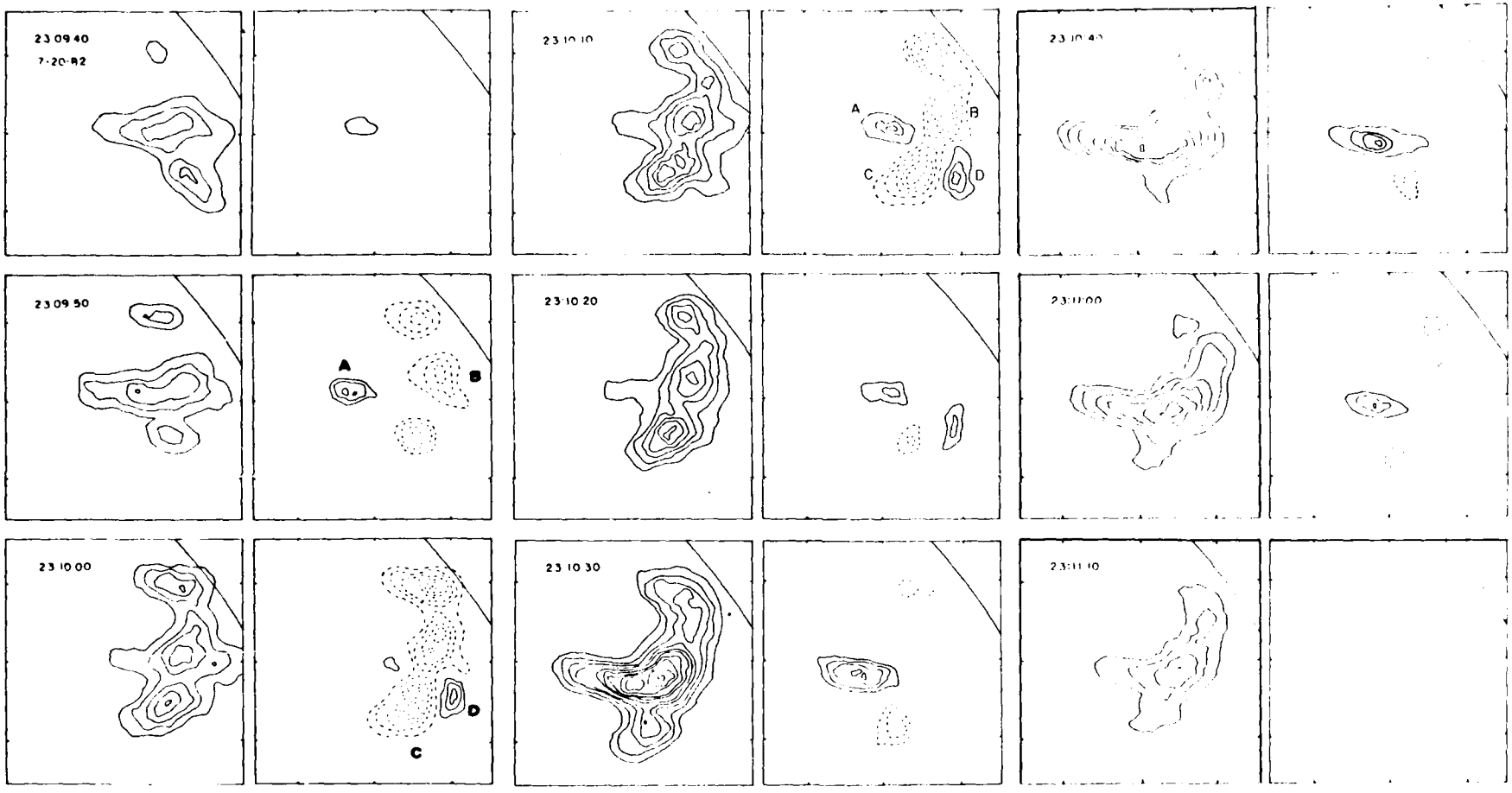

FIG. 9. A series of 10 s VLA snapshot maps of the total intensity, I, and circular polarization, V, for the burst shown in Fig. 8. The development of the preburst emission is shown between 23:09:40 and 23:10:50 UT. Maps of the impulsive phase are shown between 23:11:00 and 23:11:20 UT. The outermost contours of the preburst maps are equal to 1.7×10^6 K. The contour interval of the I and V maps are equal to 1.7×10^6 K and 8.5×10^5 K, respectively. The outermost contours of the impulsive phase maps are equal to 8.2×10^6 K. The contour interval of the I and V maps are equal to 8.2×10^6 K and 4.1×10^6 K, respectively. The curved line in the upper right-hand side of each box denotes the solar west limb. The angular scale can be inferred from the 30" spacing between fiducial marks on the axes.

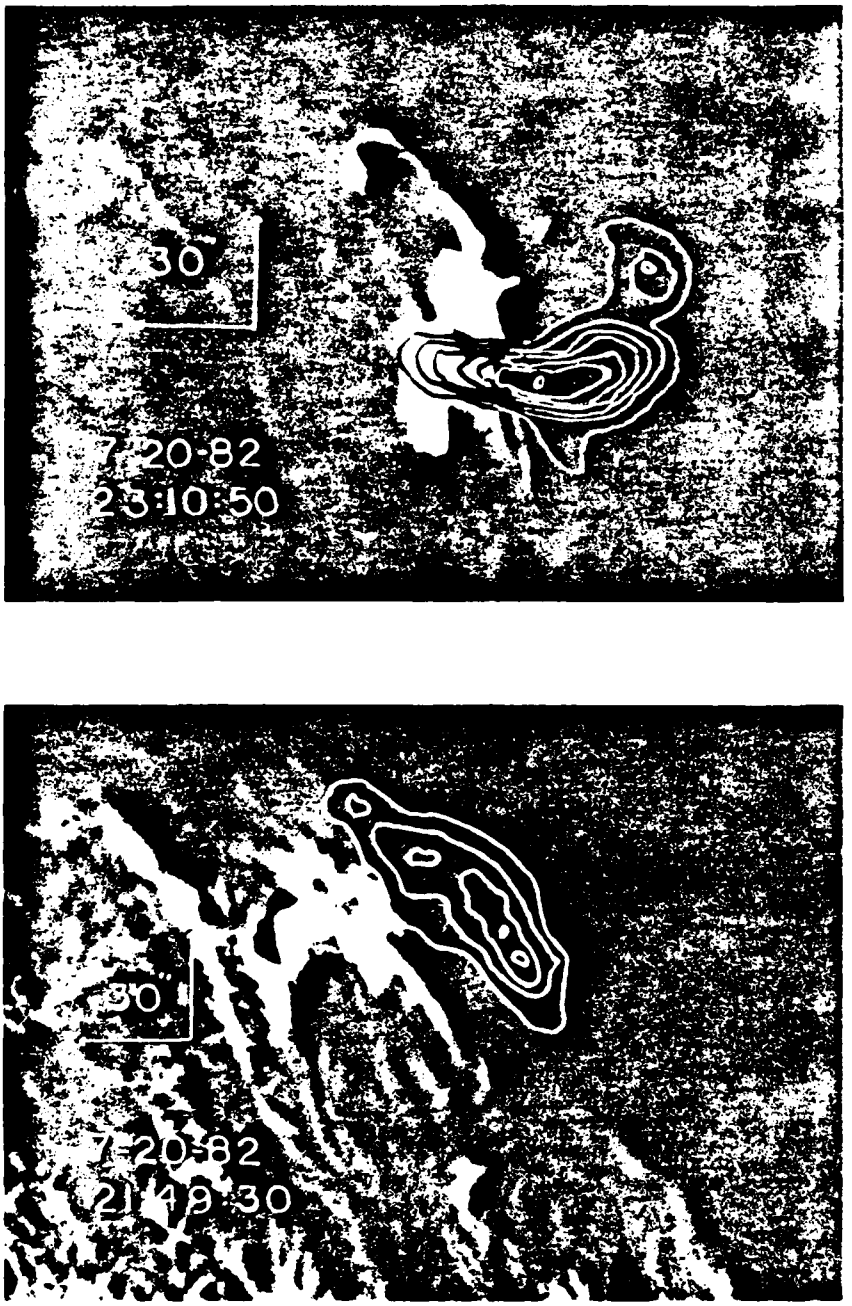

FIG. 10.—A 10 s VLA synthesis map of the impulsive phase of two bursts detected at 20 cm wavelength on 1982 July 20. The radio maps have been superposed on an Hα photograph of the optical flares taken at the same time. For both images, north is up, west is to the right. The Hα photograph was taken at the Big Bear Solar Observatory (courtesy of Margaret Liggett).

Kuznetzov 1980; Syrovotskii and Somov 1980; Webb and Kundu 1978; Webb 1980). The cause of the sudden temperature enhancements is uncertain. It is possible that we are viewing portions of magnetic loops where the opacity due to either gyroemission or thermal bremsstrahlung increased, thereby causing a temperature increase. Kundu *et al.* (1982) have speculated that if the dominant radiation mechanisms in preflare coronal loops is gyroemission, then the onset of currents in the lo[illegible] could increase the magnetic field strength to make the sou[illegible] optically thick at the third harmonic of the gyrofrequency (170 gauss at 20 cm). It is interesting to note, however, that for the burst which began at 19:04 UT on July 12, the impulsive sources were both left and right circularly polarized, whereas the newly heated preburst source was only right circularly polarized, suggesting that the impulsive and preburst sources were located in a different set of loops. In

another case we found that a loop system emerged about 20 s before the impulsive phase of the burst. Recently Kundu *et al.* (1982) observed a similar polarization change only a few tens of seconds before a 6 cm burst, which they believe to be related to the impulsive energy release. The quadrupole field configuration observed in these cases evokes flare models in which neighboring loops merge together and form current sheets between the interface of the loops, thereby triggering the impulsive phase of the burst (Gold and Hoyle 1960; Heyvaerts, Priest, and Rust 1977; Emslie 1982).

There were also cases where preburst changes were undetectable on time scales of minutes to several hours before the onset of the impulsive phase. Out of eight bursts observed at 2, 6, and 20 cm by Willson (1983), only one exhibited detectable preburst heating of the coronal loop in which the burst took place. These results suggest that preburst changes in the centimeter wavelength emission of coronal loops are not a general feature of the burst process, at least for relatively small bursts of a few solar flux units in size. A similar conclusion was reached by Kahler (1979) and Mosher and Acton (1980) who found no compelling evidence for X-ray enhancements during the few tens of minutes before weak X-ray events.

Solar radio astronomy at Tufts University is supported under grant AFOSR-83-0019 with the Air Force Office of Scientific Research. We are grateful to Margaret Liggett of the Big Bear Solar Observatory for providing the Hα photographs. The Very Large Array is operated by Associated Universities Inc., under contract with the National Science Foundation.

REFERENCES

Alissandrakis, C. E., and Kundu, M. R. 1978, *Ap. J.*, **222**, 342.
Antiochos, S. K., and Sturrock, P. A. 1982, *Solar Phys.*, **254**, 343.
Antonucci, E., *et al.* 1982, *Solar Phys.*, **78**, 107.
Baum, P. J., and Bratenahl, A. 1976, *Solar Phys.*, **47**, 331.
Clark, B. G. 1980, *Astr. Ap.*, **89**, 377.
Craig, I. J. D., and McClymont, A. N. 1976, *Solar Phys.*, **50**, 133.
Emslie, A. G. 1982, *Ap. Letters*, **22**, 41.
Felli, M., Lang, K. R., and Willson, R. F. 1981, *Ap. J.*, **247**, 325.
Gold, T., and Hoyle, F. 1960, *M.N.R.A.S.*, **85**, 553.
Heyvaerts, J., Priest, E. R., and Rust, D. M. 1977, *Ap. J.*, **216**, 123.
Kahler, S. W. 1979, *Solar Phys.*, **63**, 347.
Kahler, W. S., Krieger, A. S., and Vaiana, G. S. 1975, *Ap. J. (Letters)*, **199**, L57.
Kai, K. 1978, *Solar Phys.*, **61**, 187.
Karpen, J. T., Crannell, C. J., and Frost, K. J. 1979, *Ap. J.*, **234**, 370.
Kundu, M. R., Alissandrakis, C. E., Bregman, J. D., and Hin, A. C. 1977, *Ap. J.*, **213**, 278.
Kundu, M., and Vlahos, L. 1979, *Ap. J.*, **232**, 595.
Kundu, M. R., Bobrowsky, M., and Velusamy, T. 1982, *Ap. J.*, **251**, 342.
Kundu, M. R., Schmahl, E. J., Velusamy, T., and Vlahos, T. 1982, *Astr. Ap.*, **108**, 188.
Lang, K. R. 1974, *Solar Phys.*, **36**, 351.
Lang, K. R., and Willson, R. F. 1979, *Nature*, **278**, 24.
Lang, K. R., Willson, R. F., and Felli, M. 1981, *Ap. J.*, **247**, 338.
Lang, K. R., Willson, R. F., and Gaizauskas, V. 1983, *Ap. J.*, **267**, 455.
Lang, K. R., Willson, R. F., and Rayrole, J. 1982, *Ap. J.*, **258**, 284.
Marsh, K. A., and Hurford, G. J. 1980, *Ap. J. (Letters)*, **240**, L111.
Marsh, K. A., Zirin, H., and Hurford, G. J. 1979, *Ap. J.*, **228**, 610.
Mosher, J., and Acton, L. 1980, *Solar Phys.*, **66**, 105.
Pick, M., and Trottet, G. 1978, *Solar Phys.*, **60**, 353.
Poland, A. I., *et al.* 1982, *Solar Phys.*, **78**, 201.
Robinson, R. D. 1978, *Solar Phys.*, **60**, 383.
Syrovotskii, S. I., and Kuznetzov, V. D. 1980, in *IAU Symposium 86, Radio Physics of the Sun*, ed. M. R. Kundu and T. E. Gergeley (Dordrecht: Reidel), p. 445.
Syrovotskii, S. I., and Somov, B. V. 1980, in *IAU Symposium 91, Solar and Interplanetary Dynamics*, ed. M. Dryer and E. Tandberg-Hanssen (Dordrecht: Reidel), p. 425.
Velusamy, T., and Kundu, M. R. 1981, *Ap. J. (Letters)*, **243**, L103.
———. 1982, *Ap. J.*, **258**, 388.
Vorpahl, J. A., Gibson, E. G., Landecker, P. B., McKenzie, D. L., and Underwood, J. H. 1975, *Solar Phys.*, **45**, 199.
Webb, D. F. 1980, in *IAU Symposium 91, Solar and Interplanetary Dynamics* ed. M. Dryer and E. Tandberg-Hanssen (Dordrecht: Reidel), p. 189.
Webb, D. F., and Kundu, M. R. 1978, *Solar Phys.*, **57**, 155.
Willson, R. F. 1983, *Solar Phys.*, **83**, 285.

KENNETH R. LANG and ROBERT F. WILLSON: Department of Physics, Tufts University, Medford, MA 02155

Presented at the Solar Terrestrial Prediction Workshop - Observatoire de Paris
June 16, 1984 To be published in Artificial Satellites

E. HIGH RESOLUTION MICROWAVE OBSERVATIONS OF THE SUN AND NEARBY STARS

Kenneth R. Lang

Department of Physics and Astronomy
Tufts University
Medford, MA 02155
U.S.A.

ABSTRACT

High resolution microwave observations are providing new insights to the nature of active regions and eruptions on the Sun and nearby solar-like stars. The strength, evolution, and structure of magnetic fields in coronal loops are specified by multiple wavelength VLA observations. Unique tests of flare models can be made using VLA snapshot maps with angular resolutions of better than one second of arc in time periods as short as 3.3 seconds. Magnetic changes that precede solar eruptions on time scales of tens of minutes include magnetic shear within isolated coronal loops, emerging coronal loops, and the interaction of two orthogonal loops. Nearby main sequence stars of late spectral type emit slowly varying microwave radiation and stellar microwave bursts that show striking similarities to those of the Sun.

1. INTRODUCTION

High resolution observations of the Sun were limited for several decades to optical wavelengths that refer to a relatively thin slice of the solar atmosphere. These observations demonstrated that intense solar activity is limited to active regions containing sunspots that are linked by dipolar magnetic fields with strengths of a few thousand Gauss at the level of the visible solar surface, or photosphere. Changing magnetic fields within active regions were thought to provide the energy source for solar bursts, or flares; but the location of these changes could not be accurately specified from observations at optical wavelengths alone.

Microwave observations of the Sun in the 1960s and 1970s provided new dimensions to studies of solar active regions. Observations of the

quiescent, or non-flaring, microwave emission at different wavelengths refer to different levels of the solar atmosphere where the brightness temperatures are comparable to the local electron temperatures. The brightness temperatures, T_B, increase with increasing wavelength, λ, from $T_B \sim 10^4$ K at $\lambda = 2$ mm in the low chromosphere through $T_B \sim 10^5$ K at $\lambda = 2$ cm in the transition region to $T_B \sim 10^6$ K at $\lambda = 20$ cm in the low solar corona.

The microwave radiation of solar active regions is, with the exception of bursts, thermal in nature. The radiation at millimeter wavelengths is thermal bremsstrahlung. At centimeter wavelengths the gyroresonant radiation of thermal electrons accelerated by magnetic fields can compete with the bremsstrahlung of thermal electrons accelerated in the electric fields of ions. The dominant emission mechanism depends upon the wavelength and the physical conditions within the active region.[1]

A connection with intense magnetic fields is indicated by the high degrees of circular polarization of the microwave emission. These magnetic fields permeate every level of the solar atmosphere above active regions. The microwave observations uniquely provide direct measurements of the strength and structure of the magnetic fields in the transition region and lower corona. The sense of circular polarization is that of the extraordinary mode of wave propagation, with right-handed circular polarization corresponding to a positive magnetic field directed towards the observer. When thermal bremsstrahlung is the dominant radiation mechanism, the circular polarization is due to a propagation effect in the presence of a magnetic field, and the longitudinal magnetic field strength can be inferred from the polarization and the optical depth. When gyroresonance dominates, the circularly polarized radiation is emitted at the second or third harmonic of the gyrofrequency, enabling the magnetic field strength to be inferred from the observing frequency.[2]

The development of radio wavelength synthesis arrays in the 1970s permitted the spatial resolution of the solar microwave sources, and opened the way for comparisons with observations of similar angular resolution at optical and X-ray wavelengths. The high resolution microwave observations were initially carried out at 6 cm wavelength using the Very Large Array (VLA) and the Westerbork Synthesis Radio Telescope (WSRT). These 6 cm observations indicated that gyromagnetic effects predominate in the regions above sunspots, and that 6 cm maps of circular polarization specify the structure of the coronal magnetic field.[3]. The high resolution observations also indicated that the impulsive component of microwave bursts is usually located near the top of magnetic loops, and that brightness and polarization changes precede solar bursts on time scales of tens of minutes.[4]

Three reviews were written when the solar application of microwave aperture syntheses were at an early stage, dealing almost solely with observations at 6 cm wavelength.[5] This research area has matured in recent years, with multiple wavelength VLA observations and snapshot synthesis maps produced in time periods as short as 3.3 seconds. Here we provide a succinct review of these recent developments. We begin with the multiple wavelength studies

that specify the three dimensional structure of quiescent, or non-flaring, active regions. Perhaps the most important new development in this area has been the discovery of the microwave counterpart of the ubiquitous coronal loops that have previously only been observable using relatively expensive satellites at X-ray wavelengths. Snapshot maps of solar microwave bursts are discussed in the next section. New evidence is provided for preburst heating and magnetic changes that may trigger solar bursts. Recent observations of microwave emission from nearby stars conclude this review. Nearby stars of late spectral type are very similar to the Sun in their microwave emission, indicating the presence of active regions and intense surface magnetic fields.

2. QUIESCENT (NON-FLARING) MICROWAVE EMISSION FROM SOLAR ACTIVE REGIONS

Because the microwave emission from non-flaring active regions is only slowly varying over time scales of several hours, its detailed structure may be investigated using aperture synthesis techniques that use the Earth's rotation to create variable interferometric baselines. Synthesis maps of total intensity, I, describe the two-dimensional distribution of brightness temperature, while the synthesis maps of circular polarization, or Stokes parameter V, describe the two-dimensional structure of the longitudinal magnetic field. Observations at different wavelengths sample different levels within the solar atmosphere, with longer wavelengths referring to higher levels. The heights of the microwave structures can be inferred from their angular displacements from underlying photospheric features, and the two-dimensional maps at different wavelengths in the microwave domain can be combined to specify the three-dimensional structure of solar active regions.

Multiple wavelength synthesis observations of solar active regions have been mainly carried out at the Very Large Array (VLA) with 2, 6 and 20 cm wavelength[6]. As illustrated in Fig. 1, the emission at these wavelengths often originates at different heights within coronal loops that join sunspots of opposite magnetic polarity. The 2 cm emission has been attributed to thermal bremsstrahlung of the 10^5 K plasma that overlies sunspots at heights $h \sim 5{,}000$ km where the longitudinal magnetic field strengths $H_\ell \sim 10^3$ Gauss. Bright, highly polarized 6 cm cores mark the legs of magnetic dipoles with brightness temperatures $T_B \sim 2$ to 5×10^6 K and heights $h \sim 30{,}000$ km above the underlying sunspots. Longitudinal magnetic field strengths of $H_\ell \sim 600$ Gauss are inferred from the fact that these 6 cm cores emit gyroradiation at the third harmonic of the gyrofrequency. The 20 cm emission comes from the hot, dense plasma that is trapped within the magnetic loops that connect underlying sunspots. These 20 cm coronal loops have brightness temperatures $T_B = 2$ to 4×10^6K and extents of about 100,000 km. The 20 cm emission may be attributed to thermal bremsstrahlung and/or gyroresonant radiation.

One of the most satisfying observational results has been the detection of circularly polarized horseshoe or ring shaped structures that were predicted using the theory of gyroresonant emission from individual sunspots.[7]

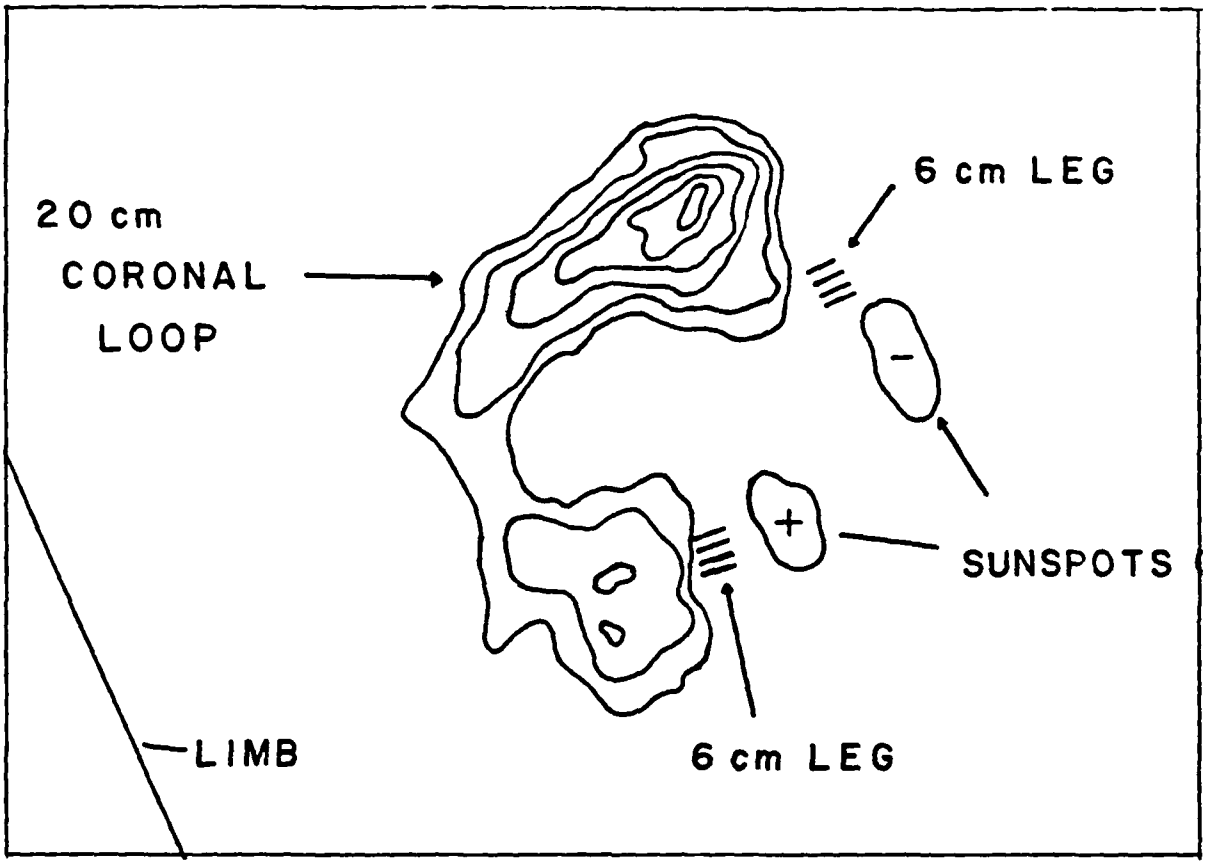

Fig. 1. A VLA synthesis map of a coronal loop at 20 cm wavelength. The contours mark levels of equal brightness temperature corresponding to 0.2, 0.4... 1.0 times the maximum brightness temperature of $T_B = 2.0 \times 10^6$ K. A schematic portrayal of the 6 cm microwave emission, which comes from the legs of magnetic dipoles, has been added together with the underlying sunspots that are detected at optical wavelengths.

Circular polarization maps at 6 cm wavelength reveal highly polarized (up to 100%) structures that lie above the curved magnetic fields of sunspot penumbrae (see Figure 2). There is no detectable circular polarization above the central sunspot umbrae whose magnetic fields project radially upwards into the hot coronal regions. The total intensity of the 6 cm radiation is often enhanced above the sunspot umbrae, with brightness temperatures of $T_B \sim 10^6$ K. A 6 cm brightness depression has also been detected above some sunspot umbrae. This depression may be attributed to cool material above sunspot umbrae, or to geometrical effects. For instance, there is negligible gyroresonant absorption when the angle between the magnetic field and the line of sight is small. Both cool material and variable absorption may be present, but the two effects cannot be easily disentangled.

Fig. 2. A 6 cm synthesis map of circular polarization V superimposed on an offband Hα photograph of the same region. The angular scale is denoted by the 30" spacing between fiducial marks on the axes. The contours mark levels of equal brightness temperature corresponding to 0.3, 0.4....0.9 times the maximum brightness temperature of $+3.0 \times 10^5$K and -2.8×10^5K.

VLA observations of coronal loops are particularly important. These ubiquitous loops are the dominant structural element in the solar corona, but they have previously only been detected during rare and expensive satellite observations at soft X-ray wavelengths. These magnetic loops have now been detected using the VLA at both 6 and 20 cm wavelength.[8] The unique aspect of these microwave observations is that they can be used to specify the structure and strength of the coronal magnetic field. This is not possible with any other technique, either at optical or X-ray wavelengths.

Although gyroresonance in the legs of magnetic loops usually dominates the 6 cm emission, weaker bremsstrahlung can sometimes be detected at 6 cm near the loop apex. The coronal loops are more reliably detected using the VLA at 20 cm wavelength where emission from the entire loop is routinely detected. The magnetic, temperature and density structure of the coronal loops are specified from the 20 cm observations. Much, if not all, of this emission is due to the thermal bremsstrahlung of the same hot plasma that gives rise to the X-ray emission. Because the magnetic energy density dominates the thermal energy density at coronal heights, this plasma remains trapped within the magnetic loops. Electron temperatures T_e = 2 to 4 x 10^6 K, electron densities $N_e \sim 10^9$ to 10^{10} cm^{-3}, loop extents $L \sim 10^9$ to 10^{10} cm are inferred from the 20 cm bremsstrahlung, while longitudinal magnetic field strengths of $H_\ell \sim 50$ Gauss are inferred from the circular polarization if it is due to propagation effects. Thermal gyroresonance emission may also sometimes play a role in the 20 cm coronal loops, and in this case stronger magnetic fields of $H_\ell \sim 200$ Gauss are inferred from the polarization data.

3. MICROWAVE BURSTS FROM SOLAR ACTIVE REGIONS

The VLA has also been recently used to detect changes in the configuration of coronal magnetic fields and temperature enhancements within coronal loops that play an important role in the excitation of solar bursts. The origin and prediction of these powerful bursts is one of the most important and interesting problems of solar physics. It has long been known that solar eruptions are intimately connected with the magnetic fields in active regions, for the ultimate source of energy for these bursts must be magnetic energy. It has only recently been realized, however, that evolving magnetic fields in the solar corona may play a dominant role in triggering solar eruptions. Theoretical considerations indicate that emerging coronal loops, magnetic shear within these loops, and interacting coronal loops can trigger solar bursts and supply their energy.[9] These effects can now be observed for the first time by using the VLA to specify the magnetic field topology in active regions with angular resolutions of better than one second of arc in time periods as short as 3.3 seconds.

It has been known for several years that preflare changes in active regions are detected as increases in the intensity and polarization of the microwave emission at centimeter wavelengths. These increases precede solar eruptions on time scales of ten minutes to an hour. They suggest that new magnetic loops are emerging or that existing magnetic fields are becoming more ordered. The high angular resolution provided by the VLA has now shown that these increases are related to preburst heating in coronal loops and to changes in the coronal magnetic field topology. The VLA snapshot maps have also enabled tests of flare models that could not be carried out at optical wavelengths.

The VLA results indicate that no single flare model is versatile enough to explain the diverse ways in which magnetic energy is dissipated in solar bursts. This is not terribly surprising in view of the magnetic complexity of solar active regions. Preburst changes can nevertheless be ordered into three major categories - changes within a single coronal loop, emerging coronal loops, and interaction between coronal loops.[10]

Single coronal loops or arcades of loops often begin to heat up and change structure about 15 minutes before the eruption of impulsive bursts. As illustrated in Figure 3, the magnetic loop heats up and twists in space. The magnetic shear produces a current sheet that triggers burst emission. Radio and X-ray data have been combined to derive a peak electron temperature $T_e = 2.5 \times 10^7$ K and an average electron density of $N_e = 10^{10}$ cm^{-3} during the preburst heating phase of the example shown in Fig. 3. Preburst heating and magnetic field changes can also occur in loops that are adjacent to, but spatially separated from, the sites of the impulsive bursts.

Preburst activity is also detected in coronal loops that are adjacent to those which emit bursts. New bipolar loops can emerge and interact with preexisting ones. When the polarity of the new emerging flux differs from that of the preexisting flux, current sheets are produced that trigger the emission of bursts. A similar process can occur when preexisting adjacent loops undergo magnetic changes and trigger eruptions in nearby coronal loops.

A third type of preburst activity occurs during the development of two bipolar loops just prior to impulsive energy release. As illustrated in Fig. 4, a quadrupole structure can be formed in which the field lines of the two loops are in orthogonal directions. A current sheet develops at the interface of the two closed loops, thereby triggering burst emission.

The microwave bursts are themselves characterized by a strongly polarized, compact (5" to 30") impulsive component with a brightness temperature of $T_B = 10^7$ to 10^{10} K lasting between 1 and 5 minutes. This is followed by a larger, longer post-burst component with relatively low polarization and brightness temperature. The impulsive bursts are due to the gyrosynchrotron radiation of mildly relativistic electrons with energies of 100 to 500 keV.

The primary release of microwave energy takes place in the coronal part of magnetic loops. The impulsive part of the microwave energy is usually released in the upper parts of coronal loops and between the flaring Hα kernels that mark the footpoints of magnetic loops (see Fig. 5). The emitting region at 6 cm wavelength occupies a large fraction of the flaring loops near their tops, while the 2 cm emission is more concentrated towards the loop apex.

A nonthermal tail of high energy electrons with energies greater than 100 keV is created near the top of a single coronal loop or an arcade of loops. Some of these electrons are trapped in the upper parts of the loops, producing the microwave bursts by synchrotron radiation. Other electrons

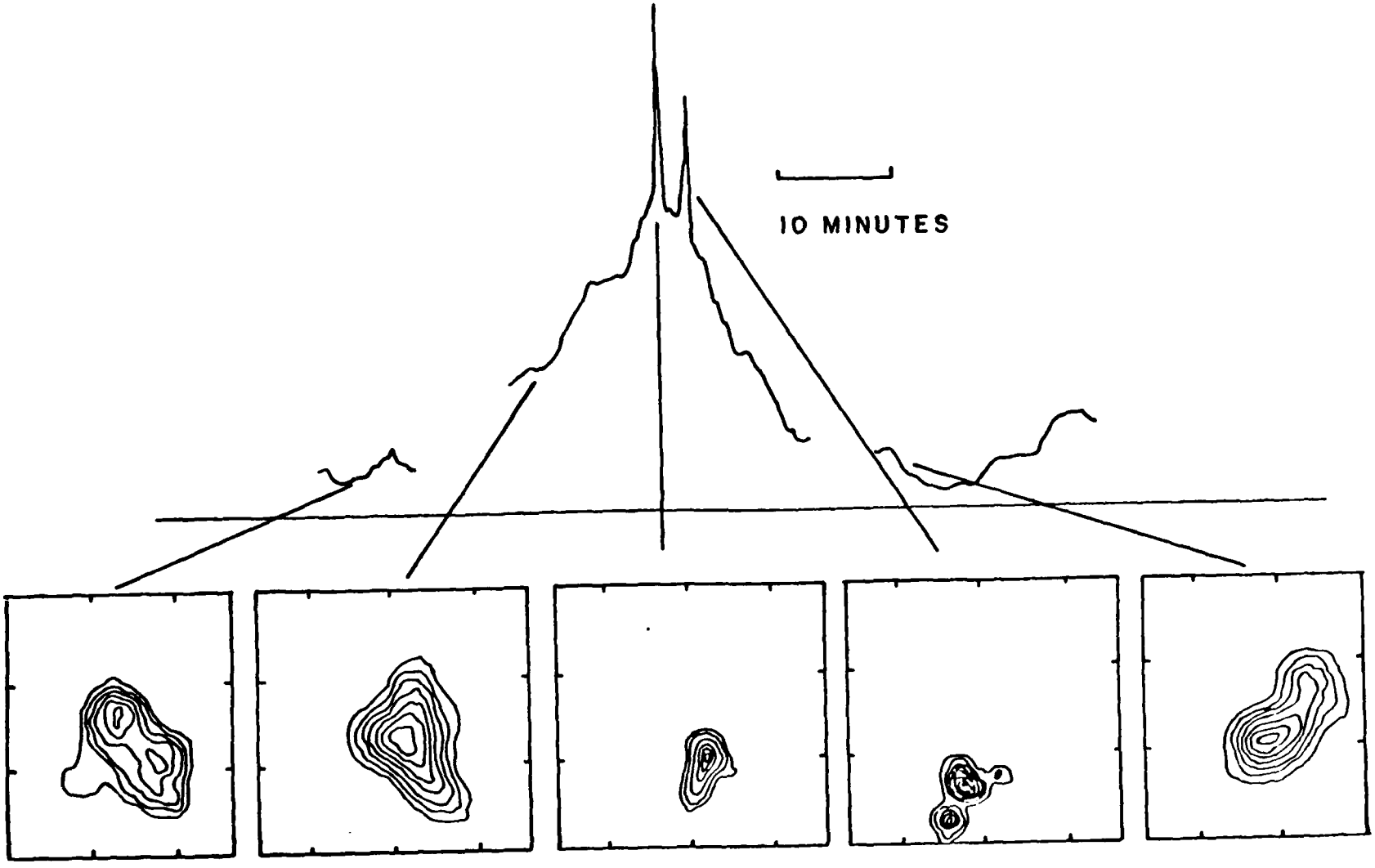

Fig. 3. The time profile of a solar burst at 20 cm wavelength illustrates heating within a coronal loop prior to the emission of two impulsive bursts. The 20 cm V.L.A. synthesis maps for ten second intervals are given below. They show that a coronal loop twisted in space.

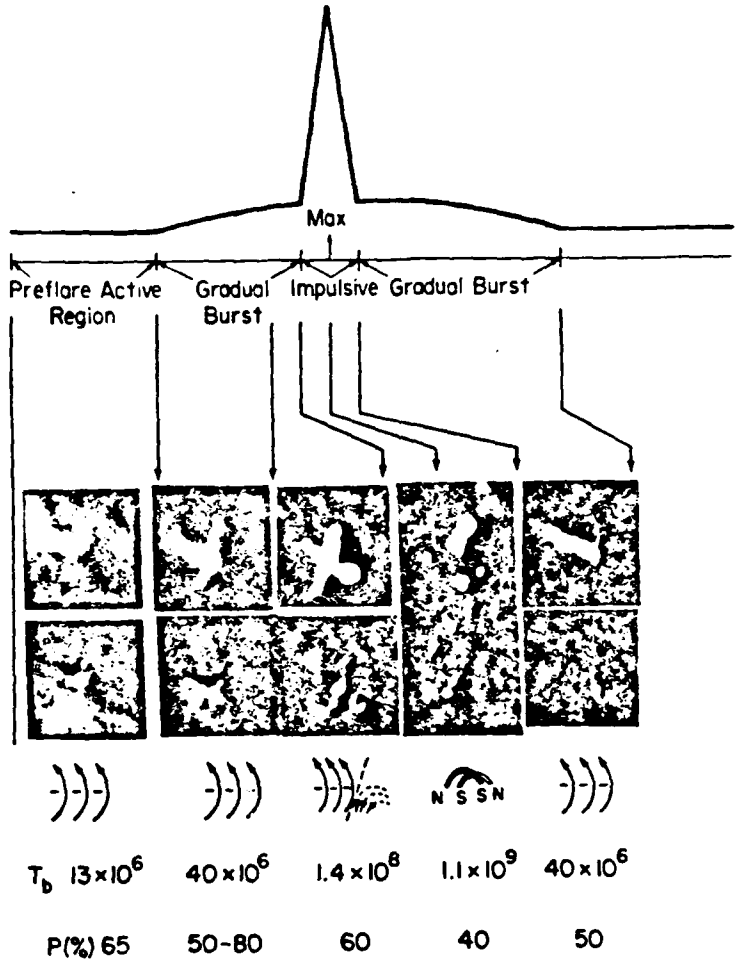

Fig. 4. The time profile and ten second VLA synthesis maps of a solar burst at 6 cm wavelength. The peak brightness temperatures, degrees of circular polarization and loop structure are given below the synthesis maps. Two dipolar loops emerged to form a quadrupolar structure. The interacting loops triggered the emission of an impulsive burst. (Adapted from M.R. Kundu, Solar Phys. 86, 205 (1983).)

stream down to the loop footpoints, producing hard X-ray bursts by thick target bremsstrahlung.

During the course of impulsive bursts, the microwave source sometimes drifts towards the limb. This apparent limbward motion can be attributed to a radial outflow at velocities of a few hundred kilometers per second. Alternatively, bursts could be sequentially triggered at higher levels in the solar atmosphere.

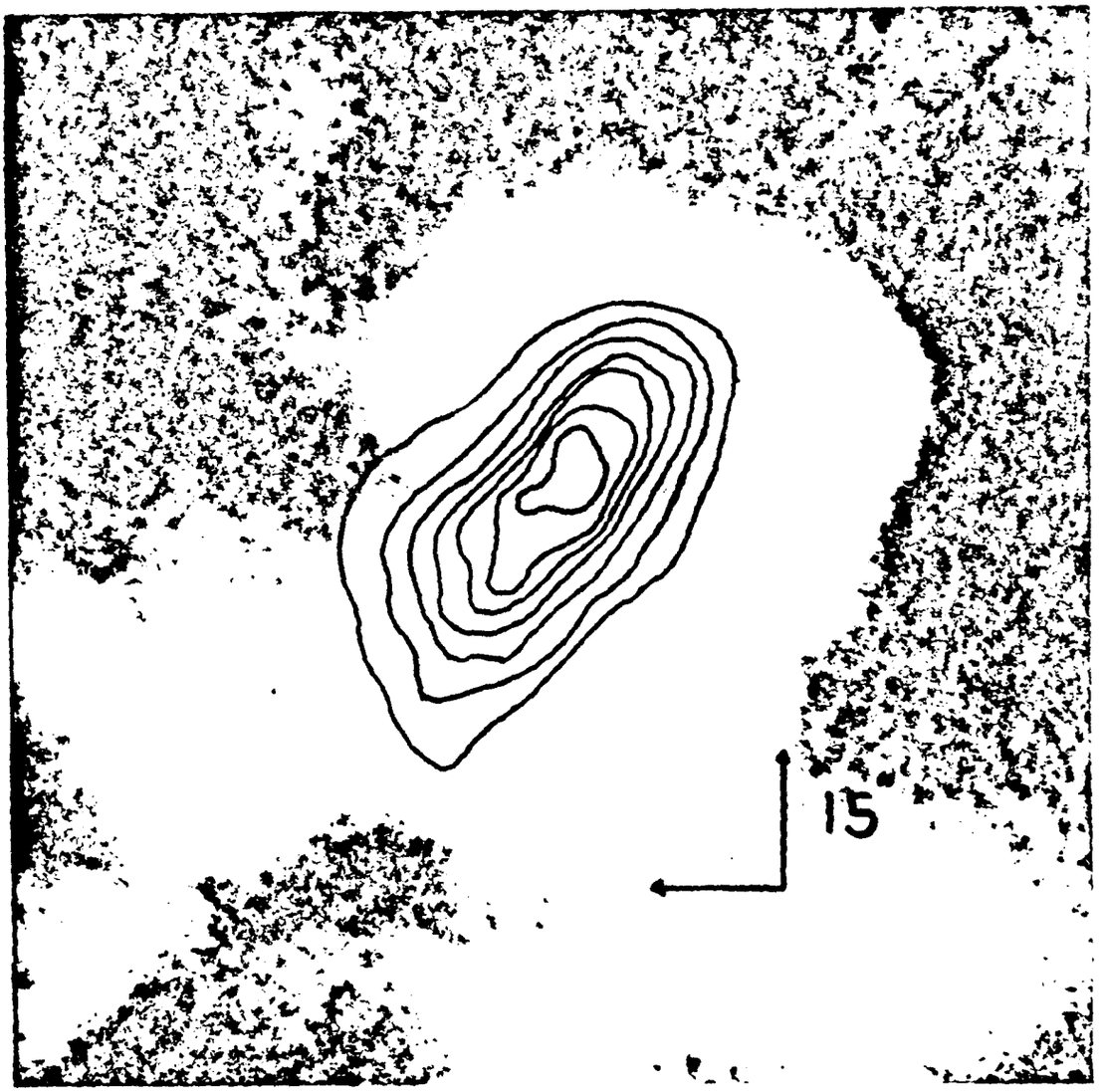

Fig. 5. A ten second VLA synthesis map of a solar burst at 6 cm wavelength is superimposed upon an Hα photograph taken at the same time at the Big Bear Solar Observatory. The contours mark levels of equal brightness temperatures corresponding to 5.5×10^6, 1.1×10^7,...3.8×10^7K. The microwave energy is released in a large part of the top of the dipolar loop, while the Hα kernels are emitted at the footpoints of the loop.

There is also evidence for the sequential triggering of microwave bursts in different loops within magnetically complicated regions. As illustrated in Fig. 6, successive intense bursts can originate in adjacent coronal loops, whereas successive weaker bursts are located in the same coronal loop.

AD-A152 027 VERY LARGE ARRAY OBSERVATIONS OF CORONAL LOOPS AND RELATED OBSERVATIONS O..(U) TUFTS UNIV MEDFORD MA DEPT OF PHYSICS K R LANG 29 JAN 84 AFOSR-TR-85-0256 2/2

UNCLASSIFIED AFOSR-83-0019 F/G 3/2 NL

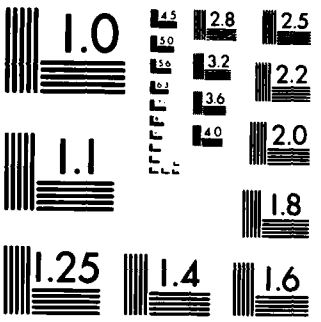

MICROCOPY RESOLUTION TEST CHART
NATIONAL BUREAU OF STANDARDS-1963-A

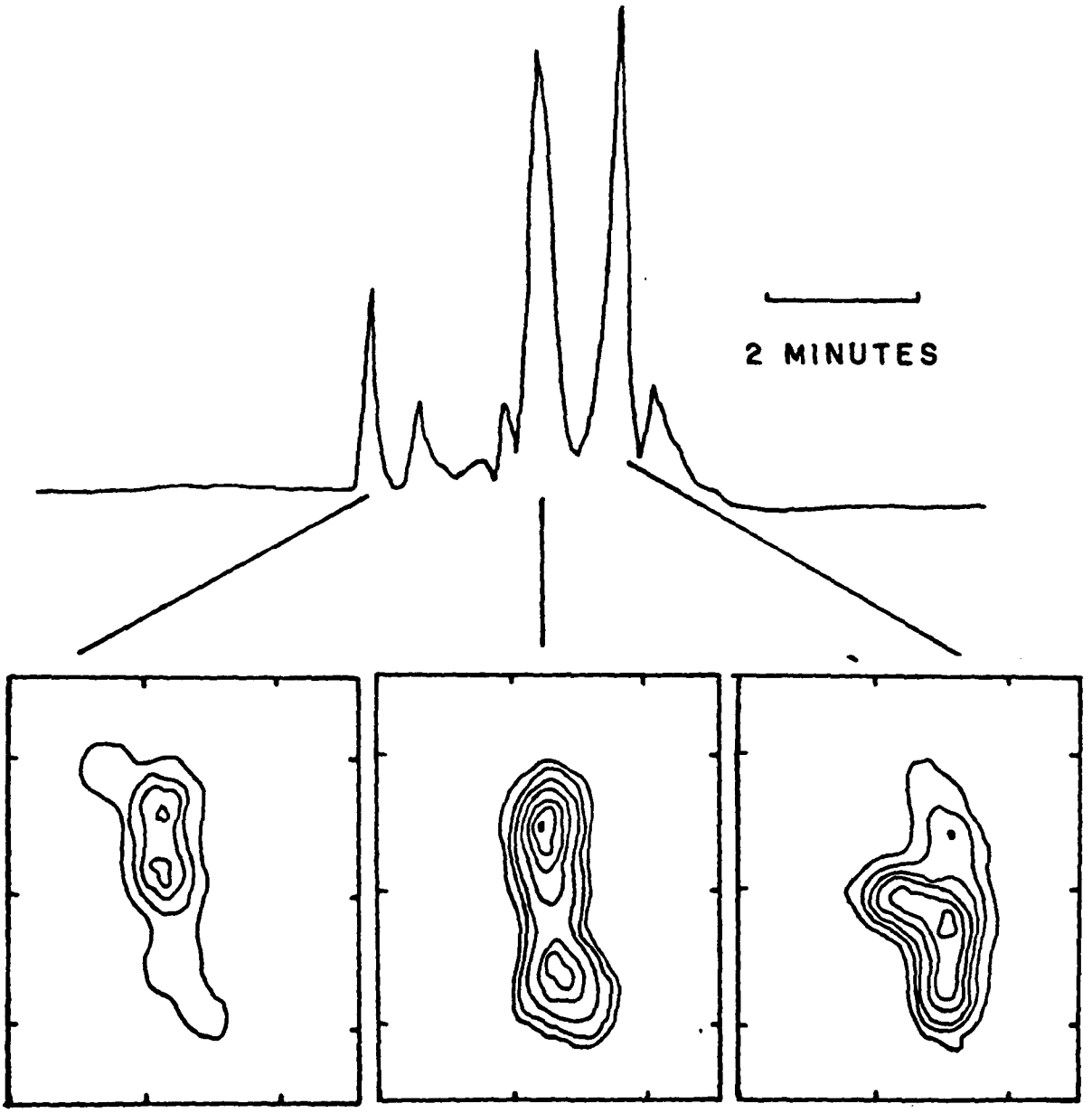

Fig. 6. The time profile of successive impulsive bursts at 20 cm wavelength is compared with ten second VLA synthesis maps at the same wavelength. Although the successive weak bursts numbered 2 and 3 were emitted from the same coronal loop as burst 1, the successive intense bursts, 1, 4 and 5, arose from spatially separated coronal loops having peak brightness temperatures of between 2×10^7 and 2×10^8 K. Here the contour intervals are in steps of 1.0×10^7 K.

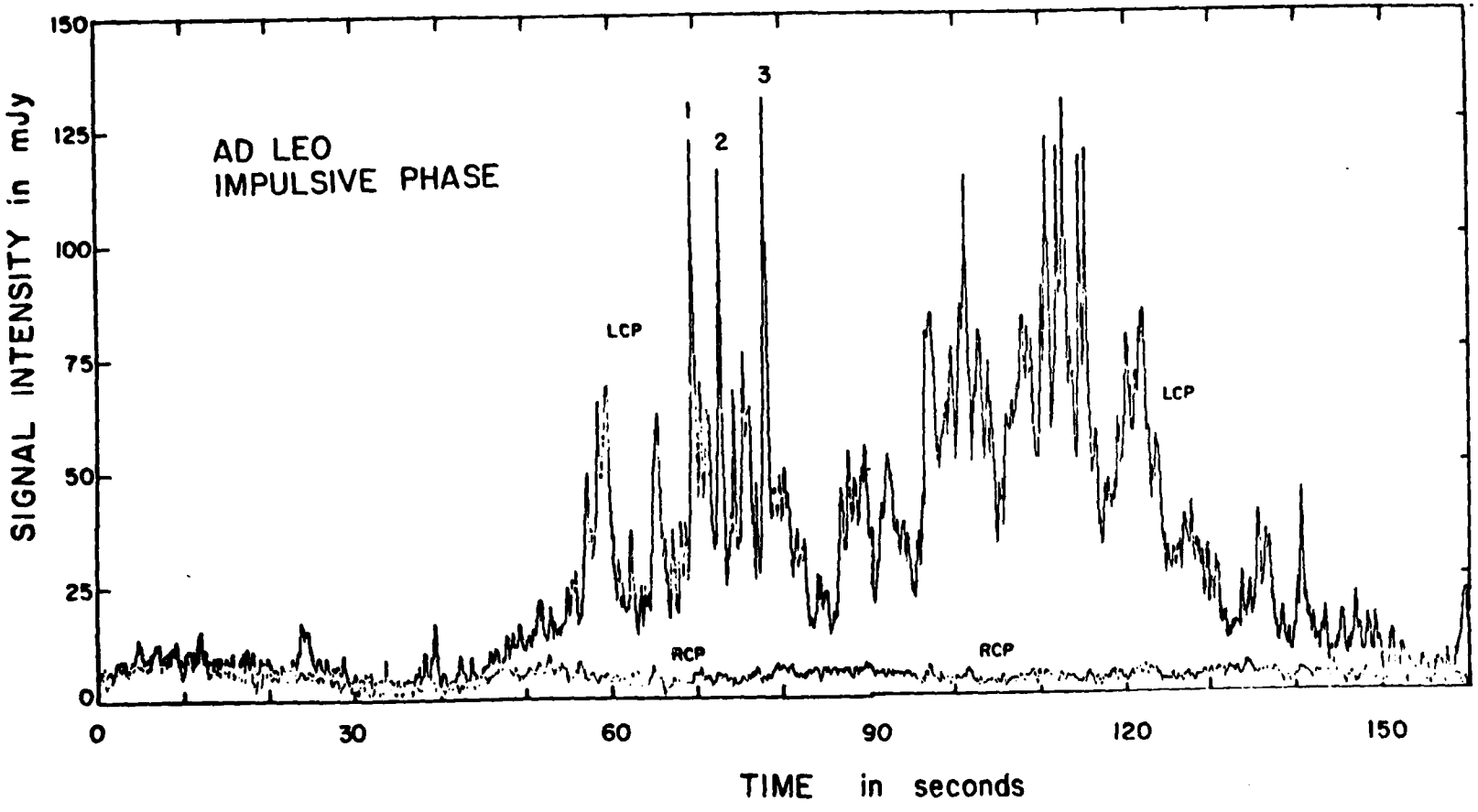

Fig. 7. Rapid, highly polarized spikes make up this 20 cm burst from the dwarf M star AD Leo. The spikes marked 1, 2 and 3 each had rise times of less than 200 milliseconds, indicating that the emitting source was less than 6 x 10^9 cm across. Brightness temperatures in excess of 10^{13} K are inferred for these spikes.

4. MICROWAVE EMISSION FROM NEARBY STARS OF LATE SPECTRAL TYPE

Nearby main sequence stars of late spectral type exhibit quiescent X-ray emission whose absolute luminosity may be as much as one hundred times that of the Sun. This suggests that these stars have large-scale coronal loops and intense magnetic fields. The solar analogy indicates that the hot coronal plasma ought to be detected at 20 cm wavelength, and that polarized 6 cm emission should reveal the presence of large scale magnetic structures.

In fact, the dwarf M flare stars exhibit slowly varying, circularly polarized microwave emission at 6 cm wavelength that is analogous to the quiescent, or non-flaring, microwave emission from solar active regions.[11] Brightness temperatures of $T_B = 10^7$ to 10^8 K are inferred if the microwave emitting source covers the entire visible surface of the star. Brightness temperatures comparable to that of the Sun's quiescent microwave emission ($T_B \sim 10^6$ K) are obtained if the stellar emitting region is three times as large as the visible star. If this is the case, the detected emission can be explained as the gyroresonant emission from thermal electrons spiralling in magnetic fields with a strength of $H_\ell \sim 300$ Gauss. Alternatively, the gyrosynchrotron emission of a small number of energetic electrons in starspots may account for the stellar microwave emission.

The dwarf M flare stars also exhibit microwave bursts that are similar to those emitted by the Sun.[12] The stellar microwave bursts are circularly polarized impulsive events with durations of a few minutes. As illustrated in Fig. 7, the impulsive burst from the dwarf M star AD Leo is composed of a rapid sequence of highly polarized (100%) spikes with rise times of less than 200 milliseconds. An upper limit to the linear size of the emitting region is 6×10^9 cm, the distance that light travels in 200 milliseconds. If the emitting starspot is symmetric, it has an area that is less than 3 percent of the star's surface area, and its brightness temperature exceeds 10^{13} K. The high brightness temperature and high degrees of circular polarization of these star bursts can be explained in terms of electron-cyclotron maser emission at the second harmonic of the gyrofrequency in longitudinal magnetic fields of strength $H_\ell \sim 250$ Gauss.

Curiously, the impulsive microwave bursts from the Sun sometimes exhibit rapid millisecond fine structure that is also 100% circularly polarized. Brightness temperatures as high as $T_B > 10^{15}$K have been inferred for the solar spikes, indicating that they are also due to a non-thermal, coherent radiation mechanism of the electron-cyclotron masing type.

ACKNOWLEDGEMENTS

This work was done in collaboration with Robert F. Willson. Radio astronomical studies of the Sun at Tufts University are supported under grant AFOSR-83-0019 with the Air Force Office of Scientific Research. Related studies of nearby stars are supported under NASA grant NAG 5-477.

REFERENCES

1. V.V. Zheleznyakov: (1962), Sov. Astron. A.J. 6, 3; T. Kakinuma and G. Swarup: (1962), Astrophys. J. 136, 975 ; M.R. Kundu: Solar Radio Astronomy (Interscience, New York, 1965); P. Lantos: (1968), Ann. d'Astrophys. 31, 101; E. Ya Zlotnik: (1968), Sov. Astron. A.J. 12, 245, 464; V.V. Zheleznyakov: (1970), Radio Emission from the Sun and Planets (Pergamon, New York), A. Kruger: (1979), Introduction to Solar Radio Astronomy and Radio Physics (Reidel, Boston).

2. J.A. Ratcliffe: The Magneto-Ionic Theory (Cambridge University Press, Cambridge, 1962); K.R. Lang: (1980), Astrophysical Formulae (Springer-Verlag, New York); C.E. Alissandrakis, M.R. Kundu and P. Lantos: (1981): Astron. Astrophys. 82, 30.

3. M.R. Kundu and C.E. Alissandrakis: (1975), Nature (London) 257, 465; M.R. Kundu, C.E. Alissandrakis, J.D. Bregman and A.C. Hin: (1977), Astrophys. J. 213, 278, K.R. Lang and R.F. Willson: (1979), Nature (London) 278, 24; K.R. Lang and R.F. Willson: (1980), Radio Physics of the Sun -I.A.U. Symp. No. 86, M.R. Kundu and T.E. Gergely, Eds. (Reidel, Dordrecht), p. 109; M.R. Kundu, E.J. Schmahl and M. Gerassimenko: (1980), Astron. Astrophys. 82, 265; M. Felli, K.R. Lang and R.F. Willson: (1981), Astrophys. J. 247, 325; R. Pallavacini, T. Sakurai and G.S. Vaiana: (1981), Astron. Astrophys. 98, 316.

4. M.R. Kundu, T. Velusamy and R.H. Becker: (1974), Solar Phys. 34, 217; K.R. Lang: (1974), Solar Phys. 36, 351; C.E. Alissandrakis and M.R. Kundu: (1978), Astrophys. J. 222, 342; K. Marsh and G.J. Hurford: (1980), Astrophys. J. Lett. 240, L111; M.R. Kundu: (1980), Radio Physics of the Sun -I.A.U. Symp. No. 86, M.R. Kundu and T.E. Gergely, Eds. (Reidel, Dordrecht, p. 157; K. Marsh, G.J. Hurford and H. Zirin: (1980), Radio Physics of the Sun -I.A.U. Symp. No. 86, M.R. Kundu and T.E. Gergely, Eds. (Reidel, Dordrecht) p. 191; K.R. Lang, R.F. Willson and M. Felli: (1981), Astrophys. J. 247, 338.

5. K.A. Marsh and G.J. Hurford: (1982), Ann. Rev. Astron. Astrophys. 20, 497; M.R. Kundu: (1982), Rep. Prog. Phys. 45, 1435; M.R. Kundu and L. Vlahos: (1982), Space Sci. Rev. 32, 405.

6. K.R. Lang and R.F. Willson: (1983), Adv. Space Res. Proc. XXIV COSPAR Pergamon, London), p. 91; K.R. Lang, R.F. Willson and V. Gaizauskas: (1983), Astrophys. J. 267, 455; R.K. Shevgaonkar and M.R. Kundu: (1984), Astrophys. J. 283, 413.

7. G.B. Gel'freikh and B.I. Lubyshev: (1979), Sov. Astron. A.J. 23, 316; C.E. Alissandrakis, M.R. Kundu and P. Lantos: (1980), Astron. Astrophys. 82, 30; C.E. Alissandrakis and M.R. Kundu: (1982), Astrophys. J. Lett. 253, L49; K.R. Lang and R.F. Willson: (1982), Astrophys. J. Lett. 255, L111.

8. M.R. Kundu and T. Velusamy: (1980), Astrophys. J. Lett. 240, L63; T. Velusamy and M.R. Kundu: (1981), Astrophys. J. Lett. 243, L103; K.R. Lang, R.F. Willson and J. Rayrole: (1982), Astrophys. J. 258, 384; G.A. Dulk and D.E. Gary: (1983), Astron. Astrophys. 124, 103; K.R. Lang and R.F. Willson: (1983), Astron. Astrophys. 127, 135; D. McConnell and M.R. Kundu: (1983), Astrophys. J. 269, 698.

9. T. Gold and F. Hoyle: (1960), Mon. Not. R. Astron. Soc. 120, 89; J. Heyvaerts, E.R. Priest and D.M. Rust: (1977), Astrophys. J. 216, 123; S.I. Syrovotskii and V.D. Kuznetsov: (1980), Radio Physics of the Sun -I.A.U. Symp. No. 86, M.R. Kundu and T.E. Gergely, Eds. (Reidel, Dordrecht), p. 445; V.D. Kuznetsov and S.I. Syrovatskii: (1981), Solar Phys. 69, 361; D.S. Spicer: (1981), Solar Phys. 70, 149; V. Petrosian: (1982), Astropnys. J. Lett. 255, L85; B.V. Somov and S.I. Syrovatskii: (1982), Solar Phys. 75, 237; E.R. Priest: (1983), Solar Phys. 86, 33.

10. M.R. Kundu, E.J. Schmanl, and T. Velusamy: (1982), Astrophys. J. 253, 963; M.R. Kundu, E.J. Schmanl, T. Velusamy and L. Vlahos: (1982), Astron. Astrophys. 108, 188; T. Velusamy and M.R. Kundu: (1982), Astropnys. J. 258, 388; M.R. Kundu: (1983), Solar Phys. 86, 205; M.R. Kundu: (1983), Adv. Space Res. -Proc. XXIV COSPAR (Pergamon, London), p. 159; M.R. Kundu, D.M. Rust and M. Bobrowsky: (1983), Astrophys. J. 265, 1084; R.F. Willson: (1983), Solar Phys. 83, 285; R.F. Willson and K.R. Lang: (1984), Astrophys. J. 279, 427; R.F. Willson: (1984), Solar Phys. 92, 189.

11. D.E. Gary and J.L. Linsky: (1981), Astrophys. J. 250, 284; K. Topka and K.A. Marsn: (1982), Astrophys. J. 254, 641; J.L. Linsky and D.E. Gary: (1983), Astrophys. J. 274, 776.

12. D.E. Gary, J.L. Linsky and G.A. Dulk: (1982), Astrophys. J. Lett. 263, L79: D.B. Melrose and G.A. Dulk: (1982), Astrophys. J. 259, 844: K.R. Lang, J. Bookbinder, L. Golub and M.M. Davis: (1983), Astrophys. J. Lett. 272, L15.

Presented at the XXV Committee On Space Research (COSPAR), Kongresszentrum, Graz, Austria, on June 26, 1984. To be published in Space Research XXV, Proceedings of COSPAR XXV, Pergamon Press.

V.L.A. OBSERVATIONS OF FLARE BUILD-UP IN CORONAL LOOPS

Kenneth R. Lang and Robert F. Willson

Department of Physics, Tufts University, Medford, MA 02155, U.S.A.

ABSTRACT

Very Large Array (V.L.A.) measurements at 20 cm wavelength map emission from coronal loops with second-of-arc angular resolution at time intervals as short as 3.3 seconds. The total intensity of the 20 cm emission describes the evolution and structure of the hot plasma that is detected by satellite X-ray observations of coronal loops. The circular polarization of the 20 cm emission describes the evolution, strength and structure of the coronal magnetic field. Preburst heating and magnetic changes that precede burst emission on time scales of between 1 and 30 minutes are discussed. Simultaneous 20 cm and soft X-ray observations indicate an electron temperature $T_e \sim 2.5 \times 10^7$ K and electron density $N_e \sim 10^{10}$ cm^{-3} during preburst heating in a coronal loop that was also associated with twisting of the entire loop in space. We also discuss the successive triggering of bursts from adjacent coronal loops; highly polarized emission from the legs of loops with large intensity changes over a 32 MHz change in observing frequency; and apparent motions of hot plasma within coronal loops at velocities V > 2,000 kilometers per second.

OBSERVING CORONAL LOOPS WITH THE V.L.A.

Because 356 interferometer pairs are sampled at the Very Large Array (V.L.A.), it is possible to create synthesis maps of solar active regions with second-of-arc angular resolution at time intervals as short as 3.3 seconds. Both the left-hand circularly polarized (LCP) and right-hand circularly polarized (RCP) signals are sampled, making it possible to create synthesis maps of the total intensity I = (RCP + LCP)/2 and circular polarization V = (RCP - LCP)/2. The total intensity maps describe the structure and evolution of the brightness temperature, whereas the circular polarization maps delineate the structure, evolution and strength of the magnetic field. Synthesis maps at longer microwave wavelengths, λ, refer to higher levels within the solar atmosphere where the brightness temperatures, T_B, are comparable to the electron temperature. Observations at $\lambda = 2$ cm refer to the footpoints of coronal loops where $T_B \sim 10^5$ K, while 6 cm observations often delineate the legs of magnetic dipoles where $T_B \sim 10^6$ K. The coronal loops are more reliably detected using the V.L.A. at 20 cm wavelength where emission from the entire loop is routinely detected /1,2,3,4,5,6/. These ubiquitous loops are the dominant structural element in the solar corona, but they have previously only been detected during rare and expensive satellite observations at soft X-ray wavelengths. Much, if not all, of the 20 cm emission is due to the thermal bremsstrahlung of the same hot plasma that gives rise to the soft X-ray emission.

The magnetic, temperature and density structure of the coronal loops can be specified from the 20 cm observations. Because the magnetic energy density dominates the thermal energy density at coronal heights, the hot plasma remains trapped within the magnetic loops. Electron temperatures $T_e = 2$ to 4×10^6 K, electron densities $N_e \sim 10^9$ to 10^{10} cm^{-3} and loop extents $L \sim 10^9$ to 10^{10} cm are inferred from the 20 cm bremsstrahlung, while longitudinal magnetic field strengths of $H_\ell \sim 50$ Gauss are inferred from the circular polarization if it is due to propagation effects. Thermal gyroresonance emission may also sometimes play a role in the 20 cm coronal loops, and in this case stronger magnetic fields of $H_\ell \sim 200$ Gauss are inferred from the polarization data.

The microwave bursts are themselves characterized by a strongly polarized, compact (5" to 30") impulsive component with a brightness temperature of $T_B = 10^7$ to 10^{10} K lasting between 1 and 5 minutes. The impulsive phase of the microwave burst is usually located near the neutral line between two Hα kernels in magnetic fields of opposite magnetic polarity. That is, the site of microwave energy release is usually at the apex of coronal loops, whereas the Hα emission occurs at the footpoints of the magnetic loops in the chromosphere /3,7,8,9,10,11/. The impulsive bursts are due to the gyrosynchrotron radiation of mildly

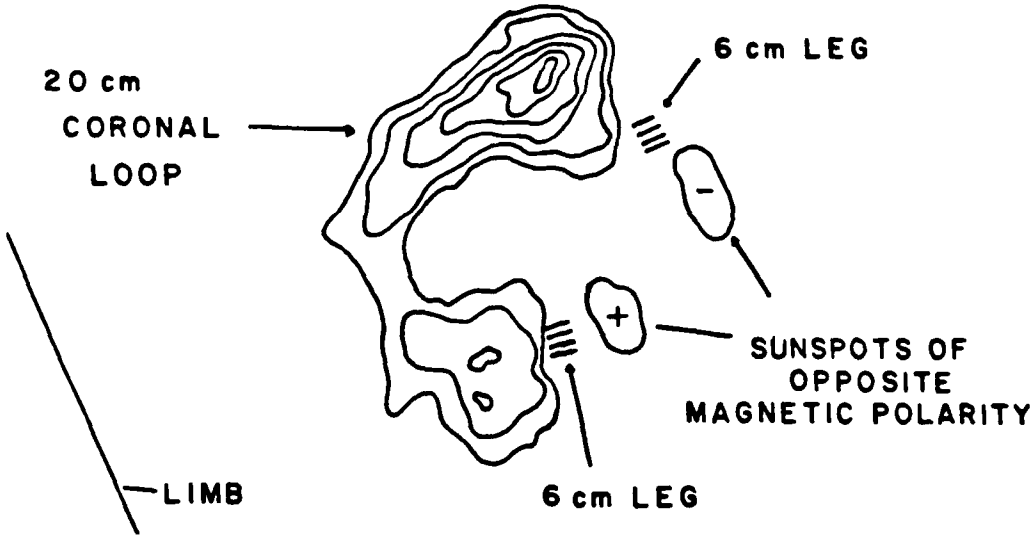

Fig. 1. A V.L.A. synthesis map of the total intensity, I, of the 20 cm emission from a coronal loop. The contours mark levels of equal brightness temperature corresponding to 0.2, 0.4,...1.0 times the maximum brightness temperature of $T_B = 2 \times 10^6$ K. A schematic portrayal of the 6 cm emission, which comes from the legs of the magnetic loops, has been added together with the underlying sunspots that are detected at optical wavelengths.

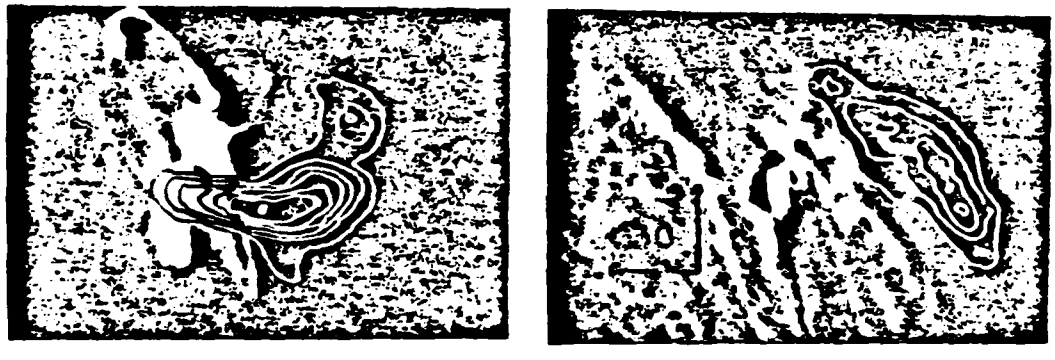

Fig. 2. The ten second V.L.A. synthesis maps of the impulsive phase of two solar bursts at 20 cm wavelength superimposed on Hα photographs of the optical flares taken at the same time at the Big Bear Solar Observatory. The 20 cm bursts originate near the tops of coronal loops that are about 40,000 km above the flaring region seen at optical wavelengths. The western solar limb is visible in both photographs.

relativistic electrons with energies of 100 to 500 keV. Some of these electrons are trapped in the upper parts of the loop, producing the microwave bursts. Other electrons stream down to the loop footpoints, producing hard X-ray bursts and the Hα kernels. This is often followed by a larger, longer post-burst component of microwave radiation with relatively low polarization and brightness temperature.

TRIGGERING SOLAR BURSTS IN CORONAL LOOPS

Preburst activity is associated with increases in the intensity and the degree of circular polarization of the centimeter wavelength emission of solar active regions /12,13/. These increases precede solar bursts on time scales of tens of minutes to an hour. The high angular resolution provided by the V.L.A. has now shown that the intensity increases are associated with preburst heating in coronal loops /10,11,14/, and that the changes in circular polarization are associated with changes in the coronal magnetic field /10,11,15/. Both the preburst heating and the magnetic field changes may trigger solar eruptions.

Single coronal loops or arcades of loops often begin to heat up and change structure about 3 minutes before the eruption of impulsive bursts. Many theoretical models of solar flares include such a preflare phase in which the coronal loop is heated, becomes unstable and then erupts /16,17,18,19/. As illustrated in Figure 3, a magnetic loop can heat up and twist in space. The magnetic shear produces a current sheet that triggers impulsive burst emission.. space. The magnetic shear produces a current sheet that triggers impulsive burst emission.. The preburst heating shown in Figure 3 was also detected at soft X-ray wavelengths with the GOES satellite. A comparison of the X-ray and radio data /14/ indicate a peak electron temperature of $T_e = 2.5 \times 10^7$ K and an average electron density of $N_e = 10^{10}$ cm^{-3} during the preburst heating. Preburst heating can also occur in coronal loops that are adjacent to, but spatially separated from, the sites of impulsive bursts /11/.

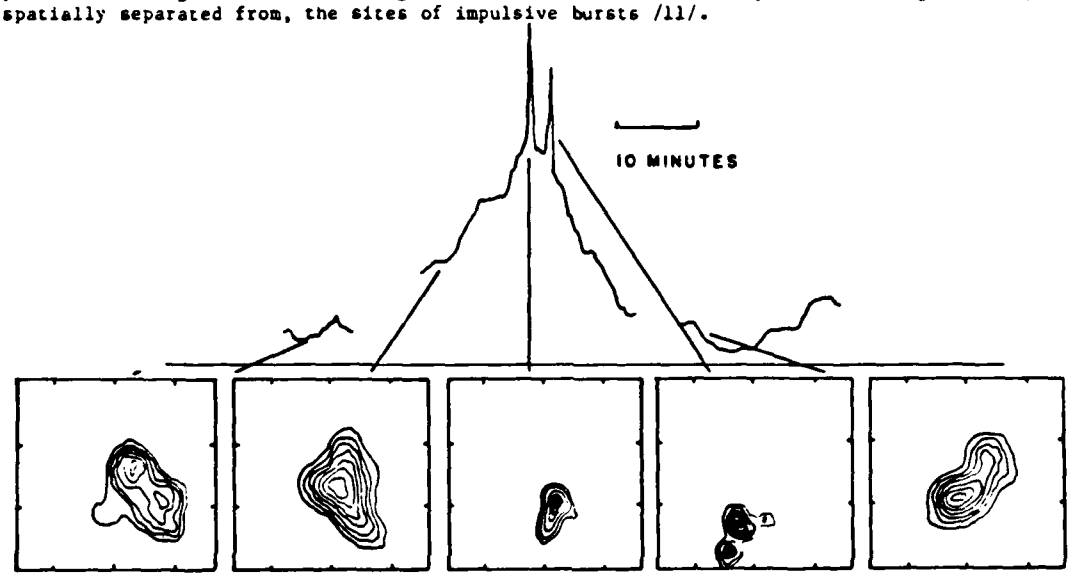

Fig. 3. The time profile of a solar burst at 20 cm wavelength illustrates heating within a coronal loop prior to the emission of two impulsive bursts. The 20 cm V.L.A. synthesis maps for ten second intervals are given below. The angular scale can be inferred from the 60" spacing between fiducial marks on the axes. The maps show that the coronal loop twisted in space, producing magnetic shear that led to impulsive burst emission from the same loop. This emission triggered a second burst from an adjacent source.

New bipolar loops can emerge and interact with preexisting ones, thereby triggering solar bursts. When the polarity of the new emerging flux differs from that of the preexisting flux, current sheets are produced that trigger the emission of bursts. A similar process can occur when preexisting adjacent loops undergo magnetic changes and trigger eruptions in nearby coronal loops.

Because of intense competition from celestial observers, it is not possible to routinely use the V.L.A. to obtain statistical data about the preburst heating and magnetic changes that trigger solar bursts. Other users of the V.L.A. have, however, reported the detection of magnetic changes that trigger bursts, including the interaction of orthogonal dipoles /15/. Preheating up to 30 minutes before flare onset has been detected for 70 percent of the flares observed at soft X-ray wavelengths using the Skylab satellite /20/, and minor energy release at 1.7 cm wavelength has preceded 25 percent of the main bursts observed at this wavelength at time intervals of between 10 to 35 minutes /21/.

Microwave bursts can be sequentially triggered within magnetically complex regions. As illustrated in Figure 4, successive intense bursts can be emitted from spatially separated coronal loops. Here the total intensity of the 20 cm burst emission is mapped. The polarization data indicate that the spatially separated structures are dipolar loops. In contrast to the intense bursts, the successive weaker bursts in the time profile were emitted from the same loop as the immediately preceding intense burst. The sequential triggering of intense impulsive bursts may be related to theoretical models of interacting loops in which an energy release in one loop triggers, through a magnetohydrodynamic disturbance, an energy release in a neighboring loop /22/.

Successive impulsive bursts can also be triggered within one leg of a coronal loop when a more gradual, oppositely polarized component is emitted from the other leg of the loop (see Figures 5 and 6). The most interesting aspect of this observation is that the last impulsive burst of the sequence (number 7) has an intensity difference of almost a factor of two over a very narrow frequency range of only 32 MHz. This might be explained by narrow-band maser emission.

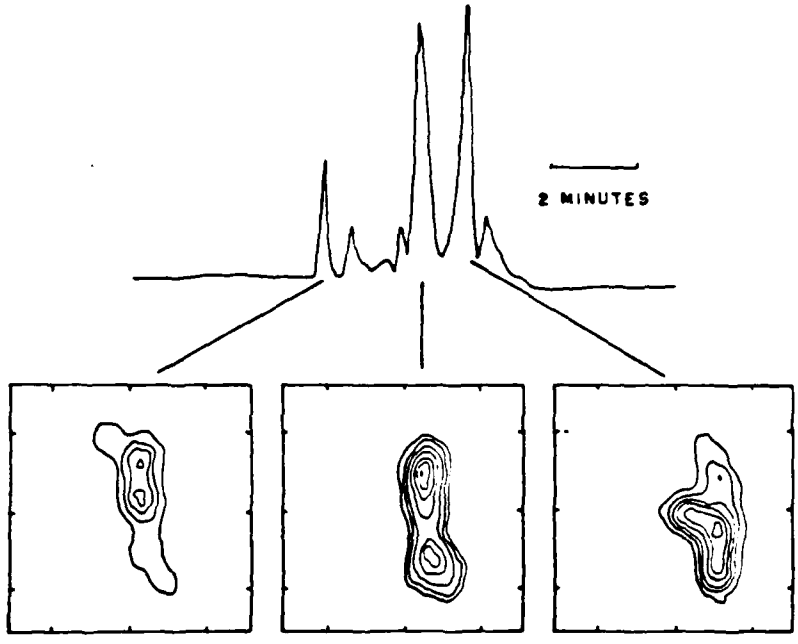

Fig. 4. The time profile of successive impulsive bursts at 20 cm wavelength is compared with ten second V.L.A. synthesis maps at the same wavelength. Here the contour intervals are in steps of 1.0×10^7 K and the angular scale can be inferred from the 30" spacing between fiducial marks on the axes.

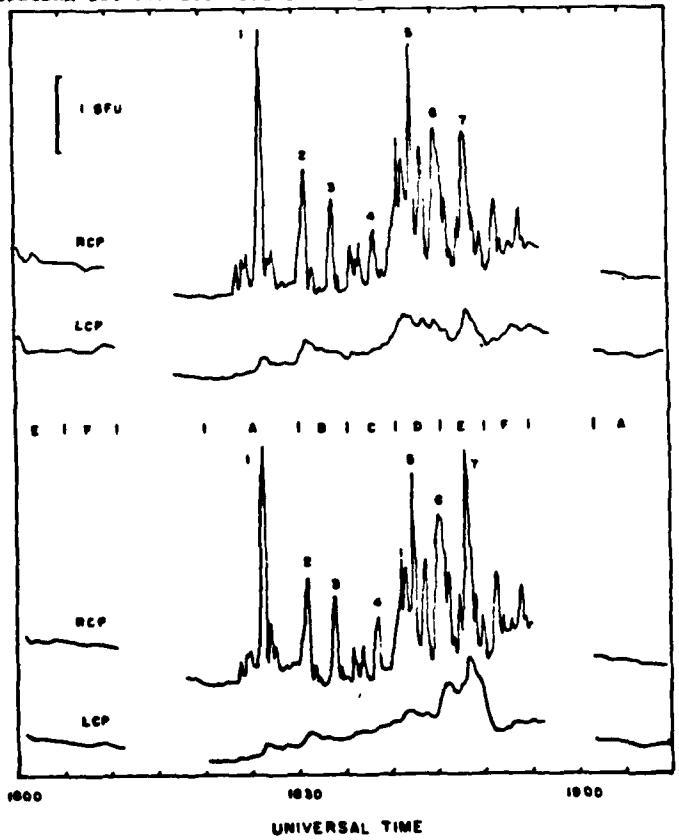

Fig. 5. A sequence of right circularly polarized (RCP) impulsive bursts observed at wavelengths near 20 cm on January 29, 1984 from AR 4398. The top and bottom profiles are at closely spaced frequencies designated by A: 1410 and 1375 MHz, B: 1480 and 1440 MHz, C: 1550 and 1515 MHz, D: 1620 and 1585 MHz, E: 1690 and 1658 MHz, and F: 1720 and 1705 MHz. Each pair of frequencies was observed for about 5 minutes. The 10 second snapshot maps at the peak of each burst are shown in Figure 6.

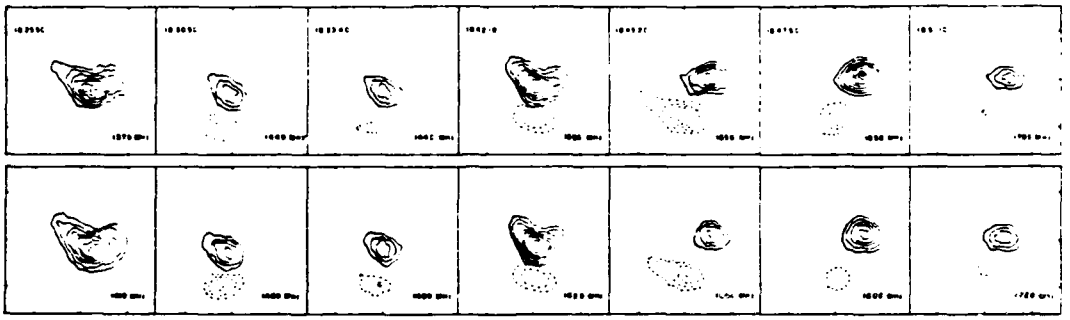

Fig. 6. Ten second snapshot maps made at the peak of the impulsive bursts shown in Figure 5. The right circularly polarized (RCP) bursts originated from a source (solid lines) that was spatially separated from the left circularly polarized (LCP) emission (dashed lines). The outermost contour and contour interval is 2.3 x 10^7 K for RCP and 9.0 x 10^6 K for LCP. Peak 7 occuring at 18^h 47^m 50^s (right) has a large difference in brightness temperature with T_B (1658) = 1.1 x 10^8 K and T_B (1690) = 6.0 x 10^7 K. The angular scale can be determined from the 30" spacing between the the hatchmarks.

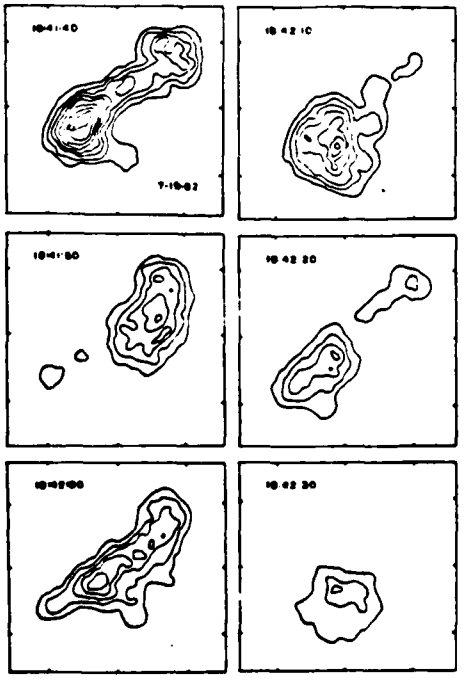

Fig. 7. A series of ten second snapshot maps of the total intensity, I, of an impulsive burst at 20 cm wavelength. The outermost contour and the contour interval are both equal to 1.3 x 10^6 K. The angular scale is determined by the 30" spacing between the fiducial marks on the axes.

As illustrated in Figure 7, the V.L.A. 20 cm snapshot maps also reveal the apparent motion of hot plasma within coronal loops at rates of more than 30" in 10 seconds, or a velocity V > 2,000 kilometers per second. Thermal conduction fronts might reach these velocities, exciting the plasma as they move through it. Although this speed is an order of magnitude higher than those detected spectroscopically during other bursts, there is abundant evidence for high speed excitations during solar bursts. Shocks with velocities of 1,000 kilometers per second are found in large flares /23/, and distant activation by electron beams travelling along large coronal loops at velocities V > 6,000 kilometers per second have been reported /24/. Electron beams moving with velocities of 100,000 kilometers per second may even have been the exciting agent for two large flares /25/.

ACKNOWLEDGEMENTS

Radio astronomical studies of the Sun and other active stars are supported under Grant AFOSR-83-0019-B with the Air Force Office of Scientific Research.

REFERENCES

1. K.R. Lang, R.F. Willson, and J. Rayrole, Astrophysical Journal 258, 284 (1982).

2. K.R. Lang, R.F. Willson and V. Gaizauskas, Astrophysical Journal 267, 455 (1983).

3. K.R. Lang and R.F. Willson, Adv. Space Res. 2, No. 11, 91 (1983).

4. D. McConnell and M.R. Kundu, Astrophysical Journal 269, 698 (1983).

5. G.A. Dulk and D.E. Gary, Astronomy and Astrophysics 124, 103 (1983).

6. R.K. Shevgaonkar and M.R. Kundu, Astrophysical Journal, in press (1984).

7. K. Marsh and G.J. Hurford, Astrophysical Journal (Letters) 240, L111 (1980).

8. K.R. Lang, R.F. Willson and M. Felli, Astrophysical Journal 247, 338 (1981).

9. M.R. Kundu and L. Vlahos, Space Science Reviews 32, 405 (1982).

10. R.F. Willson, Solar Physics 83, 285 (1983).

11. K.R. Lang and R.F. Willson, Astrophysical Journal 279, 427 (1984).

12. K.R. Lang, Solar Physics 36, 351 (1974).

13. M.R. Kundu, T. Velusamy and R.H. Becker, Solar Physics 34, 217 (1974).

14. R.F. Willson, Solar Physics, in press (1984).

15. M.R. Kundu, Solar Physics 86, 205 (1983).

16. J. Heyvaerts, E.R. Priest and D.M. Rust, Astrophysical Journal 216, 123 (1977).

17. S.I. Syrovotskii and V.D. Kuznetsov, in I.A.U. Symposium No. 86, Radio Physics of the Sun, ed. M.R. Kundu and T. Gergeley (Dordrecht: Reidel, 1980) p. 445.

18. D.S. Spicer, Solar Physics 70, 149 (1981).

19. B.V. Somov and S.I. Syrovatskii, Solar Physics 75, 237 (1982).

20. D.F. Webb, in I.A.U. Symposium No. 91, Solar and Interplanetary Dynamics, ed. M. Dryer and E. Tandberg-Hanssen (Dordrecht: Reidel, 1980), p.189.

21. K. Kai, H. Nakajima and T. Kosugi, Publications of the Astronomical Society of Japan 35, 285 (1983).

22. A.G. Emslie, Astrophysical Letters 22, 41 (1982).

23. D.M. Rust and D.F. Webb, Solar Physics 54, 403 (1977).

24. M.R. Kundu, D.M. Rust and M. Bobrowsky, Astrophysical Journal 265, 1084 (1983).

25. F. Tang and R.L. Moore, Solar Physics 77, 263 (1982).

VII. VERY LARGE ARRAY OBSERVING APPLICATIONS ACCEPTED FOR 1985

1. VLA OBSERVATIONS OF THE INNER SOLAR CORONA AT 21 CM AND 91 CM WAVELENGTH

Abstract

VLA observations at 21 and 92 cm will bridge the gap between the visible solar surface and the outer solar corona. They will provide high angular resolution measurements ($\gtrsim$ 6" at 327 MHz) of Type I or Type III bursts thereby resolving uncertainties over whether they are located at the top or legs of magnetic loops or in open field lines. Changing magnetic structures related to these bursts will also be detected. The early stages, driving mechanism and initiating source of coronal transients or mass ejections, may also be described. We will continue our search for thermal cyclotron lines and coordinate our observations with the SMM and P 78-1 satellites as well as with the K-coronameter at Mauna Loa.

2. MULTIPLE WAVELENGTH OBSERVATIONS OF M DWARF FLARE STARS AND RS CVn STAR

Abstract

We propose to use the VLA to observe six M dwarf flare stars and two RS CVn stars at 2, 6 and 20 cm wavelength. Our observations of flare stars will be used to search for impulsive and longer term variations which occur at different heights in the stellar atmospheres. Observations of RS CVn stars will be made with 3.3 second resolution in an attempt to detect impulsive events which may be superimposed on more gradual bursts.

3. COORDINATED VLA AND SOLAR MAXIMUM MISSION OBSERVATIONS OF SOLAR MASER BURST EMISSION AND CYCLOTRON LINE EMISSION

Abstract

The VLA will be used in coordination with the Solar Maximum Mission X-ray satellite to study narrow-band maser burst emission and cyclotron line

emission from the Sun. The combined data will be used to determine the location and structure of maser emission and to test theories of coronal heating by maser spikes during bursts. Observations of cyclotron line emission near 20 cm wavelength in combination with soft X-ray observations will lead to estimates of the magnetic field strengths, electron density and electron temperature in coronal loops during quiet periods and before bursts. All of these observations will provide constraints to theoretical models of solar eruptions in which a coronal loop is heated, becomes unstable and then erupts, giving rise to impulsive bursts.

4. VLA OBSERVATIONS SIMULTANEOUS WITH BALLOON OBSERVATIONS OF SOLAR HARD X-RAY MICROWAVE BURSTS

Abstract

Sensitive balloon-bourne hard X-ray spectrometer instrumentation has revealed very small hard X-ray bursts termed microflares. The microflares last from a few seconds to ten seconds, and they have a power law spectrum with the number of events increasing with decreasing flux. Such a spectrum suggests a nonthermal emission mechanism. The proposed VLA - hard X-ray balloon observations are designed to test the spectral nature of the microbursts and to also test the hypothesis that they may collectively contribute significantly to the heating of the solar corona.

VIII. PAPERS ACCEPTED FOR PRESENTATION AT PROFESSIONAL MEETINGS AND WORKSHOPS IN 1985

"V.L.A. Observations of Thermal and Non-Thermal Emission from Coronal Loops", Kenneth R. Lang and Robert F. Willson, 165th Meeting of the American Astronomical Society, Tucson, Arizona, January 13-16, 1985.

"Thermal and Non-Thermal Emission from Coronal Plasmas", Kenneth R. Lang, Solar Maximum Mission Topical Meeting on Prominence and Coronal Plasmas, sponsored by SMM-Goddard Space Flight Center, Airlie Conference Center, Warrenton, Virginia, April 9-11, 1985.

"Microwave Bursts from Coronal Loops", Kenneth R. Lang and Robert F. Willson, CESRA Workshop on Radio Continua During Solar Flares, Trieste, Italy, May 27-31, 1985.

"High Resolution Observations of the Sun and Nearby Stars", Kenneth R. Lang, Solar Maximum Analysis (SMA) Workshop on Plasma and MHD Physics Applied to Solar Flares, Irkutsk, USSR, June 16-21, 1985.

"Microwave Emission from the Sun and Nearby Stars", Kenneth R. Lang, International Astronomical Union (I.A.U.) Joint Discussion on Stellar Activity: Rotation and Magnetic Fields, New Delhi, India, November 19 to 28, 1985.

IX. PAPERS ACCEPTED FOR PUBLICATION IN 1984

"The Sun and Nearby Stars: Microwave Observations at High Resolution", Mukul R. Kundu and Kenneth R. Lang, Science (1985).

"V.L.A. Observations of Narrow Band Decimetric Burst Emission", Robert F. Willson, Solar Physics (1985).

"V.L.A. Observations of Solar Active Regions at Closely Spaced Frequencies: Evidence for Thermal Cyclotron Line Emission", Robert F. Willson, Astrophysical Journal (1985).

"The Structure of a Solar Active Region from RATAN-600 and Very Large Array Observations", Kenneth R. Lang, et. al., Astrophysical Journal (1985).

"Microwave Observations of Stars of Late Spectral Type with the Very Large Array", Roberto Pallivicini, Robert F. Willson and Kenneth R. Lang, Astronomy and Astrophysics (1985).

X. ABSTRACTS OF PAPERS ACCEPTED FOR PUBLICATION IN 1985

A. THE SUN AND NEARBY STARS; MICROWAVE OBSERVATIONS AT HIGH RESOLUTION

Mukul R. Kundu and Kenneth R. Lang

To be published in Science

Abstract

High resolution microwave observations are providing new insights into the nature of active regions and eruptions on the Sun and nearby stars. The strength, evolution, and structure of magnetic fields in coronal loops can be determined by multiple wavelength VLA observations. Flare models can be tested using VLA snapshot maps with angular resolutions of better than one second of arc in time periods as short as 10 seconds. Magnetic changes that precede solar eruptions on time scales of tens of minutes primarily involve emerging coronal loops, and the interaction of two of more loops. Magnetic reconnection at the interface of two closed loops may accelerate electrons and trigger the release of microwave energy in the coronal parts of the magnetic loops. Nearby main sequence stars of late spectral type emit slowly varying microwave radiation and stellar microwave bursts that show striking similarities to those of the Sun.

B. V.L.A. OBSERVATIONS OF NARROW BAND DECIMETRIC BURST EMISSION

Robert F. Willson

To be published in Solar Physics

Abstract

The Very Large Array was used to observe a multiply-impulsive solar radio burst at several wavelengths near 20 cm. The observations indicate that the impulsive emission was nearly 100% circularly polarized and originated in small regions of ~ 10" - 20" in size. For one of the impulsive spikes, we find evidence of narrow-band emission that could be attributed to an electron-cyclotron maser. The radio data are also compared with soft X-ray data and interpreted in light of a model in which the coronal plasma is heated by maser burst emission.

C. V.L.A. OBSERVATIONS OF SOLAR ACTIVE REGIONS AT CLOSELY SPACED FREQUENCIES: EVIDENCE FOR THERMAL CYCLOTRON LINE EMISSION

Robert F. Willson

To be published in the Astrophysical Journal

Abstract

VLA observations of a solar active region at ten closely spaced frequencies between 1440 and 1720 MHz are presented. The synthesis maps show, on two successive days, significant changes in the brightness temperature within this narrow frequency range. We show that these changes cannot be due to either thermal bremsstrahlung or gyroresonance emission from a coronal loop in which the temperature, density or magnetic field varies uniformly with height. Instead, we attribute the brightness spectrum to cyclotron line emission from a narrow layer where the temperature is elevated above the surrounding part of the loop.

D. THE STRUCTURE OF A SOLAR ACTIVE REGION FROM RATAN-600 AND VERY LARGE ARRAY OBSERVATIONS

Kenneth R. Lang et al.

To be published in the Astrophysical Journal

Abstract

Solar active region AR 3804 was observed on the same days with the RATAN-600 and the VLA in July 1982. The emission at wavelengths between 2 and 4 cm consisted of narrow ($\phi \lesssim 40"$), bright ($T_B \sim 0.2$ to 6×10^6 K) core sources surrounded by a weaker ($T_B \sim 10^4$ to 10^5 K), extended ($\phi \sim 200"$) halo. The brightest core sources are associated with sunspots and are interpreted in terms of the gyroradiation of thermal electrons at the second and third harmonics of the gyrofrequency. Two of the core sources were associated with a filament that lie above the magnetic neutral line in the photosphere. One of these filament-associated sources has a flat spectrum and is attributed to thermal bremsstrahlung. The other filament-associated source has a steep spectrum that cannot be attributed to gyroradiation because of the weak magnetic fields. It may be attributed to the gyrosynchrotron radiation of subrelativistic electrons. VLA synthesis maps at 20 cm reveal hot ($T_B \sim 10^6$ K) coronal loops that connect underlying sunspots of opposite magnetic polarity, but RATAN-600 observations reveal the presence of a much more extended source that accounts for the vast majority of the flux detected at this wavelength. This extended source may also be attributed to the gyrosynchrontron radiation of subrelativistic electrons.

E. MICROWAVE OBSERVATIONS OF STARS OF LATE SPECTRAL TYPE WITH THE VERY LARGE ARRAY

Roberto Pallavicini, Robert F. Willson and Kenneth R. Lang

To be published in Astronomy and Astrophysics

Abstract

The Very Large Array was used to search for microwave emission from 32 stars of late spectral type including RS CVn type stars, dwarf M flare stars, and stars with active chromospheres, coronae or intense magnetic fields. We have detected four RS CVn stars at 6 cm wavelength and have established upper limits for another six. Radio emission was detected from three dwarf M flare stars, UV Cet, EQ Peg and YZ Cmi. Both impulsive (<20s) and more gradual (> ten minutes) bursts were observed from the flare star YZ Cmi. We do not confirm radio emission at 6 cm from the solar type star χ^1 Ori, with an upper limit that is three times lower than the detections reported by other observers. We failed to detect microwave emission from any other solar type star of spectral class G to K. The quiescent radio emission from dwarf M flare stars is interpreted as non-thermal gyrosynchrotron emission by mildly relativistic electrons accelerated more or less continuously in the magnetic fields of sunspots.

XI. PLANS FOR FUTURE RESEARCH

The research proposed in this interim scientific report will be continued under a continuation of grant AFOSR-83-0019 in 1985. We will first complete and publish the analysis of simultaneous observations of nearby dwarf M flare stars with the Very Large Array (V.L.A.) and the International Ultraviolet Explorer (I.U.E.) satellite. They consist of six days of observations of AD Leo, UV Cet and YZ Cmi.

We will also quickly continue the analysis of simultaneous V.L.A. and Solar Maximum Mission (S.M.M.) satellite observations of solar active regions. These data, which were taken in July, 1984, include X-ray and V.L.A. 20 cm observations that should discriminate between thermal and non-thermal emission mechanisms for coronal loops.

Future research also involves continued V.L.A. observations of solar active regions. Abstracts for four of these observing programs are given in Section VII. They include V.L.A.-S.M.M. observations, V.L.A. - balloon X-ray observations, and V.L.A. observations at long wavelengths of 20 cm and 91 cm. Future observations of bursts from both the Sun and nearby stars will stress observational tests for coherent maser-like emission processes.

The 1985 research program is best summarized by the project abstract which follows:

We propose observations of solar active regions with the Very Large Array (VLA) which will lead to a new understanding of the origin and prediction of the solar bursts which disrupt communication systems and interfere with highflying aircraft. Multiple wavelength VLA observations will be used to determine the three dimensional structure of solar active regions by specifying the temperature and magnetic structure at different

heights within coronal loops. These data will be combined with simultaneous observations at ultraviolet and soft X-ray wavelengths using the recently repaired Solar Maximum Mission (SMM) satellite. The combined results will enhance the scientific return beyond that expected from using either the VLA or the SMM alone. Preburst signatures that may predict solar eruptions on time scales of tens of minutes to an hour will be studied. These include preburst heating and mangetic shear within coronal loops, as well as emerging coronal loops and interaction between coronal loops. The unique high time and spatial resolution of the VLA will be used to study the mechanisms of burst excitation, including shock waves, electron beams, and thermal conduction fronts that travel at high speeds. The VLA observations will also be able to determine the spatial location of the bright points and blue shifted components that are detected at ultraviolet wavelengths. We will carry out related investigations of the quiescent and burst emission from coronal loops on nearby stars of late spectral type. The International Ultraviolet Explorer (IUE) satellite and the VLA will be used to simultaneously observe the nearby dwarf M stars YY Gem, YZ Cmi, and AD Leo, which are known to emit frequent and powerful flares. The combined observations will provide valuable new insights to such things as the difference between coronal and chromospheric flares, the flare energy budget, the location of flare energy release, and the preburst heating or magnetic changes that trigger flare emission. The proposed studies of radio bursts from the Sun and nearby stars will lead to a deeper knowledge of the triggering mechanisms of solar bursts, and may lead to new methods of predicting when they will occur.

END

FILMED

5-85

DTIC